UiO : University of Oslo

Ashish Rauniyar

Exploring and Enhancing the Spectral and Energy-Efficiency of Non-Orthogonal Multiple Access in Next Generation IoT Networks

Thesis submitted for the degree of Philosophiae Doctor

Department of Informatics
Faculty of Mathematics and Natural Sciences

2021

To my Loving Family, Friends, and Teachers Who Has Always been Source of Inspiration, Motivation and Learning Throughout My Life

"Research is to see what
everybody else has seen,
and to think what nobody
else has thought."
Albert Szent-Gyorgyi (1893-1986)
Physiologist and Nobel Prize Recipient

Preface

This thesis is submitted in partial fulfillment of the requirements for the degree of *Philosophiae Doctor* at the Department of Informatics, Faculty of Mathematics and Natural Sciences, University of Oslo. The research work presented here was conducted at the University of Oslo and at Oslo Metropolitan University, under the supervision of Prof. Paal E. Engelstad and Telenor Senior Research Scientist Olav N. Østerbø. The research leading to this doctoral thesis has been carried out entirely in the period from September 2016 to October 2020. As part of the Ph.D. program, 40 credits course has been studied at the Department of Informatics, Faculty of Mathematics and Natural Sciences, University of Oslo. About 25 % of the time (4 years) has been dedicated to teaching courses and supervision of Master students and the remaining 75 % time was dedicated to research work for this thesis. This Ph.D. research work was fully supported by The Norwegian Ministry of Education and Research under KD Funding Schemes for Research and Innovation.

I hereby declare that I am the first author of this thesis. Paper I - XIII are based on work that has been published or submitted for publication. The related publications are co-authored by my supervisors Prof. Paal E. Engelstad and Senior Research Scientist Dr. Olav N. Østerbø.

Acknowledgements

This dissertation would not have been possible without the guidance, indispensable encouragement and motivation of all my supervisors, to whom i express my deepest appreciation.

First of all, I would like to express my sincere gratitude and appreciation to my main supervisor, Prof. Paal Engelstad for guiding me to do Ph.D. research studies under his esteemed supervision. He inspired and motivated me in understanding the scientific research and his willingness to guide me contributed greatly to this thesis. I would also like to thank him for his timely and constructive advice during our regular research meetings in order to improve my work. I still remember my initial PhD days when things were not going as i had planned. Paal supported me in all the possible ways and gave me complete research freedom to think critically and work on the things that i like. Paal is very critical when it comes to scientific writing and and the rigorousness of argumentation. I have benefited a lot from him and i think this is one of the important skills i have acquired which would help me in my scientific career. I would also like to thank for his extreme supervision, guidance, support, and encouragement from the beginning that enabled me to finish this thesis. It was really a nice experience to work under his supervision. Paal, you are a great supervisor and i could not have imagined having the best and knowledgeable main supervisor for my Ph.D. than you.

Secondly, I would like to thank my co-supervisor - Telenor Senior Research Scientist Dr. Olav N. Østerbø. Olav is a mathematical genius and i am in complete awe of him. I really had a nice time solving complex analytical frameworks of this PhD dissertation. Whenever, i am stuck in my Ph.D. research, Olav is always there to guide me. I still remember long discussions on solving the complex equations together on the big board at Paal's office. The discussions with you on the mathematics part for all the papers gave me a motivation to deeply understand the underlying principles of the wireless communication field. Olav is full of energy and his critical and timely suggestions on our scientific works has contributed a lot to this Ph.D. dissertation. Olav, you are one of the best supervisor that any PhD student would like to have. I have learned a lot from you.

Thirdly, I would also like to thank Prof. Anis Yazidi. Anis is always positive and keep sharing me his invaluable scientific knowledge. I have had the privilege to co-work with him in some of the scientific works and I have learned a lot from him. I would also like to thank Head of Department of Computer Science - Laurence Marie Anna Habib of Oslo Metropolitan University. Laurence is very helpful and i really appreciate her for providing me all the support required during my PhD.

Like they say, Ph.D. is a long and daunting process and one cannot enjoy it without the support and care of amazing friends and colleagues. Since the beginning of my Ph.D, I am blessed to have support of my friends like Dr. Desta Haileselassie Hagos, Ramtin Aryan, Debesh Jha, Dr. Laura Andreína Marcano Canelones and Dr. Flavia Dias Casagrande, without whom my Ph.D. life in Oslo

might not have been so much fun. I miss our silly and interesting discussions over lunch and numerous gatherings. We had so much fun. Whenever, I felt low during my Ph.D., you guys were always there and i am truly indebted to you guys. You all are awesome. Thank you so much.

I would like to thank Dr. Samiksha Koirala, Anushree, Archana and Ichchha for your time out of your busy schedule. You all have provided me a tremendous support and motivation during my PhD. I would also like to thank my friend Siva Leela Krishna Chand Gudi for the extra-curricular activities like pitching of ideas at different international events and rigorous scientific discussions. A special thanks also goes to my friend Bineeth, Simon and Daniel for all the memorable time i had with you guys during my PhD. There are also other very close friends, and colleagues who have had the chance to share thoughts about my Ph.D. thesis work. They are too many to list them all, to whom I owe a great debt of sincere thanks.

Last but not the least, I would like to thank most important people in my life to whom this dissertation is dedicated: my dad Mr. Ashok Rauniyar, mom Mrs. Gayatri Rauniyar, my brother Saurab Rauniyar and my joint family. Without your extreme love, support and care, none of what I've done and all the miles I've travelled so far in my life would have been possible. I owe everything I've ever done in my entire life to you all.

I am really thankful to almighty God for his long uninterrupted blessings with full of encouragement and motivation.

Ashish Rauniyar
Oslo, February 2021

Abstract

The proliferation of technologies like Internet of Things (IoT) and Industrial IoT (IIoT) has led to rapid growth in the number of connected devices and the volume of data associated with IoT applications. It is expected that more than 125 billion IoT devices will be connected to the Internet by 2030. With the plethora of wireless IoT devices, we are moving towards the connected world which is the guiding principle for the IoT. The next generation of IoT network should be capable of interconnecting heterogeneous IoT sensor or devices for effective Device-to-Device (D2D), Machine-to-Machine (M2M) communications as well as facilitating various IoT services and applications. Therefore, the next generation of IoT networks is expected to meet the capacity demand of such a network of billions of IoT devices. The current underlying wireless network is based on Orthogonal Multiple Access (OMA) by assigning orthogonal resources to multiple users. OMA cannot serve multiple IoT devices simultaneously and hence cannot maximize the resource efficiency. Therefore, OMA is considered spectrally inefficient for the design and optimization of the next-generation wireless systems. In this context, to provide massive connectivity requirements of IoT sensor and devices and to ameliorate their capacity demands, Non-Orthogonal Multiple Access (NOMA) has been considered as a potential candidate for the Fifth-Generation (5G) and the next-generation networks. Fundamentally, in NOMA, multiple signals or messages for users with distinct channel conditions are multiplexed in power domain. Specifically, multiple signals can overlap in same time, frequency and code in order to achieve a balanced trade-off between system throughput and user fairness. Moreover, in addition to improving the Spectral Efficiency (SE), which is the main motivation of NOMA, another key objective of the next-generation wireless IoT networks is to maximize the energy-efficiency so as to support massive IoT device communication and data transmission. To this end, Simultaneous Wireless Information and Power Transfer (SWIPT) has been contemplated as an energy efficient viable solution to self-sustainable communication in IoT networks.

In this dissertation, different from the state-of-the-art methods and architectures, we investigate and propose several spectral and energy-efficient NOMA architectures for next-generation IoT networks. This dissertation first proposed an architecture to demonstrate how bi-directional communications can be achieved in a NOMA-SWIPT enabled IoT relay networks. Then pairing issues in NOMA are discussed, since efficient user pairing between multiple users is needed to enhance the capacity of NOMA systems. Thus, a new adaptive user pairing strategy that enhances the capacities of a cell for NOMA systems is proposed and thoroughly examined. Then this dissertation sheds lights on the issue of distributed localization in the IoT, since accurate and precise localization

can help the IoT sensor nodes for efficient user pairing and energy harvesting. Therefore, we propose Social Learning based Particle Swarm Optimization (SL-PSO), which is a new distributed localization algorithm inspired from nature. Following this, several architectures for cooperative NOMA-SWIPT are proposed where outage probability, throughput, sum-throughput, Ergodic capacity and Ergodic sum capacity is investigated for a delay limited and delay tolerant transmission mode. Their analytical derivations are mathematically derived and corroborated with the simulation results under both perfect Signal-to-Interference Cancellation (SIC) and imperfect SIC scenarios. Moreover, NOMA is based on the principle of SIC, which is known to be very fragile to interference, as the decoding failure propagates in the SIC chain to weaker users. Therefore, we propose and investigate a simple and energy-efficient distributed power control in downlink NOMA using Reinforcement Learning (RL) based Game Theoretic approach. Finally, this dissertation proposes and investigates different models by consolidating direct links in a way that significantly enhances the performance of the cooperative NOMA-SWIPT systems. We believe that our works proposed in this dissertation will be useful for designing spectral and energy-efficient NOMA in next-generation IoT networks. We further believe that the study and results presented in this dissertation might be potentially useful to network operators, researchers and scientists in the wireless networking community from both academia and industry who want to assess the characteristics of NOMA to design next-generation IoT networks.

List of Papers

This Ph.D. dissertation is based on the following papers numbered from I to XIII.

Paper I

Rauniyar, A., Engelstad, P., and Østerbo, O. N. "On the Performance of Bidirectional NOMA-SWIPT Enabled IoT Relay Networks". In: *IEEE Sensors Journal* Vol. 21, no. 2 (2020), pp. 2299 - 2315. DOI: 10.1109/JSEN.2020.3018905.

Paper II

Rauniyar, A., Engelstad, P., and Østerbo, O. N. "An Adaptive User Pairing Strategy for Uplink Non-Orthogonal Multiple Access". In: *2020 IEEE 31st Annual International Symposium on Personal, Indoor and Mobile Radio Communications, London,UK, 31 August - 3 September* (2020), pp.pp. 1–7. DOI: 10.1109/PIMRC48278.2020.9217383.

Paper III

Rauniyar, A., Engelstad, P., and Moen, Jonas. "A New Distributed Localization Algorithm Using Social Learning based Particle Swarm Optimization for Internet of Things". In: *2018 IEEE 87th Vehicular Technology Conference (VTC Spring), Porto, Portugal, 3-6 June* (2018), pp. 1–7. DOI: 10.1109/VTCSpring.2018.8417665.

Paper IV

Rauniyar, A., Engelstad, P., and Østerbo, O. N. "Exploiting SWIPT for IoT NOMA-based Diamond Relay Networks". In: *EAI MobiQuitous 2020 - 17th EAI International Conference on Mobile and Ubiquitous Systems: Computing, Networking and Services, Darmstadt, Germany, December 7 - 9* (2020), pp. 1–10. DOI: 10.1145/3448891.3448931.

Paper V

Rauniyar, A., Engelstad, P., and Østerbo, O. N. "RF Energy Harvesting and Information Transmission Based on Power Splitting and NOMA for IoT Relay Systems". In: *2018 IEEE 17th International Symposium on Network Computing*

and Applications (NCA), Cambridge, MA, USA, 1-3 November (2018), pp. 1–8. DOI: 10.1109/NCA.2018.8548068.

Paper VI

Rauniyar, A., Engelstad, P., and Østerbo, O. N. "RF Energy Harvesting and Information Transmission in IoT Relay Systems based on Time Switching and NOMA". In: *2018 28th International Telecommunication Networks and Applications Conference, Sydney, NSW, Australia, 21-23 November* (2018), pp. 1–7. DOI: 10.1109/ATNAC.2018.8615403, **(Best Paper Award)**.

Paper VII

Rauniyar, A., Engelstad, P., and Østerbo, O. N. "RF Energy Harvesting and Information Transmission Based on NOMA for Wireless Powered IoT Relay Systems". In: *Sensors Journal, Special Issue: Selected Papers from the 28th International Telecommunication Networks and Applications Conference,* Vol. 18, no. 10 (2018), pp. 3254–3275. DOI: 10.3390/s18103254.

Paper VIII

Rauniyar, A., Engelstad, P., and Østerbo, O. N. "Ergodic Sum Capacity Analysis of NOMA-SWIPT Enabled IoT Relay Systems". In: *Internet Technology Letters, Wiley* Vol. 00, no. 00 (2020), pp. 1–6. DOI: 10.1002/itl2.218.

Paper IX

Rauniyar, A., Yazidi, A., Engelstad, P., and Østerbo, O. N. "A Reinforcement Learning based Game Theoretic Approach for Distributed Power Control in Downlink NOMA". In: *2020 IEEE 19th International Symposium on Network Computing and Applications (NCA), Cambridge, MA, USA, 26-28 November.* (2020), pp. 1–10. DOI: 10.1109/NCA51143.2020.9306737.

Paper X

Rauniyar, A., Engelstad, P., and Østerbo, O. N. "Performance Analysis of RF Energy Harvesting and Information Transmission based on NOMA with Interfering Signal for IoT Relay Systems". In: *IEEE Sensors Journal* Vol. 19, no. 17 (2019), pp. 7668–7682. DOI: 10.1109/JSEN.2019.2914796.

Paper XI

Rauniyar, A., Engelstad, P., and Østerbo, O. N. "Ergodic Capacity Performance of NOMA-SWIPT Aided IoT Relay Systems with Direct Link". In: *IEEE 18th*

International Symposium on Modeling and Optimization in Mobile, Ad Hoc and Wireless Networks (WiOpT 2020), Volos, Greece, 15-19 June (2020), pp. 1–8.

Paper XII

Rauniyar, A., Engelstad, P., and Østerbo, O. N. "Capacity Enhancement of NOMA-SWIPT IoT Relay System with Direct Links over Rayleigh Fading Channels". In: *Transactions on Emerging Telecommunications Technologies, Wiley, Special Issue: Cross-layer Innovations in Internet of Things,* Vol. 00, no. 00 (2020), pp. 1–18. DOI: 10.1002/ett.3913.

Paper XIII

Rauniyar, A., Engelstad, P., and Østerbo, O. N. "Ergodic Capacity Performance of D2D IoT Relay NOMA-SWIPT Systems with Direct Links". In: *IEEE 43rd International Conference on Telecommunications and Signal Processing (TSP), Milan, Italy, 7-9 July* (2020), pp. 1–7. DOI: 10.1109/TSP49548.2020.9163552, **(Best Paper Award)**.

Other Scientific Activities

List of Other Publications Not Included in This Thesis

J1 Ramesh Upreti, **Ashish Rauniyar**, Jeevan Kunwar, Hårek Haugerud, Paal Engelstad, Anis Yazidi, "Adaptive Pursuit Learning for Energy Efficient Target Coverage in Wireless Sensor Networks." Concurrency and Computation Practice and Experience Journal, Wiley, April 2020.

J2 **Ashish Rauniyar**, Desta Haileselassie Hagos, Manish Shrestha. "A Crowd-based Intelligence Approach for Measurable Security, Privacy, and Dependability in Internet of Automated Vehicles". *International Journal of Mobile Information Systems, March 2018, Vol 2018:1-14, Article ID 7905960*, **Best Paper Award** at AI-DLDA 2018 International Summer School on Artificial Intelligence, Udine-Italy.

J3 Ramesh Pokhrel, **Ashish Rauniyar**, Anis Yazidi, "A Stochastic Learning Approach in the Pursuit of Trade-off between Job Parallelism and Throughput for Adaptive Parameter Tuning of Hadoop." Concurrency and Computation Practice and Experience Journal, Wiley, March 2020. **Status: Under Review**

C1 Ramesh Pokhrel, **Ashish Rauniyar**, Anis Yazidi, "In the Quest of Trade-off between Job Parallelism and Throughput in Hadoop: A Stochastic Learning Approach for Parameter Tuning on the Fly." *20th International Conference on Parallel and Distributed Computing, Applications and Technologies (PDCAT 2019), 5-7 December 2019, Gold Coast, Australia.*

C2 **Ashish Rauniyar**, Jeevan Kunwar, Hårek Haugerud, Anis Yazidi, Paal Engelstad, "Energy Efficient Target Coverage in Wireless Sensor Networks Using Adaptive Learning." *Distributed Computing for Emerging Smart Networks (DiCES-N) in conjunction with 16th International Colloquium on Theoretical Aspects of Computing October 30, 2019, Hammamet, Tunisia.*

C3 **Ashish Rauniyar**,Paal Engelstad, Boning Feng and Do Van Thanh. "Crowdsourcing-based Disaster Management Using Fog Computing in Internet of Things Paradigm." *In Proceedings of Collaboration and Internet Computing (CIC), 2016 IEEE 2nd International Conference on. IEEE, 2016, Pittsburgh, USA, November 2016.*

Honours and Awards During PhD

- Our research paper titled 'Ergodic Capacity Performance of D2D IoT Relay NOMA-SWIPT Systems with Direct Links' has been awarded as **Best Paper Award** at 2020 43rd IEEE International Conference on Telecommunications and Signal Processing (TSP), July 7 $\sim$ July 9, 2020, Milan, Italy.
- Selected as **Top 200 Young Scientists** to attend 8th Global Young Scientists Summit, from 14-17 January 2020, Singapore.
- Our research paper titled 'RF Energy Harvesting and Information Transmission in IoT Relay Systems based on Time Switching and NOMA' has been awarded as **Best Paper Award** at 28th IEEE International Telecommunication Networks and Applications Conference (ITNAC), November 21 $\sim$ November 23, 2018, Sydney, Australia.
- Our research paper titled 'A Crowd-based Artificial Swarm Intelligence Approach for Measurable Security in Internet of Automated Vehicles with Vehicular Fog Computing' has been awarded as **Best Paper Award** at AI-DLDA 2018 International Summer School on Artificial Intelligence, Udine-Italy | 2-6 July 2018.
- Selected as **Top 50 Young Global Changer** and invited to attend Global Solutions Summit, May 24 - 29 2018, Berlin, Germany.
- Selected as **Norway Regional Winner for European Satellite Navigation Competition**, November 7, 2017, Tallinn, Estonia.
- Selected as **Top 200 Young Researcher** to attend 5th Heidelberg Laureate Forum from September 23 to September 30, 2017 at Heidelberg, Germany.

Master Thesis Supervision

- "In the Quest of Trade-off between Job Parallelism and Throughput: Adaptive Parameter Tuning of Hadoop." University of Oslo, Norway, January 2018 $\sim$ September 2018.

Teaching and Tutoring

- ADSE1310 Internet of Things Course to Engineering Undergraduate Students, Spring 2020 (Class Size: 150 Students).
- MEK1200 Introduction to IT for Engineers Course to Undergraduate Engineering Students at OsloMet, Autumn 2019 (Class Size: 100+ students).

- ADSE1310 Internet of Things Course to Second Year Undergraduate Students, Spring 2019 (Class Size: 80 Students).
- DAVE3605-Effective Programming in C and C++ Course to Final Year Undergraduate Students, Spring 2017 (Class Size: 110 Students).

PhD Panel

- PhD Panel for the European Commission Radical Innovation Breakthrough Inquirer (RIBRI) Project, April 2018

Mentorship

- Mentor for Young Sustainable Impact (YSI) Innovation Program, August 2018.
- Mentor for OsloMet Summer School Innovation Camp 2018, July 2018.
- Mentor for Young Sustainable Impact (YSI) Innovation Program, August 2017.

Talks

- "Crowdsourcing-based Disaster Management using Fog Computing in Internet of Things Paradigm", COINS Ph.D. Student Seminar, University of Bergen, 27-28 November 2016, Bergen, Norway.

Technical Programme Committee (TPC) Member and Reviewer

- TPC member for IEEE International Symposium on Personal, Indoor and Mobile Radio Communications (IEEE PIMRC), 2018, 2019, 2020, & 2021.
- Reviewer for 2018 IEEE 87th Vehicular Technology Conference: VTC2018-Spring, June 2018, Porto, Portugal.
- Reviewer for IEEE Communication Letters Journal.
- Reviewer for IEEE Sensors Letters Journal.
- Reviewer for IEEE Networking Letters Journal.
- Reviewer for IEEE Internet of Things Journal.
- Reviewer for IEEE Sensors Journal.

- Reviewer for IEEE Transactions on Vehicular Technology Journal
- Reviewer for IEEE Transactions on Systems, Man, and Cybernetics Journal
- Reviewer for IEEE Transactions on Industrial Informatics Journal.
- Reviewer for IEEE Access Journal.
- Reviewer for Evolving Systems Journal, Springer.
- Reviewer for Journal of Experimental & Theoretical Artificial Intelligence, Taylor & Francis.
- Reviewer for International Journal of Electronics, Taylor & Francis.
- Reviewer for International Journal of Distributed Sensor Networks.

List of Abbreviations

3GPP 3rd Generation Partnership Project

5G Fifth-Generation

AF Amplify-and-Forward

AI Artificial Intelligence

BER Bit Error Ratio

BPSO Binary Particle Swarm Optimization

BR Bi-directional Relaying

BS Base Station

CI Confidence Interval

C-NOMA Conventional Non-Orthogonal Multiple Access

DF Decode-and-Forward

D2D Device-to-Device

EC Ergodic Capacity

EE Energy Efficiency

EH Energy Harvesting

ESC Ergodic Sum Capacity

FDMA Frequency Division Multiple Access

FU Far User

ipSIC Imperfect Signal-to-Interference Cancellation

ID Information Decoding

IoT Internet of Things

LA Learning Automata

LA-GT Learning Automata based Game-Theoretic

LTE Long Term Evolution

MPA Message Passing Algorithm

M2M Machine-to-Machine

MRC Maximal Ratio Combining

MUST Multi-User Superposition Transmission

ML Machine Learning

NE Nash Equilibrium

NOMA Non-Orthogonal Multiple Access

NDR NOMA-based Diamond Relaying

NR New Radio

NU Near User

OFDMA Orthogonal Frequency Division Multiple Access

OMA Orthogonal Multiple Access

OWR One Way Relaying

pSIC Perfect Signal-to-Interference Cancellation

PS Power Splitting

PSR Power Splitting Relaying

PF Proportional Fairness

PSO Particle Swarm Optimization

QoS Quality of Service

RF Radio Frequency

RL Reinforcement Learning

RSSI Received Signal Strength Identification

SCMA Sparse Code Multiple Access

SE Spectral Efficiency

SIC Signal-to-Interference Cancellation

SL-PSO Social Learning based Particle Swarm Optimization

SNR Signal-to-Noise Ratio

SDS Single Signal Decoding Scheme

SWIPT Simultaneous Wireless Information and Power Transfer

TDMA Time Division Multiple Access

TDOA Time Difference of Arrival

TOA Time of Arrival

TS Time Switching

TSR Time Switching Relaying

TWR Two Way Relaying

WSN Wireless Sensor Network

Contents

List of Figures

List of Tables

Chapter 1

Introduction

1.1 Background and Motivation

The proliferation of technologies like Internet of Things (IoT) has led to rapid growth in the number of connected devices and volume of data associated with IoT applications [4]. It has been predicted that by 2025, 80 billion Internet of Things (IoT) devices will be connected to the Internet, and the global data traffic will reach up to 175 trillion gigabytes [71].

In simple terms, IoT is a network of physical objects such as sensors which are further embedded with software, electronics and network connectivity that allows these physical entities to collect and exchange data between them [86][38]. There are numerous applications of IoT such as routing, target tracking, monitoring homes, cities, automation, health monitoring, transportation management and environment [53].

All these applications of IoT are possible due to the deployment of sensor nodes that continuously monitor the surrounding environment and entities, collect and send sensed data according to the application requirement in IoT. IoT technologies such as Machine-to-Machine (M2M), Device-to-Device (D2D) communication complemented with intelligent data analytics are expected to drastically change landscape of various industries. Therefore, the realization of automation is fully possible without any human intervention.

The upcoming Fifth-Generation (5G) and next generation networks are expected to support these massive connectivity requirements of the IoT devices [9][28]. However, it is to be noted that these IoT devices are usually battery powered. Essentially, energy is a limited resource of eminent importance as much longer operation lifetime is expected in the next generation wireless networks such as IoT networks for self-sustainable green communications [34].

Meeting the capacity and energy demands of the IoT devices and networks is a challenge that needs to be resolved [76]. Thus, among the various challenging requirements of 5G and next-generation networks, spectral and energy efficiency are the two key requirements. Therefore, new, energy and spectral efficient protocols to ameliorate the capacity and energy demands of the massive IoT networks need to be designed. In this regard, to provide a higher data rate, higher capacity, and massive connectivity requirements of the IoT device, Non-Orthogonal Multiple Access (NOMA) has been contemplated as a promising radio access technique for the 5G and next-generation IoT networks to meet their heterogeneous capacity demands [42][19][22]. Different from conventional Orthogonal Multiple Access (OMA) schemes, the principal concept of NOMA is to assist multiple users in the same frequency band, time and code [20].

In addition, Simultaneous Wireless Information and Power Transfer (SWIPT)

has emerged as a potential technology to meet the energy demands of IoT nodes.

1.2 Non-orthogonal Multiple Access

In the OMA approach, the different MA techniques such as Frequency Division Multiple Access (FDMA), Time Division Multiple Access (TDMA) and Orthogonal Frequency Division Multiple Access (OFDMA), allow only a single user to be served under the same time/frequency resource block. In contrast to OMA approach, NOMA allows multiple users to be served under the same time/frequency/code. NOMA can primarily be classified into two categories, namely code domain NOMA and power domain NOMA. In code domain NOMA, each user is assigned a unique code-book, which is complex-valued, multidimensional and sparse in nature. A prominent code-domain NOMA technique is Sparse Code Multiple Access (SCMA) that utilizes the Message Passing Algorithm (MPA) for multi-user detection [65]. However, the complexity of the MPA increases exponentially with the number of interfering users. Moreover, in order to increase the number of users supported by code domain NOMA system, we have to increase the number of codebook patterns. However, adding new codebook patterns increases the decoding complexity and reduces the reliability of the system [7]. For more details on code domain NOMA, we refer the reader to a NOMA survey by Tao et. al [84]. In the other hand, the Long Term Evolution (LTE) standard uses a power domain NOMA method called Multi-User Superposition Transmission (MUST) [22]. Therefore, we restrict ourselves to power domain NOMA in this dissertation as it is being used by LTE standard. Specifically, in power domain NOMA, multiple user signals are superimposed in the power domain at the transmitter side, and the user signals are separated using the Signal-to-Interference Cancellation (SIC) technique at the receiver side [77].

1.2.1 Downlink NOMA

The working principle of downlink NOMA is shown in Figure 1.1. In downlink NOMA, the users with strong channel conditions decode the signals of weak users and cancel them through a SIC technique before decoding its own signal. The user with weak channel conditions treats the signals of strong users as noise when decoding its own signal. In a downlink NOMA transmission, the power allocated to a user depends on the power of the other users due to the total power constraint of the Base Station (BS) [82].

1.2.2 Uplink NOMA

The working principle of uplink NOMA is shown in Figure 1.2. In uplink NOMA, the signals of users with strong channel conditions are likely to be the strongest at the BS. Therefore, these signals are decoded first at the BS. Then, the BS applies the SIC technique to remove the signals of users with strong channel conditions to successfully decode weak user signals. The power transmitted per

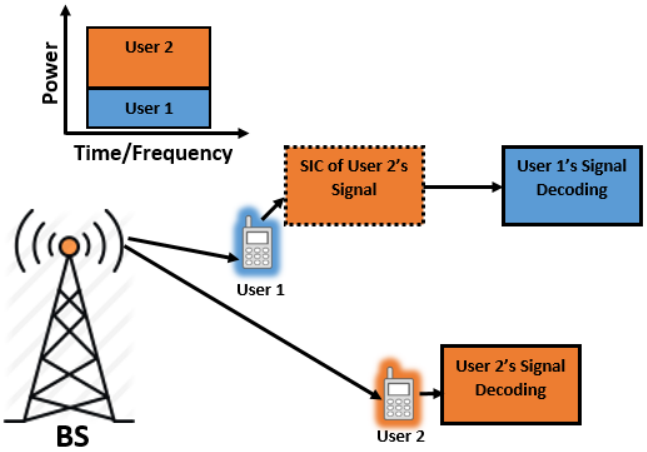

Figure 1.1: Downlink NOMA Transmission

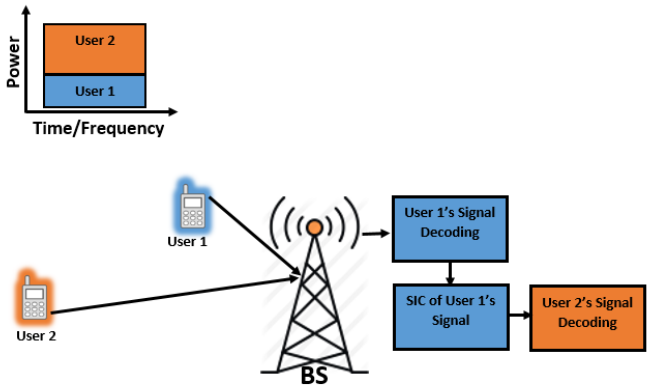

Figure 1.2: Uplink NOMA Transmission

user is restricted by the overall battery power of the user. Unlike downlink NOMA, all users can use their battery power individually to the maximum limit, as long as the channel gains of the users are sufficiently distinct [82].

1.3 Simultaneous Wireless Information and Power Transfer (SWIPT)

Sensors are the principal components that make the idea of IoT into reality. However, in IoT these sensor devices are usually battery operated, which limits

their lifetime operation. Moreover, it is difficult to replace the battery of a IoT sensor node that is deployed in a hostile or hazardous environment, like in a nuclear reactors or in toxic environments where sensors and IoT devices, such as indicators, detectors and alarms are often employed for effective operation [61]. In such areas, it is difficult to manually replace the battery of the sensor nodes or IoT devices and often it is also difficult to connect all of them through wired connections.

Moreover, cooperative communication has been widely considered to combat wireless impairments, such as fading and other environmental factors [54][70][41][31]. Also, cooperative communication can be used for extending the coverage area [106]. However, the cooperation for relaying the information comes at the cost of extra energy consumption of the relay node. This may prevent the battery operated IoT nodes or devices to take an efficacious part in relaying.

Recently, Energy Harvesting (EH) from Radio Frequency (RF) signals have emerged as a promising candidate to fulfill the energy requirements of the massive IoT sensor and devices [57][93]. The IoT sensor or devices can be recharged through EH mechanism by the directed RF signal from the source node [35]. In [51], it is shown that to charge a 5V super-capacitor utilizing RF wireless EH technology, their proposed system was able to work with a minimum input power of a 10 dBm (0.1 mW). Further, the authors in [30] demonstrated that the wireless sensor node received 3.14 mW of power through the air at a distance of 1m from a 3W source by RF EH. This amount of power is sufficient for the operation of the sensors nodes which indicates the usefulness of RF EH in wireless sensor networks [85]. The energy consumption of various components used in IoT is listed in Table 1.1.

Since RF signal carries both energy and information simultaneously, the IoT sensors or nodes can recharge themselves through RF EH and at the same time decode the information data and then relay or transmits the information of the source node to its destination [8]. Therefore, SWIPT is being considered as an energy-efficient viable approach for self-sustainable communication in IoT networks [52][90]. Due to the practical considerations of the EH circuit of the receivers, SWIPT cannot be directly applied for the EH and Information Decoding (ID) at the same time. Therefore, Power Splitting (PS) and Time Switching (TS) relaying are two popular EH architectures widely considered for SWIPT [64].

In RF energy transfer, the amount of energy that can be received by a receiver in free space can be modeled as the Friis equation, as follows [6]:

$$P_R = P_s \frac{G_T G_R \lambda^2}{(4\pi d)^2 L} \tag{1.1}$$

where P_s is the transmit power of the transmitter, P_R is the receive power of the receiver, G_T and G_R are the transmit and receive antenna gains respectively, L is the path loss factor, λ is the wavelength of the RF signal, and d is the distance between the transmit and receive antennas. Note that in Equation (1.1), it only denotes the amount of energy that can be received by a receiver in free space. However, the amount of energy or power received by a receiver in different fading

Table 1.1: Energy Consumption of Various Components Used in IoT [108]

	Component	Power/Current Consumption
Wireless Technology	Wi-Fi	835 mW
	Zigbee node	36.9 mW
	Bluetooth	215 mW
	BLE	10 mW
	Cellular	0.1-0.5 mW
	LoRa	100 mW
Typical Sensing Devices	Temperature/humidity	0.2-1 mA
	Infrared (IR) sensor	16.5 mA
	Ultrasonic	4 - 20 mA
	Light	0.65 μA
	Camera	270-585 mA
IoT node/gateway	WASP mote	9 mA
	Pi	100-500 mA
	Arduino	3.87 - 13.92 mA

channel scenario other than free space would be different as it also depends on the energy conversion efficiency of the circuits of the receiver.

The free-space model consider deterministic parameters of RF signal propagation. In a model, the randomness of signal propagation needs to be captured. A realistic probabilistic model is thus widely adopted, i.e., the Rayleigh model. For a Rayleigh fading channel, the amount of energy at a receiver is calculated as follows [66]:

$$P_R = P_{Rdet} 10^L |r|^2 \tag{1.2}$$

where P_{Rdet} is the received RF power obtained from a deterministic model, L is a path loss factor and r is a random number following a complex Gaussian distribution.

1.3.1 Power Splitting Relaying (PSR)

A basic PS relaying protocol for energy harvesting and information processing at the node is shown in Figure 1.3. In this PS relaying scheme, a power constrained node first harvests the energy from the signal of source node using εP_s, where ε is the power splitting factor, and P_s is the power of the source node transmit signal. The power constrained node uses the remaining power$(1-\varepsilon)P_s$ for the information decoding.

The harvested energy at the node can be determined by:

$$E_H^{PSR} = \eta\varepsilon|h|^2 P_s(\frac{T}{2}) \tag{1.3}$$

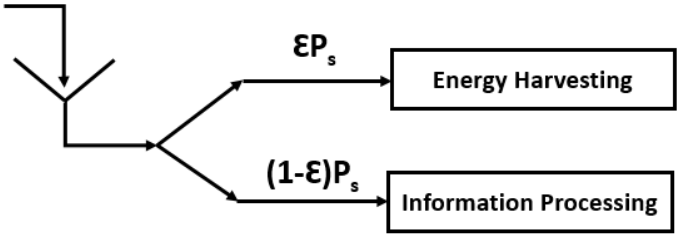

Figure 1.3: Power Splitting Relaying Architecture

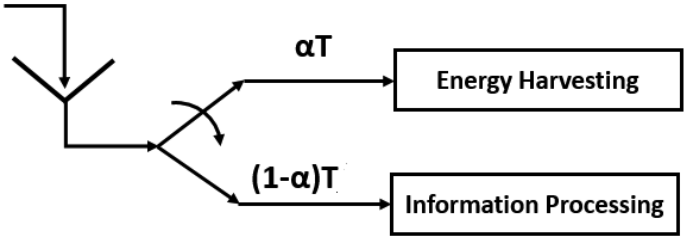

Figure 1.4: Time Switching Relaying Architecture

where $0 < \eta < 1$ denotes the EH efficiency at the energy receiver and it depends on the rectifier and EH circuitry deployed at the node. $|h|^2$ represents the channel gain between the EH node and the source node. T is the total block time.

1.3.2 Time Switching Relaying (TSR)

A basic TS relaying protocol for energy harvesting and information processing at the node is shown in Figure 1.4. In this TS relaying scheme, a power constrained node first harvests the energy from the source node signal for a duration of αT, where α is the time switching factor, and T is total time duration. The power constrained node uses the remaining time $(1-\alpha)T$ for the information decoding.
For TSR, the harvested energy at the node can be determined by:

$$E_H^{TSR} = \eta\alpha|h|^2 P_s T \tag{1.4}$$

1.4 Research Aims and Objectives

The main research aims and objectives of this dissertation is to explore and enhance spectral and energy efficiency of NOMA in the next-generation of IoT networks and to provide some new deeper insights. The focus is on a wireless communication engineering perspective. Figure 1.5 gives an overview of the

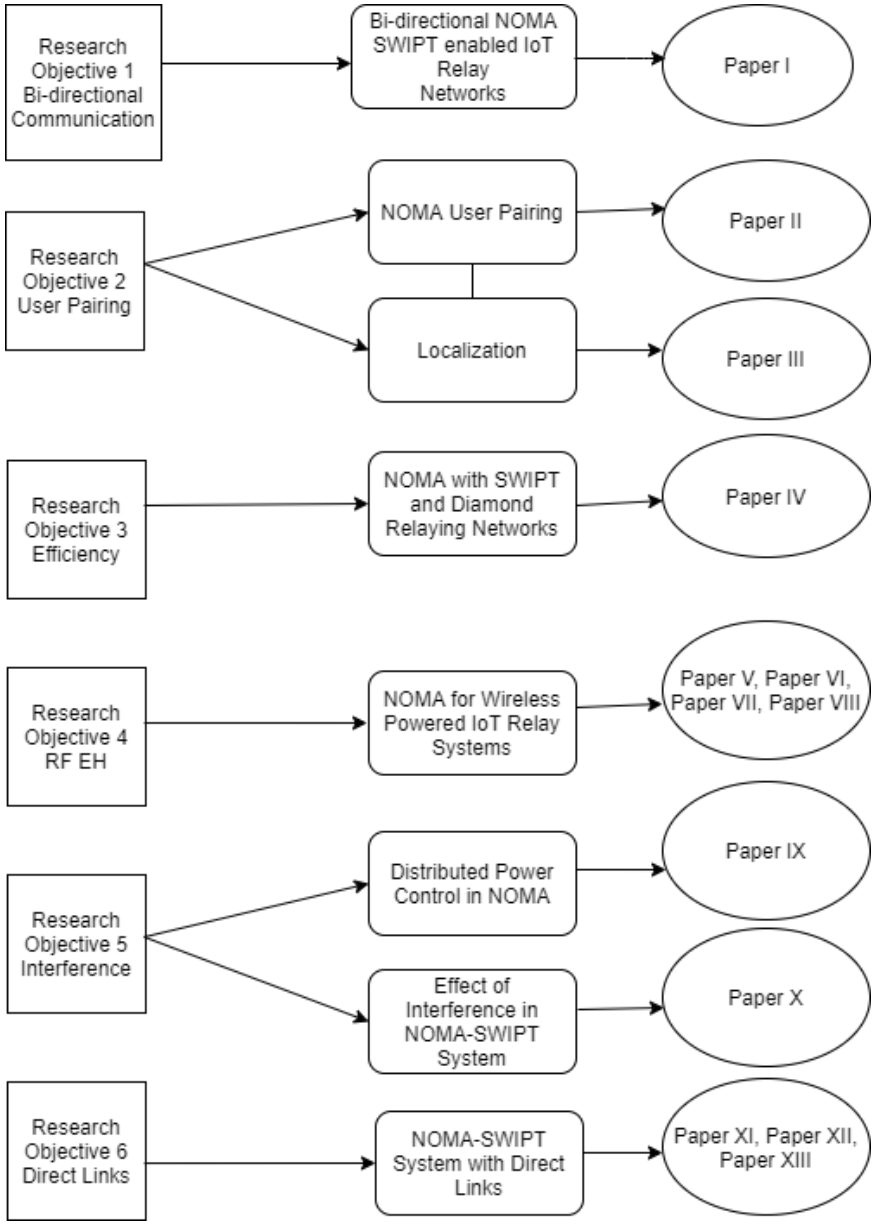

Figure 1.5: Overview of Research Objectives and Contributions with Linkage to Individual Papers in this Ph.D. Dissertation.

research objectives and contributions of this Ph.D. dissertation with linkage to the individual papers. We consider six main research aims and objectives related to the following areas:

1. **Bi-directional communication in NOMA-SWIPT systems.**
2. **User pairing issues in NOMA and localization.**
3. **Spectral and energy efficiency of NOMA with SWIPT and diamond relaying networks.**
4. **Radio frequency energy harvesting for wireless powered IoT systems.**
5. **Interference issue in NOMA and NOMA-SWIPT systems.**
6. **NOMA-SWIPT system with direct links.**

Now, to address key research aims and objective of this dissertation, we consider the following six main research questions:

1. **How bi-directional communications can be achieved in a NOMA-SWIPT enabled IoT relay networks?**
    - Due to different factors such as bad pairing between the users, hardware limitation, channel estimation, and power allocation of the paired users causes interference on the SIC process and leads to SIC imperfection on the system. We address the issue of how such imperfect SIC (ipSIC) affects the Bi-directional relaying (BR) NOMA-SWIPT system performance?
    - How uplink and downlink NOMA can be used to achieve bi-directional communications for BR NOMA-SWIPT systems?
    - To see the performance gain, the impact of node's location, user pairing, outage probability of the nodes, sum-throughput and achievable sum capacity of the BR NOMA-SWIPT system needs to be investigated. Moreover, a fair comparison of BR NOMA-SWIPT system with BR OMA-SWIPT system needs to be examined to show the performance enhancement.
2. **Since efficient user pairing between multiple users is needed to enhance the capacity of NOMA systems, how should NOMA users be paired is a key issue that needs to be investigated?**
    - For even number of nodes around the BS, what is the optimal user pairing scheme for the NOMA systems?
    - An additional problem arises when there is an odd number of nodes around the BS. In this scenario, how to accommodate the unpaired user to the already formed pairs?
    - How to find best pair of nodes to serve the unpaired node in order to improve overall sum capacity? What is the impact of perfect SIC (pSIC) and imperfect SIC (ipSIC) on the user pairing strategy and how does it affects the overall sum capacity performance?

- The location of the nodes plays an important role for user pairing and energy harvesting. Can we accurately localize the nodes by using bio-inspired algorithms that are known to converge faster and are computationally efficient? What is the performance gain in terms of average localization error of the proposed bio-inspired algorithm compared to traditional localization algorithms?

3. **How to to increase the spectral, energy efficiency and capacity enhancement of the system by combining NOMA with SWIPT and diamond relaying networks compared to OMA-SWIPT network?**

    - NOMA based Diamond Relaying (NDR) network provides an effective strategy to improve the achievable rate of the system compared to a traditional two-relay cooperative communication protocol. Moreover, a diamond network topology has been established as a standard cooperative relaying model in the 3rd Generation Partnership Project (3GPP). In short, the diamond relay network is an efficient cooperative networking configuration in which the source node cooperates with two selected neighbors.
    - Contrary to research objective 1, how downlink and then uplink NOMA can be used to achieve higher spectral, energy efficiency and capacity enhancement of the NDR-SWIPT system?
    - How NOMA power allocation factor and relay node's location affects the NDR-SWIPT system performance?

4. **Can we have a system model where an IoT relay node can be used to relay the information to the destination of the source node and at the same time transmits or offload data to its destination node? What is the effect of different EH parameters on the considered system model based on TSR and PSR architecture with NOMA for delay limited and delay tolerant transmission mode under both pSIC and ipSIC scenarios?**

    - Although a myriad of works have been carried out in the literature for EH, the absolute vast majority of those works only consider RF EH at relay node and transmission of source node data successfully to its destination node. Those approaches do not consider the data transmission of the relay node that may be an IoT node which needs to offload or transmit its data along with the source node data to their respective destinations. Thus, such approaches are clearly ineffective for energy efficient IoT relay systems.
    - The optimized TS and PS factor for the considered system needs to be examined for delay limited and delay tolerant transmission mode under both pSIC and ipSIC scenarios to have optimum performance gain.

- Furthermore, which architecture is more energy efficient needs to be explored?

5. **This research objective is dedicated to examining the distributed power control in NOMA and the effect of interference in NOMA-SWIPT systems respectively?** This research objective is sub divided into two as:

   a) Can we utilize Reinforcement Learning (RL) and Game Theory for distributed power control in multi cell downlink NOMA systems that is maximizing the achievable rate fairness of the system?

   b) Considering the interference from the external entity, can we study and extend the NOMA-SWIPT model considered in the research objective 4 and examine it under the influence of interference from an external entity?

   - Since resources are not used in an orthogonal manner in NOMA, it is important to efficiently manage interference among multiple users to maximize the system throughput or capacity. This is particularly more important in large scale networks where BSs might be densely placed to serve their associated multiple NOMA users.
   - If power control optimization is not used, the BS serving at a higher power levels to satisfy the individual achievable data rate of its associated NOMA users will create interference on the NOMA users associated with other BSs and thus jeopardize their achievable data rates.
   - Most of the power control schemes in the literature are based on scheduling, optimization techniques, heuristics, sub-carrier allocation, and power allocation techniques. These techniques may not be globally efficient and thus may result into sub-optimal solutions. Furthermore, latter techniques are usually centralized and require large message exchanges between BSs and users.
   - As BSs aspire to maximize the individual data rate of its associated NOMA users, they might act selfishly by raising their power level at the detriment of other users from other BSs which might get affected by the interference and thus fail in the SIC phase.
   - There has recently been a growing interest in examining distributed power control in wireless networks from a game-theoretical perspective. Game theory is a powerful modeling tool in many systems where the outcome of a player does not only depend on its decision or action, but also on the decisions taking by other players. On the other hand, RL would ultimately yield the optimum strategy as the learning parameter gets sufficiently small.
   - Can we model the distributed power control in downlink NOMA as a strategic game and derive the Nash Equilibrium (NE) of the game and show its convergence?

Table 1.2: Linking the Research Aims and Objectives Area With Our Included Papers

Research Aims and Objectives Area	Included Papers
1. Bi-directional Communication in NOMA-SWIPT Systems	Paper I
2. User Pairing Issues in NOMA and Localization	Paper II, Paper III
3. Efficiency of NOMA with SWIPT and NDR Network	Paper IV
4. Radio Frequency Energy Harvesting with NOMA	Paper V, Paper VI, Paper VII, Paper VIII
5 a). Power Control and Interference Issue in NOMA	Paper IX
5 b). Interference Issue in NOMA-SWIPT systems	Paper X
6. NOMA-SWIPT System with Direct Links	Paper XI, Paper XII, Paper XIII

- Usually, in the practical environment, such as IoT networks or systems are subjected to external interference factors which often results in the loss of the system rate. Considering the NOMA-SWIPT system model proposed in research objective 4, a thorough comparison with the TS and PS protocol with NOMA under the influence of interference from the external entity on the outage performance, throughput performance of the source user and IoT relay user needs to be examined. How to optimize EH parameters such as TS and PS factor to achieve higher sum-throughput of the system?

6. **Examining the impact of direct links in NOMA SWIPT systems is important as incorporating direct links could significantly enhance the performance of cooperative NOMA SWIPT systems. What is the impact of Single Signal Decoding Scheme (SDS) and Maximal Ratio Combining (MRC) scheme on the TS and PS relaying EH architecture with NOMA in the presence of direct links?**

   - To the best of our knowledge, there is no published literature that investigates the Ergodic Capacity (EC) and Ergodic Sum Capacity (ESC) of the NOMA-SWIPT aided IoT relay systems with the direct link, in which one source or BS transmits symbol to two destination nodes through the direct link and with the help of EH based relay node.
   - Further EC performance of D2D IoT relay NOMA-SWIPT systems where the relayed communication is supported with direct link needs to be examined.
   - Can a D2D user offloading scheme enhance the spectral efficiency of the system? What is the impact of single signal decoding and MRC decoding scheme on the proposed D2D IoT relay NOMA-SWIPT systems?

For a clear representation, the linking of the research areas related to the research questions of this Ph.D. dissertation with our included papers is shown in Table 1.2.

1.5 Methods Used in This Dissertation

In our work, we have favored of using mathematical techniques such as analytical modeling to analyze the performance of the various wireless system models presented in this dissertation. Using this method, we obtain useful insights that aid in designing next-generation of spectral and energy-efficient IoT networks. Moreover, we have used the Monte-Carlo simulations, based on the same physical assumptions as of the analytical derivations, to corroborate the correctness of the analytical derivations of the system model.

An advantage of analytical modeling, is that the derivations provide further insights and understanding of the workings of the system, and especially closed-form solutions can be very informative. Moreover, an asymptotic closed-form solution also provides mathematical tractability and simplified analysis. Essentially, we can extract tractable expressions that contribute to more general characterizations of results and gives intuition through the analytical modeling.

A disadvantage is that we often have to limit ourselves to look at fairly simple network setups. Studying complex networks will require other methods than analytical, like pure event-driven simulations. However, we believe that by studying simpler networking models, much of the insights gained through a mathematical techniques, such as analytical modeling, are transferable to larger systems as well. Thus, it might be helpful when analyzing the performance of wireless communication in general and provide insights that aid in designing a better wireless world.

1.6 Organization of the Dissertation

The rest of this dissertation is organized as follows.

- Chapter 2 starts with briefly introducing the state-of-the arts methods in the field of NOMA, cooperative communications and SWIPT. It also discusses the issue and shortcomings of the previous works that lead us to define our research objectives.
- In Chapter 3, we provide the summary, contributions and main results of each of the papers dealing with our research objectives and questions as explained in Chapter 1.
- Finally, Chapter 4 concludes the thesis, with a summary of main findings and contributions, and also discusses possible future works.
- In Part II, we include all our published scientific papers that are part of this Ph.D. dissertation.

Chapter 2

Related Works

NOMA has been widely studied with cooperative relaying to combat wireless impairments, such as fading and other environmental factors, to improve the system capacity and reliability of wireless networks [98][44]. However, the cooperation for relaying comes at an extra energy consumption of the relay nodes, which may be battery operated in the context of IoT, and this may prevent it from taking an active part in cooperative relaying. Due to significant Spectral Efficiency (SE) of NOMA, as compared to OMA, NOMA has also been extensively researched in combination with other technologies, such as cooperative NOMA [21] and NOMA-SWIPT [24].

This chapter briefly presents a summary of the relevant related works found in the literature for the six research objective areas that we presented in Chapter 1.

2.1 Bi-directional NOMA SWIPT enabled IoT Relay Networks

Here we summarize the most important related works for research objective 1 from our Paper I.

A two-phase cooperative relaying strategy is proposed using the concept of uplink and downlink NOMA in [47] where the authors successfully analyzed the capacity and outage probability of a dual-hop Decode-and-Forward (DF) relay-aided NOMA scheme. In downlink NOMA, the strong channel users achieve throughput gains by successively decoding and cancelling the messages of the weak channel users, prior to decoding their own signals. In the uplink NOMA, the BS successively decodes and cancels the messages of strong channel users before decoding the signals of weak channel users to enhance the throughput of weak channel users [80]. A comprehensive difference between uplink and downlink NOMA is given in [82]. A full/half duplex user relaying scheme in NOMA systems is proposed in [102] where strong NOMA users act as relays for weak NOMA users. Further, the authors in [97] proposed a novel receiver design for cooperative NOMA systems where dedicated relays are used to assist NOMA users. Among several research directions of NOMA in cooperative networks, NOMA-SWIPT is being considered as the most promising active research area by researchers for the development of next-generation wireless networks. A cooperative network where a source node communicates with two NOMA users through an EH based relay is analyzed in [99] to investigate the impact of power allocation policies in NOMA-SWIPT networks. Joint power allocation and time switching control for energy efficiency optimization in a TS-based NOMA-SWIPT system is proposed in [83]. A SWIPT-aided NOMA transmission scheme to support energy-efficient uplink NOMA transmissions, helping the

source node in receiving the signals with distinguished power levels, is proposed in [105]. However, all of these schemes are only based on a One Way Relaying (OWR) scheme where messages are relayed or transmitted only in one direction. Two-Way Relaying (TWR) or BR where two users can simultaneously exchange information through a common relay has gained much attention because of its high SE as compared to OWR [69].

Aiming to increase the SE further, NOMA and BR can be integrated together. There are already a few proposals that have successfully applied NOMA for BR, such as [17][103][46]. The algorithm to find the optimal power allocation that maximizes the user fairness and sum-rate is studied in [17] for a bidirectional cooperative NOMA in a two user scenario without full channel state information. Here, the bidirectional cooperation is considered between two NOMA users for improved decoding of the signal of the user that is not performing the SIC. A TWR-NOMA system is investigated in [103] where two groups of NOMA users can exchange the messages with the aid of one half-duplex DF relay. The authors also investigated the effect of ipSIC and pSIC on a TWR-NOMA system. With the model presented in [103], the authors in [46] proposed a similar BR-NOMA model where they studied the ergodic sum capacity and outage capacity to evaluate the performance of the system. All these models have only integrated BR in cooperative NOMA networks. Moreover, these works have ignored the impact of EH in their considered network. To the best of our knowledge, there is no existing work or contribution on BR for NOMA-SWIPT networks. The reason for combining BR and NOMA with SWIPT in cooperative networks is obvious and simple, as bidirectional NOMA improves the SE and SWIPT provides incentives to the IoT relay node through RF EH to take an active part in relaying. Therefore, in Paper I, we propose and examine in detail, the performance of BR NOMA-SWIPT system under both psIC and ipSIC scenarios. Specifically, we show how uplink and downlink NOMA can be used to achieve bi-directional communications for BR NOMA-SWIPT systems.

2.2 NOMA User Pairing and Localization

Here we summarize the most important related works for our research objective 2 from our papers - Paper II and Paper III.

An efficient user pairing strategy is needed to enhance the capacity of NOMA systems. Usually, a high capacity gain can be achieved if the two users in a cluster have a significant disparity in channel gain [112]. For an even numbers of the users around the BS, two users can form a cluster for user pairing. However, a problem arises in user pairing when there are an odd numbers of users around the BS. In such a scenario, if pairing between the two users is performed then, one user will remain unpaired.

A user pairing algorithm with SIC in a NOMA system is proposed in [109]. The authors presented the channel state sorting pairing and the user difference selecting access algorithm. However, the unpaired user is assigned resources

individually in their proposed algorithm. Furthermore, the work in [75] presents a uniform channel gain difference pairing and hybrid pairing scheme in which the cell mid users are accommodated by maintaining a relatively uniform channel gain difference between in-pair users of all pair. A fast Proportional Fairness (PF) scheduling based user pairing and a power allocation algorithm are proposed in [39]. The idea is to form user pairs around the users with the highest PF metrics with a fixed power allocation. Two user pairing algorithms based on neighbor search methods, specifically the hill climbing and the simulated annealing, are proposed in [111]. However, [75], [39] and [111] considered even number of users in their proposed algorithms. For a non-uniform distribution of users, a virtual pairing scheme in the NOMA system is proposed in [74]. The authors considered that a cell-centered user could be paired with two cell edge users provided they have similar channel gain. The authors in [60] extend the model presented in [74] to multi-user multiple inputs multiple out downlink channels. The authors in [95] proposed a user pairing strategy where the performance of a cell edge user is improved with the help of pairing with two cell center users.

These works mainly concentrated on the user pairing for downlink NOMA. There are considerably fewer published studies of user pairing in uplink NOMA. A user pairing scheme based on channel quality indicator for uplink NOMA is presented in [62]. A framework to analyze multi-cell uplink NOMA systems is presented in [81]. A user selection and power allocation for the uplink NOMA beamforming system is presented in [11]. However, all of these models considered an even number of $2N$ users in their system model. When there is an odd number of users, i.e. $2N + 1$ around the BS, we will end up with one user who will remain unpaired. Such unpaired users cannot be paired in another cluster as it will create an inter-set interference from the low/weak channel gain user. Usually, the unpaired user can be served through OMA. Using the Conventional NOMA (C-NOMA) technique, the unpaired user can be grouped together in a cluster, if two users can be paired and served through NOMA, while the other user will be served through OMA. It is obvious that the performance of the latter is better in terms of capacity as compared to using only OMA. The objective of this Paper II is to propose and analyze a scheme that will be able to serve the unpaired user by adapting it into one of the paired clusters and thereby increase the overall capacity. Moreover, finding the right cluster for the unpaired user is also important so that the overall capacity can be increased. Therefore, to address these issues, we propose and study an adaptive user pairing scheme for uplink NOMA systems under both pSIC and ipSIC scenarios.

Pairing between nodes is highly dependent on the channel conditions which in turn depends on the nodes location. Therefore, it is important to find the precise location of the IoT nodes so that the nodes can be rightly paired and performance gain of NOMA can be achieved.

An unknown IoT sensor node's location (X, Y) can be estimated if it is in the communication range of at least three anchor nodes which have a priori knowledge about their location information as (X_1, Y_1), (X_2, Y_2), (X_3, Y_3) respectively [68]. The process of localization consists of two phases namely ranging phase and estimation phase. In the ranging phase, an unknown sensor node estimate their

distance based on Received Signal Strength Identification (RSSI), Time of Arrival (TOA) of received signal, Time Difference of Arrival (TDOA) of received signal [5] etc. The results obtained during the ranging phase is affected by the noise factor and thus likely to be inaccurate [14]. In the estimation phase, the position of an unknown sensor node is calculated using the ranging information from the first phase. This can be done either by using conventional mathematical optimization algorithms such as solving a set of simultaneous equations or by using stochastic optimization algorithms that minimizes the localization error. The focus of the Paper III is on bio-inspired stochastic optimization algorithms.

Many localization algorithms have been proposed for the Wireless Sensor Network (WSN) to surmount the localization accuracy and increase lifetime of wireless sensor nodes and have been documented in the literature [67][58]. A WSN node localization based on bio-inspired Particle Swarm Optimization (PSO) has been proposed in [32][50]. However, PSO is likely to get trapped in local minima of the optimization problem. Different variants of the PSO algorithm has been widely researched and proposed in the literature. A distributed localization for WSN using Binary PSO (BPSO) is proposed in [107]. The authors showed the fast computation of the BPSO algorithm on the WSN sensor node localization process at the expense of increased localization error. A distributed localization of WSN node based on differential evolution approach is proposed in [10]. The authors demonstrated results for different scenarios delimited by walls and tested with inner obstacles to obtain a suboptimal solution. A recursive shortest path routing algorithm with it's application in WSN localization is proposed in [18]. Their proposed recursive shortest path routing algorithm is capable of estimating the shortest distance between two non-neighbouring sensors in multi-hop WSN. A localization scheme for IoT is proposed in [12]. The authors proposed scheme consists of two phases namely the partition phase and localization refinement phase. In partition phase, the target region is first divided into small grids. Then in localization refinement phase a higher accuracy of localization can be obtained by applying a compact algorithm which can easily implement two-dimensional plane localization with a regular deployment of reference nodes. An effective bio-inspired cuckoo search algorithm for sensor node localization in WSN is proposed in [13]. The author showed the effective performance of cuckoo search algorithm on reducing the average localization error and increasing the convergence rate. Bio-inspired algorithms are known to be computationally efficient algorithms and are widely used for solving optimization problems. Out of all proposed bio-inspired algorithms in the literature so far, PSO is widely chosen optimization algorithm because of its simplicity and ease of implementation. An interesting new variant of the PSO algorithm inspired from social behaviour found in animals, which they called 'SL-PSO' is proposed in [15]. The authors showed the superior performance of the 'SL-PSO' algorithm in solving scalable optimization problems. This 'SL-PSO' algorithm serves as the basis for our proposed distributed localization algorithm in IoT in Paper III. We first surveyed the bio-inspired algorithms, such as PSO and its variants - BPSO and Modified BPSO algorithm, to tackle the distributed localization issue in IoT. We then formulate and propose a new distributed Social Learning based Particle Swarm

Optimization (SL-PSO) localization algorithm to find the precise location of the IoT nodes and show its superiority over PSO and its variants in terms of average localization error and computation time.

2.3 NOMA with SWIPT and Diamond Relaying Networks

Here we summarize the most important related works for our research objective 3 from our Paper IV.

NOMA based diamond relaying network was first proposed in [94], provides an effective strategy to improve the achievable rate of the system compared to a traditional two-relay cooperative communication protocol. Here two relay nodes assist the source node in transmitting its data to a destination node. A protocol for NDR networks is investigated, and the joint power allocation problem is examined in [40]. Further, a full duplex NDR network is proposed in [89]. The authors studied the ESC performance of the system under ipSIC. All of these works did not examine the impact of SWIPT on the NDR networks. Moreover, there is not much work investigated on the NDR networks. The reason for combining NDR networks with SWIPT is obvious. Since, NDR is an effective strategy to improve the system's achievable rate, integrating NDR networks with SWIPT will further provide incentives to the relay nodes to take an active part in relaying and thereby enhancing the energy efficiency of the system. Note that such a network topology considered in our proposed Paper IV has been established as a standard cooperative relaying model in the 3rd Generation Partnership Project (3GPP) [2]. Contrary to research objective 1, in Paper IV, we show how downlink and then uplink NOMA can be used to achieve higher spectral, energy efficiency and capacity enhancement of the NOMA-NDR SWIPT system.

2.4 NOMA for Wireless Powered IoT Relay Systems

Here we summarize the most important related works for our research objective 4 from our papers - Paper V, Paper VI, Paper VII and Paper VIII.

RF EH is considered as an appealing solution in extending the lifetime of these IoT sensors and devices from months to years and even decades, that ultimately enable their self-sustaining operations [59]. In wireless communication systems, SWIPT is another emerging paradigm that allows the wireless nodes to recharge themselves through RF signals directed to them from the source node and then relaying or transmitting the information [110].

Nasir *et al.* studied Amplify-and-Forward (AF) relaying network based on TS and PS relaying schemes [63]. They derived the analytical expressions for outage probability and the ergodic capacity for delay-limited and delay tolerant transmission modes. Du *et al.* investigated outage analysis of multi-user cooperative transmission network with TS and PS relay receiver architectures [26]. They theoretically analyze the system outage probability based on TS and PS relaying protocols. A cooperative SWIPT NOMA protocol is studied in [56].

Here, near NOMA users that are close to source node acted as a EH based relay to help far NOMA users. Considering user selection schemes, they derived the closed-form expressions for the outage probability and system throughput. Ha *et al.* [36] studied the outage performance of EH based DF relaying NOMA networks by deriving the closed form equation of the outage probability. Two copies of same information from the source node direct link and EH based relay link were received at the destination nodes. Kader *et al.* [45] studied TS and PS with EH and NOMA in a spectrum sharing environment. The secondary transmitter acts as an EH based relay and then transmits the primary transmitter data along with its data using NOMA protocol. Jain *et al.* [43] also proposed an EH-based spectrum sharing protocol for wireless sensor networks. However, although a myriad of such EH works have been carried out in the literature, EH considering the energy-efficient data transmission of source and IoT relay node together based on TS, PS and NOMA suitable for IoT relay systems has not been considered in the previous works. This motivated us to propose an RF EH and information transmission based on TS, PS and NOMA for IoT relay systems and analyze their performance by deriving the analytical expressions for outage probability, throughput and sum-throughput in delay-limited transmission mode in Paper V, Paper VI, and Paper VII.

Moreover, in delay-limited transmission mode, the system throughput is limited by a fixed rate. However, for the delay tolerant transmission mode, the source transmits at any constant rate upper bounded by the EC [114]. Zaidi *et al.* [104] evaluated the ergodic rate in SWIPT-aided hybrid NOMA in which the users transmits on the uplink by utilizing the harvested energy on the downlink. Considering the EC as a fundamental performance indicator, in Paper VIII, we investigated the ESC analysis of the NOMA-SWIPT enabled IoT relay systems in delay tolerant transmission mode under the both pSIC and ipSIC scenarios.

2.5 Distributed Power Control in NOMA and Effect of Interference in NOMA-SWIPT System

Here we summarize the most important related works for our research objective 5 from our papers Paper IX, and Paper X.

Since resources are not used in an orthogonal manner in NOMA, it is important to efficiently manage interference among multiple users to maximize the system throughput or capacity. Most of the power control schemes in the literature are based on scheduling, optimization techniques, heuristics, sub-carrier allocation, and power allocation techniques. These techniques may not be globally efficient and thus may result into sub-optimal solutions. Furthermore, latter techniques are usually centralized and require large message exchanges between BSs and users. As BSs aspire to maximize the individual data rate of its associated NOMA users, they might act selfishly by raising their power level at the detriment of other users from other BSs which might get affected by the interference and thus fail in the SIC phase. There has recently been a growing interest in examining distributed power control in wireless networks

from a game-theoretical perspective. Game theory is a powerful modeling tool in many systems where the outcome of a player does not only depend on its decision or action, but also on the decisions taking by other players. Rational users make calculated decisions to achieve maximise their pay-off functions. On the other hand, some RL strategies, such as Learning Automata (LA) [101], would ultimately yield the optimum strategy as the learning parameter gets sufficiently small [73, 91, 100]. LA is one of the simplest and yet efficient RL schemes that are shown to reach NE in a large set of games [73]. Therefore, in Paper IX, we explore if can utilize RL and game theory for distributed power control in multi cell downlink NOMA systems that is maximizing the achievable rate fairness of the system.

Fu et al. studied distributed downlink power control for the NOMA system with two interfering cells [29]. The authors formulated the distributed downlink power control mathematically as an optimization problem that aimed to minimize the total transmit power of the two BSs. Similarly, Sung et al. investigated game theoretic analysis of uplink power control with two interfering cells for the uplink NOMA systems [79]. Furthermore, a game-theoretic approach is studied in [16] where NOMA is applied to ALOHA for deciding the transmission probability. Based on the Glicksberg game, Aldebes et al. proposed a power allocation algorithm for cellular downlink NOMA networks [3]. In particular, for the power allocation algorithm, the authors proposed a price-based user's utility function, which is shown to be restrictive if the allocated power beyond a threshold value causes a decrease in the utility value. In [88], a joint utility-based power control via S-modular theory in multi-service wireless networks is addressed. A RL-based power control scheme for downlink NOMA in the presence of smart jamming is studied in [96], where the authors formulated a Stackelberg equilibrium of the antijamming NOMA transmission game. A power control based on evolutionary game theory for uplink NOMA systems is examined in [72]. A power allocation based on optimization and deep reinforcement learning approach for cache-aided NOMA systems is proposed in [25]. Moreover for a hybrid NOMA systems, a joint channel selection and power control based on game theory is proposed in [87]. Although a lot of work for power allocation for NOMA and wireless networks based on game theory has been carried out in the literature, some interesting questions still remain to be answered. How to optimize distributed power control, especially for multicell NOMA networks where multiple BSs compete with each other based on the fairness of achievable data rate among its users so as to achieve overall system fairness for the downlink NOMA systems. Therefore, in Paper IX, we propose distributed power control in a multicell downlink NOMA system based on the joint application of RL and game theory.

In the practical environment, IoT networks or systems are subjected to the external interference factors which often results in the loss of the system rate [92]. An interference aided energy harvesting model is proposed for cooperative relaying systems in [33]. The author studied the TS and PS relaying scheme where the relay harvests the energy from the source RF signal and co-channel interference and then transmit the information to the destination node. The authors investigated their scheme on the three terminal model namely source-

relay-destination. The authors in [27] studied three relaying protocols, the TSR protocol, the PSR protocol and hybrid TSR-PSR protocol in the presence of an interfering signal. The authors derived the analytical expressions for the outage probability and throughput for the aforementioned three protocols. However, the investigated model was limited to three terminal model-source-relay-destination with the interfering signal. The authors in [23] investigated the performance of dual-hop AF relaying networks under the impact of co-channel interference at the two source nodes and the EH based relay node. The authors derived the closed-form expressions for outage probability and Bit Error Ratio (BER) to analyze the system performance. In our previous Paper VII, we proposed and investigated RF energy harvesting and information transmission based on NOMA for Wireless Powered IoT relay systems. However, no interference constraint was considered in our work in Paper VII. In the practical environment, external interference factors often results in the loss of the system rate [92]. Therefore, it is important to study the effect of interference on the system. Hence, we extend our work presented in Paper VII by introducing the interfering signal in our system model. We investigate the performance analysis of RF EH and information transmission based on TS, PS and NOMA for IoT relay systems and study the effect of interference in proposed NOMA-SWIPT system in Paper X.

2.6 NOMA-SWIPT System with Direct Links

Here we summarize the most important related works for our research objective 6 from our papers Paper XI, Paper XII and Paper XIII.

In cooperative communications research, a general assumption is often that a direct link to the node is not available, and the communication of data is only possible through relaying. However, in wireless communication it is known that when direct links between the BS and the users exist and are non-negligible, consolidating direct links could significantly enhance the performance of the cooperative relaying systems [48],[49]. The performance analysis of the SWIPT relaying network in the presence of a direct link is carried out in [113]. The authors analyzed the optimal throughput performance by considering a simple system model with a source node, a relay node, and a destination node in the presence of a direct link. A DF relay is analyzed in [55] for a cooperative NOMA system with direct links. Although three different relay schemes are analyzed by the authors, EH is not considered in their system model. Analyzing and studying the impact of EH in the cooperative NOMA-SWIPT systems is important for increasing the spectral and energy-efficiency demands of IoT networks. The spectral and energy efficiency of the next generation IoT networks is possible through the combined approach of NOMA with SWIPT. Thus, the authors in [37] studied the outage probability of a NOMA-SWIPT network in the presence of direct links. However, the authors only studied and analyzed the outage probability for the NOMA-SWIPT network with the direct link, while the EC and ESC were not studied. Motivated by the works in [55] and [37] and taking the EC as a fundamental performance indicator, in this paper, we investigate

the EC performance of cooperative NOMA-SWIPT aided IoT relay systems in which one BS sends two symbols to two users UE_1 and UE_2 through the direct link and via an EH based relay node in papers - Paper XI and Paper XII and show the impact of SDS and MRC decoding scheme on the considered system model with direct links.

In Paper XIII, we consider a two-user case where a BS transmits symbols to two NOMA users and to the EH based relay node via a direct link. The PS EH based relay node harvests the energy from the BS's signal and again transmits a superimposed composite NOMA signal intended for the user with poor channel condition and for its D2D user. The reason we have considered a D2D user in the considered system is to assist the EH based relay node for offloading its data traffic and thereby further enhancing the spectral efficiency of the considered system.

Chapter 3

Summary, Contributions and Main Results of Papers

In this chapter, we give a brief summary and contributions of the included papers in the dissertation. We also highlight some important results from each of the papers.

3.1 Paper I: Summary, Contributions and Main Results

Summary

Paper I demonstrates how bi-directional communications can be achieved in a NOMA-SWIPT enabled IoT relay networks. To the best of our knowledge, there is no existing study or research on BR NOMA with SWIPT. A scenario consisting of multiple NOMA users in one group that can communicate or exchange information with multiple NOMA users in another group through a common energy harvesting based relay is examined. The EH based relay exploits the RF energy supplied by the two NOMA user groups to recharge itself, and then it exchanges the information between them. Specifically, the two groups of NOMA users transmit the information intended for the exchange to the relay node using the uplink NOMA protocol. The relay node first harvests the RF energy through the signals of the two group of NOMA users, and then it carries out the exchange of information between two NOMA user groups by using the downlink NOMA protocol to achieve energy-efficient bi-directional communication in the system. We also study the effect of both pSIC and ipSIC on the proposed BR NOMA-SWIPT system. Analytical expressions for the outage probability, EC and ESC are mathematically derived. The analytical results of our proposed system model are validated by the simulation results, and representative performance comparisons are presented thoroughly. The results provide practical insights into the effect of different system parameters on the overall network performance. It also demonstrates that our proposed BR NOMA-SWIPT can attain significant throughput and capacity gains as compared to conventional BR multiple access schemes.

Contributions

As pointed out in Section 2.1, most of the previous works have ignored the impact of EH in their considered network. To the best of our knowledge, there is no existing work or contribution on BR for NOMA-SWIPT networks. The reason for combining BR and NOMA with SWIPT in cooperative networks

is obvious and simple, as bidirectional NOMA improves the SE and SWIPT provides incentives to the IoT relay node through RF EH to take an active part in relaying. Therefore, in Paper I, we propose and examine in detail, the performance of BR NOMA-SWIPT system under both psIC and ipSIC scenarios. Specifically, we show how uplink and downlink NOMA can be used to achieve bi-directional communications for BR NOMA-SWIPT systems.

The major contributions of Paper I can be summarized as:

- To the best of our knowledge, this is one of the first study or research on BR NOMA with SWIPT.
- We propose and examine in detail, the performance of BR NOMA-SWIPT enabled IoT relay networks where users in one NOMA group can exchange information with other users in another NOMA group with the help of an energy harvesting based relay node R to achieve bi-directional communication.
- The outage probability, throughput, and ergodic capacity of each user and the sum-throughput and ergodic sum capacity of the proposed system are analytically derived under the both pSIC and ipSIC scenarios.
- For a fair comparison and benchmarking of our results, we devise and investigate the TWR/BR-OMA SWIPT system considering TDMA and compare it with our proposed system model. This demonstrates the significant improvement in the throughput and ergodic capacity of our BR NOMA-SWIPT system.
- We also study the effect of user pairing for the exchange of information in different groups and show the sum capacity enhancement of the BR NOMA-SWIPT system.
- We provide thorough practical insights into the effect of different system parameters on the overall network performance. We also show that our derived analytical results match exactly with the simulation results, to demonstrate that our analytical derivations are correct.

Main Results

The proposed BR NOMA-SWIPT system model scenario is shown in Figure 3.1. There are two NOMA users in each group, S and D i.e., S_1 and S_2 are NOMA users in group S, and D_1 and D_2 are NOMA users in group D, which can exchange information and communicate via the bidirectional IoT relay node R. Both group S and D works on a channel that is orthogonal to each other.

Figure 3.2 shows the effect of user pairing on the performance of sum capacity maximization of the proposed BR NOMA-SWIPT system of Paper I at time switching factor $\alpha = 0.5$. We consider the user pairing case where a NOMA user in group S with good channel condition i.e., S_1 exchanges information with another NOMA user in group D with good channel condition of group

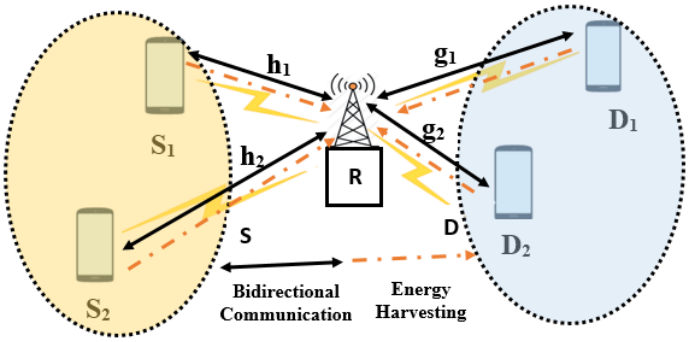

Figure 3.1: Proposed BR NOMA-SWIPT System Model of Paper I

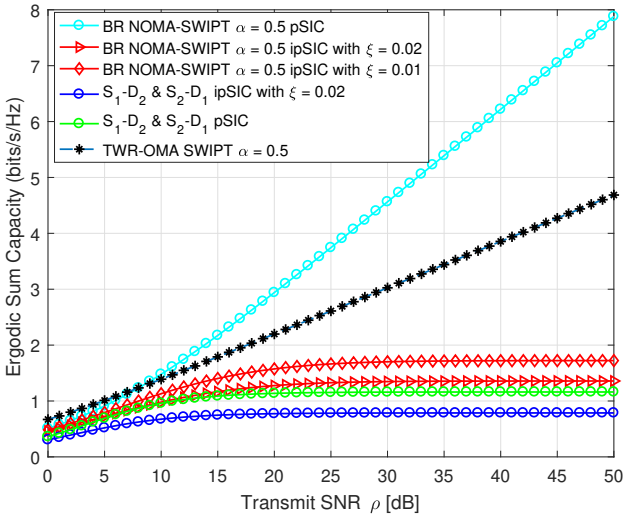

Figure 3.2: Ergodic Sum Capacity Comparison of the BR NOMA-SWIPT System with Different User Pairing

D i.e., D_2 and a NOMA user in group S with poor channel condition i.e., S_2 exchanges information with the NOMA user in group D with poor channel condition i.e., D_1 with the help of the EH based relay R. We see that the ergodic sum capacity of such a system is greatly affected when such user pairing is done, and the performance is severely degraded compared to our proposed BR NOMA-SWIPT and TWR-OMA SWIPT system. This is because SIC is performed on different NOMA users during the uplink and downlink, and hence a user will not gain the appropriate benefits of SIC and cooperative diversity. For our proposed BR NOMA-SWIPT system, SIC is performed on the same user during the uplink and downlink so that the sum capacity is maximized.

This indicates that the user pairing has significant impact on the capacity enhancement of the system. Also, in Figure 3.2, we observe that as SIC factor ξ decreases from 0.02 to 0.01, the ergodic sum capacity of the BR NOMA-SWIPT system is improved. This specifies that with the use of a better SIC technique, a significant improvement of the ergodic sum capacity can be achieved.

3.2 Paper II: Summary, Contributions and Main Results

Summary

Paper II shows a new and exciting result about an adaptive user pairing strategy for uplink NOMA systems. As pointed out in Paper I, an efficient user pairing between multiple users is needed to enhance the capacity of NOMA systems. This paper investigates and proposes a new user pairing strategy that enhances the capacities of a cell for uplink NOMA systems. In general, NOMA separates nodes into two equally-sized groups where half of nodes with the best channel conditions are allocated to one group, while the other half of nodes are allocated to the other group. Then, NOMA pairs each node in one group with another node in the other group. First, we investigate an efficient pairing scheme that maximizes the sum capacity for the uplink NOMA system, with an even number of nodes, i.e. when there is an equal number of cellular users in each group. An additional problem arises when there is an odd number of nodes, and the number of users in one group is thus one larger than in the other, leaving one node potentially unpaired. Instead of using regular OMA for the unpaired node, we propose an efficient adaptive user pairing strategy where the unpaired node is allowed to pair with one of the other pairs, forming a cluster of three nodes. The objective of our proposed scheme is to find the best pair of nodes to serve the unpaired node in order to increase the overall sum capacity. Moreover, the impact of perfect and imperfect SIC is studied on the user pairing strategy for uplink NOMA systems. Numerical results verify the effectiveness of our proposed adaptive user pairing strategy over the user pairing scheme utilizing conventional NOMA and OMA schemes.

Contributions

As pointed out in Section 2.2, there are considerably fewer published studies of user pairing in uplink NOMA. When there is an odd number of users around the BS, we will end up with one user who will remain unpaired. Usually, the unpaired user can be served through OMA. Using the conventional NOMA technique, the unpaired user can be grouped together in a cluster, if two users can be paired and served through NOMA, while the other user will be served through OMA. It is obvious that the performance of the latter is better in terms of capacity as compared to using only OMA. The objective of this Paper II is to propose and analyze a scheme that will be able to serve the unpaired user by adapting it into

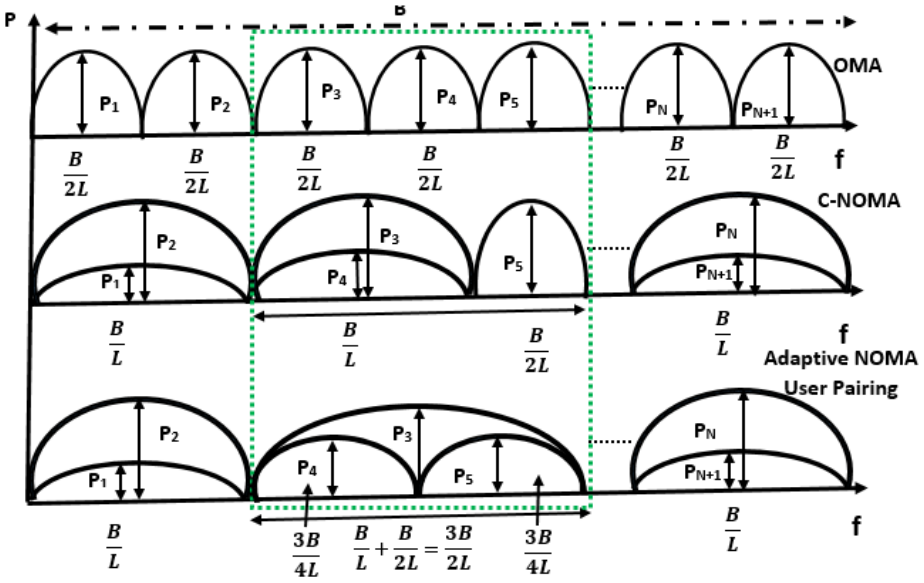

Figure 3.3: Conventional OMA, NOMA and Proposed Adaptive User Pairing Scheme

one of the paired clusters and thereby increase the overall capacity. Moreover, finding the right cluster for the unpaired user is also important so that the overall capacity can be increased. Therefore, to address these issues, we propose and study an adaptive user pairing scheme for uplink NOMA systems under both pSIC and ipSIC scenarios.

The principal contributions of Paper II are as follows:

- First, a fundamental study of user pairing strategy that enhances the capacities of a cell for uplink NOMA is investigated for even numbers of users around the BS.

- Then for uneven distribution of users around the BS, an efficient Adaptive user pairing strategy for uplink NOMA systems is proposed in order to accommodate the unpaired user into the formed clusters. Our proposed scheme finds the right paired cluster to serve the unpaired user by accommodating it so as to increase the overall sum capacity.

- We also study the effect of perfect SIC and imperfect SIC on the proposed Adaptive user pairing strategy for uplink NOMA systems.

- We demonstrate the effectiveness of our proposed Adaptive user pairing strategy over the user pairing scheme using conventional NOMA and OMA schemes.

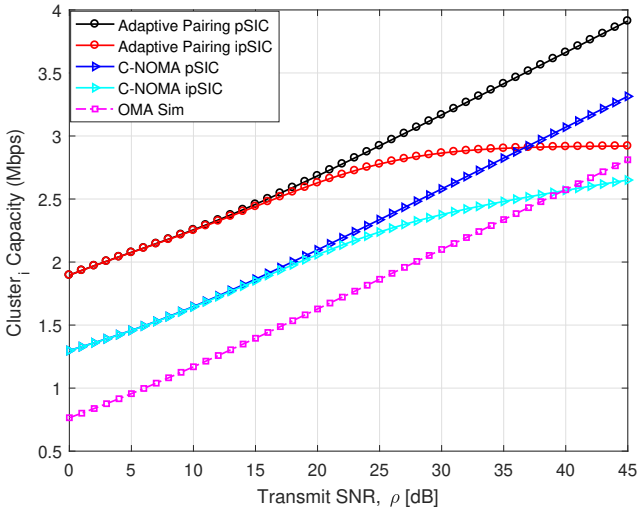

Figure 3.4: Cluster$_i$ Sum Capacity

Main Results

The conventional OMA, NOMA and the proposed Adaptive user pairing scheme is shown in Figure 3.3. We named our scheme as an Adaptive user pairing scheme as in our scheme, the paired cluster is able to adapt or accommodate the unpaired user and hence forming a three user cluster from the two user cluster.

The cluster$_i$ sum capacities for three user cluster when $N = 21$ as found through our Adaptive user pairing scheme is shown in Figure 3.4. The difference in the overall $cluster_i$ sum capacity for the Adaptive user pairing scheme, C-NOMA, and OMA scheme is clearly visible against all transmit SNR (ρ) values. Since our proposed adaptive user pairing approach aims to find a suitable cluster to accommodate the unpaired user with the paired user, the sum capacity of $cluster_i$ is significant, which can contribute to the improvement of overall sum capacity for our proposed Adaptive user pairing scheme. Also, since SIC imperfection leads to capacity degradation, we can see that the cell capacities for OMA actually exceed the cell capacities for ipSIC C-NOMA for ρ greater than 40 dB. However, even the cell capacities for ipSIC of our proposed adaptive user pairing scheme remains higher than the OMA which indicates the performance gain of our proposed user pairing scheme.

3.3 Paper III: Summary, Contributions and Main Results

Summary

Paper III focuses on the issue of distributed localization in the IoT. There are numerous applications of IoT such as routing, target tracking, monitoring homes, cities, automation, health monitoring, transportation management and environment. All these applications of IoT are possible due to the deployment of sensor nodes which continuously monitor the surrounding environment and entities. Accurate localization of sensor nodes is the prerequisite to run these emerging applications of IoT as it is staggeringly difficult to differentiate sensed data and employ sensing information of the nodes without location information. Besides, accurate localization of sensor nodes also help to tackle problem such as geographic routing, energy harvesting,intrusion detection, traffic monitoring and so on. However, accurate localization of deployed sensors nodes is a classical optimization problem which falls under NP-hard class of problems. Therefore, in this paper, we propose and study a new distributed localization algorithm inspired from nature which we call as Social Learning based Particle Swarm Optimization (SL-PSO) for IoT. Experimental results depicts that a precise localization of deployed IoT sensors nodes can be achieved with reduced computational complexity that will further enhance the lifetime of these resource constrained IoT sensor nodes. Experimental results demonstrate that SL-PSO algorithm can not only increase convergence rate but also significantly reduce average localization error compared to traditional PSO and its other variants.

Contributions

Pairing between nodes is highly dependent on the channel conditions which in turn depends on the nodes location. Therefore, it is important to find the precise location of the IoT nodes so that the nodes can be rightly paired and performance gain of NOMA can be achieved. As discussed in Section 2.2, bio-inspired algorithms are known to be computationally efficient algorithms and are widely used for solving optimization problems. Out of all proposed bio-inspired algorithms in the literature so far, PSO is widely chosen optimization algorithm because of its simplicity and ease of implementation. Therefore, in Paper III, we formulate and propose a new distributed SL-PSO localization algorithm to find the precise location of the IoT nodes and show its superiority over PSO and its variants in terms of average localization error and computation time.

The main contribution of Paper III can be outlined as:

- We first survey the bio-inspired algorithms, such as PSO and its variants BPSO and Modified BPSO algorithm, to tackle the distributed localization issue in IoT.
- We then formulate and propose a new distributed SL-PSO localization algorithm and show its superiority over PSO and its variants.

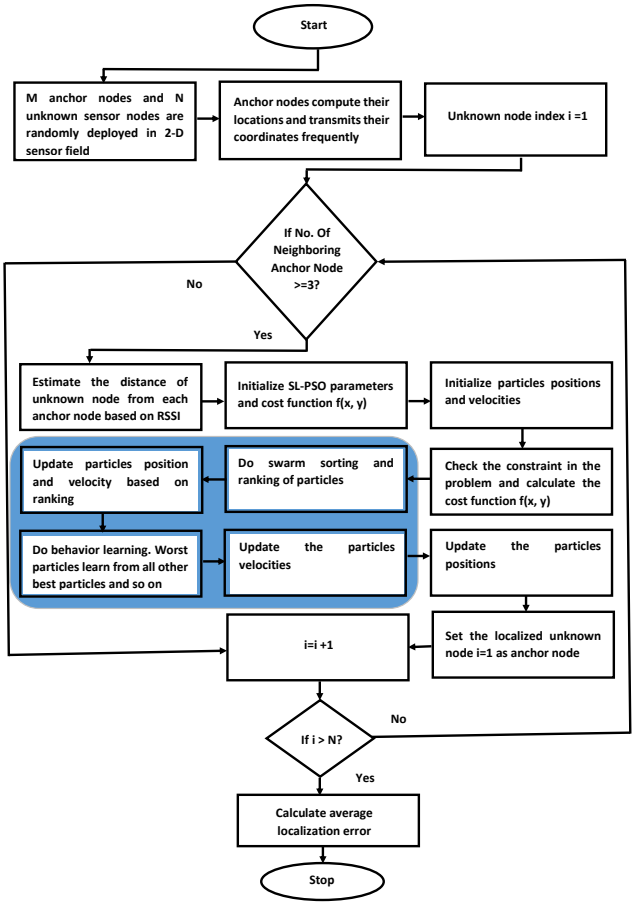

Figure 3.5: Procedural Flow of SL-PSO Algorithm for Localization

- We performed extensive simulation to verify that the SL-PSO algorithm significantly reduces average localization error and that it is computationally more efficient than PSO and its variants.

Main Results

The procedural flow of SL-PSO algorithm for localization is shown in Figure 3.5. The mean of square of localization error between the anchor nodes and unknown sensor node is formulated as the cost/objective function $f(x_n, y_n)$ which is given

Table 3.1: Comparison of Localization Error

Algorithm	Average Localization Error, E_{ALE} (m)	95% CI Lower Range, $LwrCI$ (m),	95% CI Upper Range, $UppCI$ (m)
SL-PSO	0.0024	0.0014	0.0040
PSO	0.0710	0.0674	0.0806
BPSO	0.2494	0.1684	0.3098
Modified BPSO	0.2494	0.1684	0.3098

Table 3.2: Comparison of Computation Time

Algorithm	Computation Time (s)
SL-PSO	63.63875
PSO	139.34383
BPSO	100.43645
Modified BPSO	66.65743

as:

$$f(x_n, y_n) = \frac{1}{M} \sum_{m=1}^{M} (\sqrt{(x_n - x_m)^2 + (y_n - y_m)^2} - \hat{d}_{nm})^2 \tag{3.1}$$

where $\hat{d}_{nm}$ is the measured distance of the node, $M \geq 3$ is the number of anchor nodes within communication range, an n^{th} unknown sensor node can estimate its location coordinate (x_n, y_n) by running the SL-PSO algorithm which minimizes the cost/objective function $f(x_n, y_n)$.
If (X_n, Y_n) is the actual unknown sensor node location and (x_n, y_n) is the computed location through SL-PSO algorithm then the average localization error (E_{ALE}) can be given as:

$$E_{ALE} = \frac{\sum_{n=1}^{N} \sqrt{(X_n - x_n)^2 + (Y_n - y_n)^2}}{N} \tag{3.2}$$

where N is the total number of nodes to be localized.

The E_{ALE} within Confidence Interval $(CI)_{95\%}$ range and computation time for each of these bio-inspired localization algorithms are shown in Table 3.1 and Table 3.2 respectively. From Table 3.1, we can see that the SL-PSO algorithm can significantly reduce localization error compared to PSO and its variants BPSO and Modified-BPSO. BPSO and Modified-BPSO algorithm have almost identical localization performance. Further, as shown in Table 3.2, our proposed SL-PSO algorithm takes less computation time to run the localization algorithm. It is due to the fact that the SL-PSO algorithm learns from all other better particles and also learns from the mean value of the particles in the current

swarm which helps to converge to optimized solution rapidly compared to PSO, BPSO and Modified-BPSO where the implicit learning process takes through only P_{best} and G_{best} vectors. With less computation time, our proposed SL-PSO algorithm can enhance the lifetime of these resource constrained and battery operated IoT sensor nodes.

3.4 Paper IV: Summary, Contributions and Main Results

Summary

Paper IV focuses on increasing the spectral, energy efficiency and capacity enhancement of the system by combining NOMA with SWIPT and cooperative relaying networks. In cooperative communications, NOMA based diamond relaying network, provides an effective strategy to improve the achievable rate of the system compared to a traditional two-relay cooperative communication protocol. The diamond relay network is an efficient cooperative networking configuration in which the source node cooperates with two selected neighbors. Moreover, a diamond network topology has been established as a standard cooperative relaying model in the 3GPP. Therefore, in this paper, we propose and investigate SWIPT for IoT NOMA-based diamond relay networks wherein a source node transmits two symbols to a destination node through two EH based decode-and-forward relay nodes using the principle of downlink NOMA in the first time slot. The two EH based relay nodes harvest the energy from the source's signal and then transmits the decoded symbol to the destination node using the uplink NOMA protocol in the next time slot. Analytical expressions for the achievable rate of the symbols and the achievable rate of the considered system are derived and verified with the simulation results. Moreover, an asymptotic closed-form solution for the achievable rate is also provided for mathematical tractability and simplified analysis. Our results demonstrates that significant performance gain could be achieved with our considered system model as compared to the OMA-SWIPT system. Since we exploited SWIPT for the considered system, we also found the optimal power splitting factor ϵ that can achieve optimum performance for the achievable rate of the considered system. Our results also indicate that the NOMA power allocation co-efficient plays an important role. With a proper selection of the NOMA power allocation factor and ρ, it can increase the achievable performance of the system. Finally, our results also demonstrates that the relay node R_1 node should be placed close to the source to have a higher achievable rate performance of the system.

Contributions

NOMA based diamond relaying network, provides an effective strategy to improve the achievable rate of the system compared to a traditional two-relay cooperative communication protocol. As pointed out in Section 2.3, previous works did not examine the impact of SWIPT on the NDR networks. Moreover, there is

not much work investigated on the NDR networks. The reason for combining NDR networks with SWIPT is obvious. Since, NDR is an effective strategy to improve the system's achievable rate, integrating NDR networks with SWIPT will further provide incentives to the relay nodes to take an active part in relaying and thereby enhancing the energy efficiency of the system. Note that such a network topology considered in our Paper IV has been established as a standard cooperative relaying model in the 3GPP. Contrary to research objective 1, in Paper IV, we show how downlink and then uplink NOMA can be used to achieve higher spectral, energy efficiency and capacity enhancement of the NOMA-NDR SWIPT system.

The principal contributions of Paper IV are as follows:

- We propose and investigate the achievable rate of the considered system that exploits the SWIPT for IoT NOMA based diamond relay networks, in which one source or BS transmits two symbols to the destination node via the help of two EH based relay node adopting PS architecture.
- We derive the analytical expressions for the achievable rate of the symbols and the achievable rate for the considered system model and validate it through the simulation results, which shows that our derived analytical expressions are intact.
- Moreover, asymptotic closed form solution for the achievable rate is also provided for mathematical tractability and simplified analysis.
- For a fair and logical comparison of the considered NOMA-SWIPT system, we devised the model using OMA-SWIPT and compared them.
- Our results demonstrate the effect of energy harvesting parameters, NOMA power allocation co-efficients, relays distance, and effectiveness of the considered system over the similar system model using conventional OMA-SWIPT scheme.

Main Results

Figure 3.6 shows the considered diamond relaying based NOMA-SWIPT system model, where a source node, i.e, S transmits two data symbols x_1 and x_2 to the destination node D via two EH based relaying nodes R_1 and R_2 using downlink NOMA protocol. We have assumed that there is no direct link from the source to the destination node due to deep fading or blockage. Hence, S only relies on R_1 and R_2 for transmission of data to D. We have also assumed that $h_2 < h_1$. Similarly, $g_1 < g_2$. The power-constrained relaying nodes R_1 and R_2 act as decode-and-forward EH based relay nodes. They first harvest the energy from the source node's signal using the PS protocol, and then they decode the symbols x_1 and x_2 transmitted by S in the first stage. The relay nodes R_1 and R_2 then forward the decoded symbols x_1 and x_2 using the uplink NOMA protocol to the destination node in the second stage.

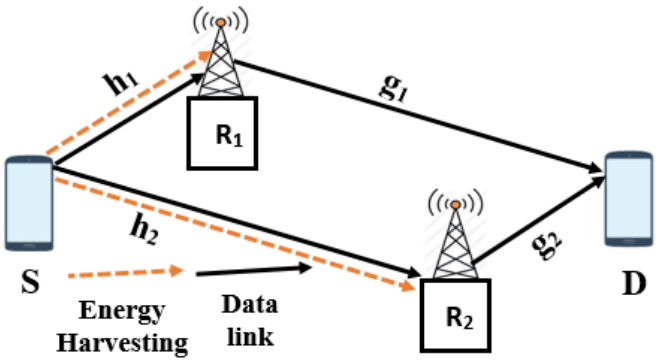

Figure 3.6: Considered Diamond Relaying based NOMA-SWIPT System Model

Figure 3.7 shows the achievable rate of the considered system and OMA-SWIPT

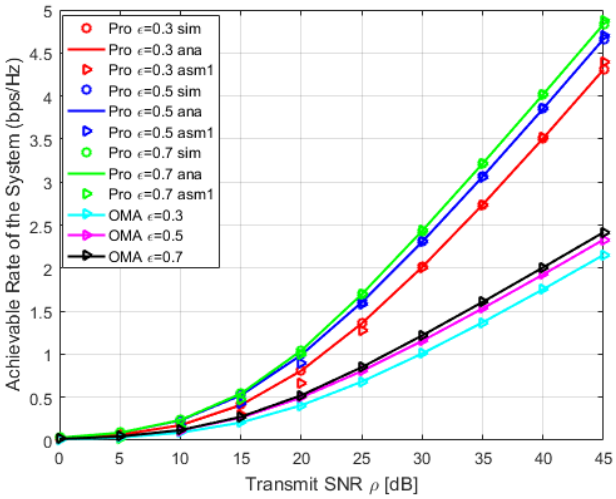

Figure 3.7: Achievable Data Rate of the Diamond Relaying based NOMA-SWIPT System

system. It should be noted that for the OMA-SWIPT system, we allocate full power for the transmission of x_1 and x_2 symbols. However, for our considered system model, the transmit power of the source node is divided between x_1 and x_2. We observe that the achievable rate for the considered system is higher than that of the OMA-SWIPT system, especially when ρ is greater than 10 dB. Also, as we increase the ϵ factor from 0.3 to 0.7, the achievable rate for both the OMA-SWIPT system and the considered system increases which indicates

that a higher power splitting factor ϵ is required to have a higher achievable rate performance.

3.5 Paper V: Summary, Contributions and Main Results

Summary

Paper V presents our system model on RF energy harvesting and information transmission where a power constrained IoT relay node first harvests the energy from the source node RF signal to power up itself using power splitting protocol and then transmits the source node information along with its information data using NOMA protocol. As opposed to conventional EH based relaying techniques, where a EH based relay node only helps the source user to transmits its data successfully, this paper also considers the data of the IoT relay user to be transmitted along with the source node data using NOMA protocol. This is particularly important for data offloading by the IoT relay node to its own D2D user or destination node. We derive the analytical expressions for the outage probability, throughput and sum-throughput for the proposed system where we corroborate our theoretical analysis with the simulation results. Effects of different EH parameters have been studied to get an insight of the considered system. It is evident that the proposed system model is feasible for ubiquitous IoT relay systems for self-sustainable energy efficient communication and data transmission.

Contributions

As pointed out in Section 2.4, unlike previous works where the participating relay node is used only to transmit source node data, in Paper V, we have also considered to transmit/offload the data of the IoT relay node along with source node data using PS and NOMA to respective destination nodes.

The major contribution of Paper V can be outlined as:

- Realizing the energy constrained nature of IoT nodes, we have considered and investigated an RF EH-based on power splitting and NOMA for IoT relay systems. Unlike several of the previous works, where the participating relay node is used only to transmit source node data, we have also considered to send the IoT relay node data along with source node data to respective destination nodes using PS and NOMA.
- We derive the analytical expressions for outage probability, throughput and sum-throughput for our considered scenario based on PS and NOMA.
- The developed analysis is corroborated through Monte-Carlo simulations that proves that our derived analysis are correct.
- Moreover, we find the optimal power splitting factor that maximizes the sum-throughput of our proposed model through iterative Golden section

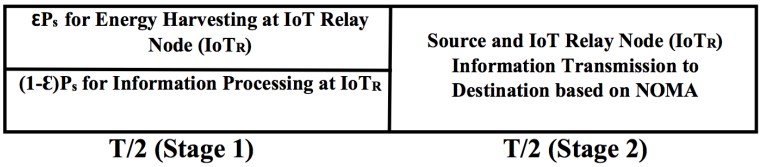

Figure 3.8: System Model based on Power Splitting and NOMA.

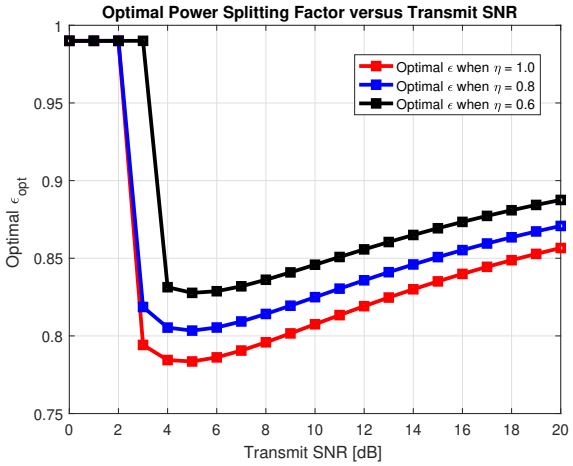

Figure 3.9: Optimal ε for Sum-throughput Maximization

search method. Also, some representative performance comparisons with different EH parameters are presented.

Main Results

The proposed system model based on PS and NOMA protocol is shown in Figure 3.8. In this PS relaying scheme, power constrained (IoT_R) node first harvests the energy from the source node signal using εP_s where P_s is the power of the source node's transmit signal and ε is the power splitting factor. IoT_R uses remaining power $(1-\epsilon)P_s$ for information decoding in the first stage. In the second stage, IoT_R node transmits the source node and IoT_R data to their respective destination nodes using NOMA.

It should be noted that higher the value of power splitting factor ε, higher is the sum-throughput. In reality, we cannot have high ε as there will be less power allocated for information decoding. Hence, there will be an outage in the system as no communication data will be transferred to the respective destinations. Therefore, we need to find optimal ε^* that maximizes the sum-throughput for the proposed system. In Figure 3.9, we found out optimal ε^* that maximizes the

sum-throughput of the proposed system through Golden section search method and plotted it against the transmit SNR. We observe that the optimal ε^* first decreases and then slightly tends to increase with the increase in transmit SNR at which the sum-throughput for the considered system using PS and NOMA is maximized.

3.6 Paper VI: Summary, Contributions and Main Results

Summary

Paper VI presents our system model on RF energy harvesting and information transmission based on TS protocol and NOMA protocol. Although a myriad of works have been carried out in the literature for EH, the absolute vast majority of those works only consider RF EH at relay node and transmission of source node data successfully to its destination node. Those approaches do not consider the data transmission of the relay node that may be an IoT node which needs to offload or transmit its data along with the source node data to their respective destinations. Thus, such approaches are clearly ineffective for energy efficient IoT relay systems. Unlike Paper V, in this paper, we rather focus on RF EH and information transmission based on TS relaying and NOMA for IoT relay systems. Analytical expressions for outage probability, throughput and sum-throughput for our proposed system have been mathematically derived. Effects of different EH parameters such as time switching factor, energy harvesting efficiency factor and transmit SNR were studied to get an insight of the considered system based on TS and NOMA.

Contributions

As pointed out in Section 2.4, previous works have not consider the data transmission of the relay node that maybe an IoT node which needs to offload or transmit its data along with the source node data to their respective destinations. Thus, such approaches are clearly ineffective for energy efficient data transmission in IoT relay systems. Therefore, in Paper VI, we propose RF EH and information transmission based on TS relaying and NOMA for IoT relay systems.

The principal contribution of Paper VI can be outlined as:

- We have proposed an RF EH-based on TS and NOMA suitable for IoT relay systems.
- Previous works and approach in this domain, have not considered the data transmission of the relay node that may be an IoT node which needs to transmit or offload its data along with the source node data to their respective destinations. In this Paper VI, we rather focus on RF EH and information transmission based on TS relaying and NOMA for IoT relay systems.

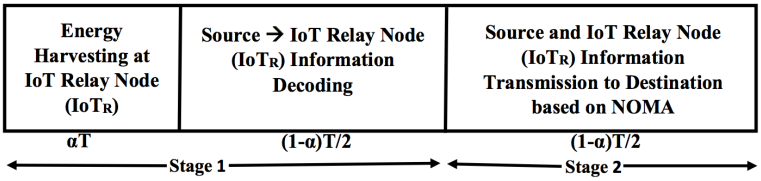

Figure 3.10: System Model based on Time Switching and NOMA.

- We derive the analytical expressions for outage probability, throughput and sum-throughput for our proposed system based on TS and NOMA.
- We also formulate an iterative algorithm-Golden section search method to find the optimal time switching factor for sum-throughput maximization.
- Our proposed system analytical results are validated by the simulation results to show that are derived analysis are correct.

Main Results

The proposed system model based on TS and NOMA is shown in Figure 3.10. In this TS relaying scheme, power constrained IoT_R node first harvests the energy from the source node's RF signal for αT duration and uses the time $\frac{(1-\alpha)T}{2}$ for information decoding in the first stage. IoT_R uses the remaining $\frac{(1-\alpha)T}{2}$ for information transmission to the source and IoT user using NOMA protocol in the second stage. Here, α is the time switching factor and T is the total time.

In Figure 3.11, we find out optimal α^* that maximizes the sum-throughput of the proposed system through Golden section search method and plot it against transmit SNR. In Figure 3.11, we can observe that optimal α^* linearly decreases with increase in transmit SNR. Finding optimal α^* is important to avoid an outage in the proposed system and maximizing the sum-throughput of the considered system based on TS and NOMA.

3.7 Paper VII: Summary, Contributions and Main Results

Summary

Paper VII is an extended version of the Paper V and Paper VI as Paper VI was chosen for the **Best Paper Award** at the 2018 28th IEEE International Telecommunication Networks and Applications Conference (ITNAC), Sydney, Australia and invited to extend the paper for the Sensors journal.

In this extended version paper, we envisioned a RF EH and information transmission system based on the TSR, PSR and NOMA which is suitable for wireless powered IoT relay systems. A thorough comparison between the TS and PS protocol with NOMA is made to show the effect of EH parameters on the

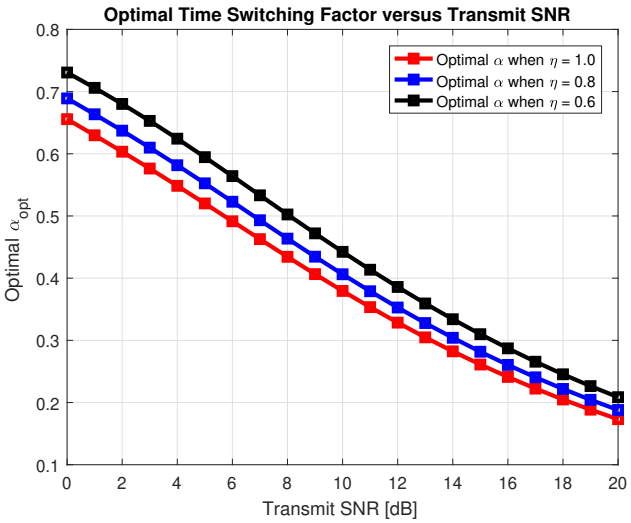

Figure 3.11: Optimal α for Sum-throughput Maximization

considered system. In reality, we cannot have a high TS and PS factors as there will be less time and power allocated for information processing. Hence, there will be an outage in the system as no communication data will be transferred to the respective destination nodes. Therefore, through Golden section search method, we found out the optimal time switching and power splitting factor that maximizes the sum-throughput of the proposed model. It is revealed that the PS with NOMA performs better at higher transmit SNR than the TS with NOMA. For a smaller values of transmit SNR, TS with NOMA performs than the PS with NOMA. Moreover, for a higher sum-throughput of the considered system, a higher PS factor is required for PS with NOMA than the corresponding TS factor for TS with NOMA.

Contributions

As mentioned above, Paper VII is an extended version of the Paper V and Paper VI. Although a myriad of works have been carried out in the literature for RF-EH, the absolute vast majority of those works only considered RF EH at the relay node and transmission of source node data successfully to its destination node. Those approaches do not consider the data transmission of the relay node that may be an IoT node which needs to transmit or offloads its data along with the source node data to their respective destinations. Therefore, in this Paper VII, we propose an RF-EH and information transmission based on the TS, PS relaying and NOMA for IoT relay systems.

The major contributions of Paper VII are as follows:

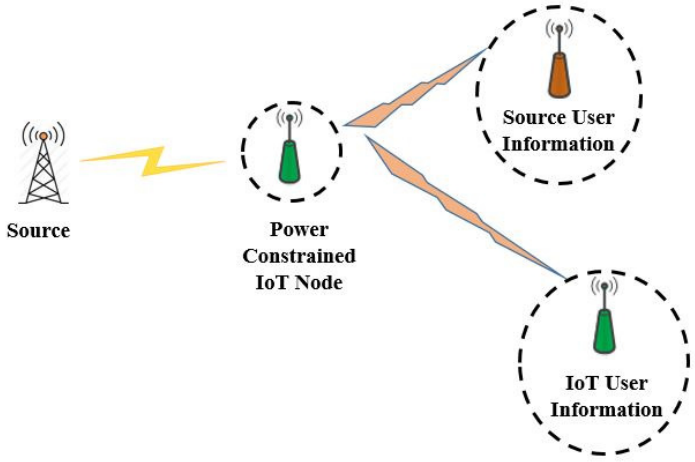

Figure 3.12: Proposed System Model Scenario

- Realizing the energy constrained nature of IoT nodes, we have considered and investigated an RF EH-based on the TS, PS and NOMA for IoT relay systems.
- We mathematically derived the analytical expressions for outage probability, throughput and sum-throughput for our proposed system based on the TS, PS relaying and NOMA.
- Our proposed system analytical results for the TS and PS with NOMA are validated by the simulation results. A thorough comparison between TS and PS with NOMA are presented. Effects of different energy harvesting parameters are also studied to get an insight of the considered system based on TS, PS relaying and NOMA.
- We also formulate an iterative algorithm - Golden section search method to find the optimal time switching and power splitting factors for sum-throughput maximization.

Main Results

We have considered a cooperative relaying EH scenario as shown in Figure 3.12, where a source has to transmit its information data to the destination. Due to fading or weak link between a source-destination pair, the source node seek the help of IoT relay node (IoT_R) for relaying its information data. Here, the source node may be an IoT node which has abundant energy supply from the other sources. Cooperative communication with single relay is a simple but effective communication scheme especially for energy constrained networks such as IoT networks [115]. Furthermore, using more than one relay increases the complexity

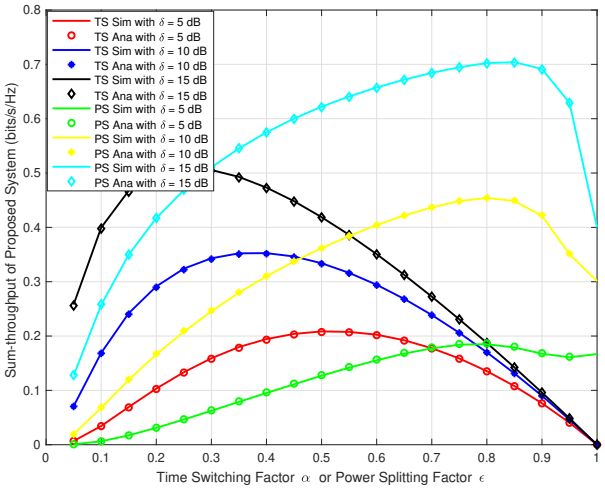

Figure 3.13: Sum-throughput of the Proposed System v/s α or ϵ with Different Transmit SNR δ.

of the systems greatly [78]. Therefore, we have considered a single IoT_R node for our system model. However, it can be extended to multiple IoT_R node scenario as well.

IoT_R is rather power constrained node that acts as a DF relay. It first harvests the RF energy from the source signal using either time switching protocol or power splitting protocol in the first stage. Then it transmits the source information data along with its own data using NOMA protocol in next subsequent stage. The dual purpose of energy harvesting and forwarding the information data is thus served by IoT_R. The receiving end for the source and IoT_R node serves as the destination for data transmission.

Figure 3.13 shows the sum-throughput of the proposed system at different time switching factor α and power splitting factor ε for both - TS and PS protocol. We plot the sum-throughput against the α and ε varying from 0 to 1 and at $\delta = 5$, 10, & 15. In Figure 3.13, we can observe that the sum-throughput first increases with the increase in α, ε, and δ, reaches to the maximum and then it decreases. This confirms that the sum-throughput is maximum at some optimal time switching factor α^* and optimal power splitting factor ε^*. In reality, we cannot have high α and ε as there will be less time and power allocated for information processing. Hence, there will be an outage in the system as no communication data will be transferred to the respective destinations.

3.8 Paper VIII: Summary, Contributions and Main Results

Summary

Paper VIII extends the works presented in Paper V, Paper VI and Paper VII and studies the ESC analysis of NOMA-SWIPT enabled IoT relay systems in delay tolerant transmission mode. In delay-limited transmission mode, the system throughput is limited by a fixed rate as seen in Paper V, Paper VI and Paper VII. However, for the delay tolerant transmission mode, the source transmits at any constant rate upper bounded by the EC. Therefore, considering the EC as a fundamental performance indicator, specifically, in this Paper VIII, we study and analyze the ESC of the NOMA-SWIPT enabled IoT relay systems in the delay tolerant transmission mode under both pSIC and ipSIC scenario. Analytical expressions for the ESC of the proposed system are derived and verified with the Monte-Carlo simulations. The impact of imperfect SIC, energy efficiency and effect of NOMA power coefficient is thoroughly examined on the ESC performance of the system. Our results demonstrate that PS relaying with NOMA is more energy-efficient than TS relaying with NOMA for the proposed system. Our results also confirmed that the SIC imperfection only affect the ESC performance and it does not show any effect on the TS or PS factors at which ESC is maximized.

Contributions

As pointed out above and in Section 2.4, in a delay-limited transmission mode, the system throughput is limited by a fixed rate. However, for the delay tolerant transmission mode, the source transmits at any constant rate upper bounded by the EC. Therefore, considering the EC as a fundamental performance indicator, in Paper VIII, we investigated the ESC analysis of the NOMA-SWIPT enabled IoT relay systems in delay tolerant transmission mode under the both pSIC and ipSIC scenarios by extending the works presented in Paper V, Paper VI and Paper VII.

The principal contribution of this Paper VIII are outlined as follows:

- We investigate and propose to use IoT node for the dual role of relaying the source node data and offloading data to its own destination based on TS and PS relaying with NOMA under both pSIC and ipSIC scenario.
- We derive the analytical expressions for the ESC of the proposed system and verified with the Monte-Carlo simulations.
- Our results demonstrate that PS relaying with NOMA is more energy-efficient than TS relaying with NOMA for the proposed system.
- Our results also confirmed that the SIC imperfection only affect the ESC performance and it does not show any effect on the α or ϵ at which ESC is maximized.

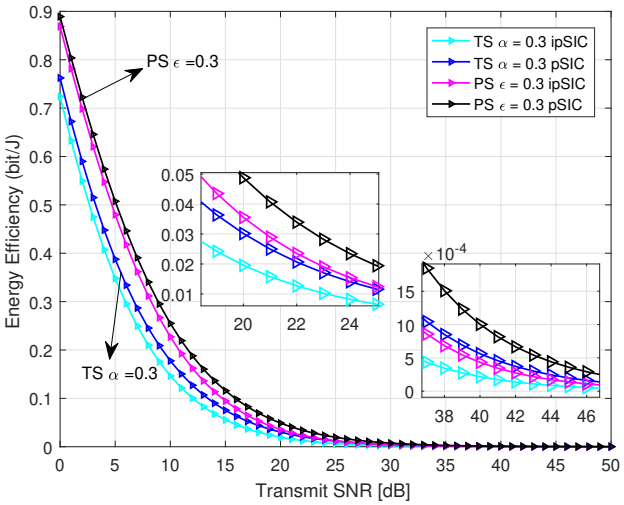

Figure 3.14: Energy Efficiency Comparison

Main Results

In Figure 3.14, we plot the Energy Efficiency (EE) of the proposed system for both TS and PS relaying with NOMA under pSIC and ipSIC scenarios. The EE can be calculated as the ratio of total achievable data rate to the total power consumption in the entire network [102]. From Figure 3.14, we can observe that PS with NOMA under both pSIC and ipSIC is more energy efficient than the TS with NOMA for the same value of EH parameters, i.e. $\alpha = 0.3$ and $\epsilon = 0.3$ especially at transmit SNR less than 25 dB. For transmit SNR greater than 35 dB, the EE performance gap of the proposed system reduces because at such high transmit SNR, the IoT_R node can harvest more energy for both TS and PS relaying with NOMA.

3.9 Paper IX: Summary, Contributions and Main Results

Summary

Paper IX proposes a simple and energy-efficient distributed power control in downlink NOMA using RL based game theoretic approach. Since resources are not used in an orthogonal manner in NOMA, it is important to efficiently manage interference among multiple users to maximize the system throughput or capacity. Moreover, NOMA is based on the principle of SIC which is known to be very fragile to interference as the decoding failure propagates in the SIC chain to weaker users. Therefore, the power must be properly allocated such

that the interfering signals can be correctly decoded and subtracted from the certain users' received signal to recover the desired signal. This is particularly more important in large scale networks where BSs might be densely placed to serve their associated multiple NOMA users. If power control optimization is not used, the BS serving at a higher power levels to satisfy the individual achievable data rate of its associated NOMA users will create interference on the NOMA users associated with other BSs and thus jeopardize their achievable data rates.

A scenario consisting of multiple BSs serving their respective Near User(s) (NU) and Far User(s) (FU) is considered. The aim of the game is to optimize the achievable rate fairness of the BSs in a distributed manner by appropriately choosing the power levels of the BSs using trials and errors. By resorting to a subtle utility choice based on the concept of marginal price costing where a BS needs to pay a virtual tax offsetting the result of the interference its presence causes for the other BS, we design a potential game that meets the latter objective. As RL scheme, we adopt Learning Automata (LA) due to its simplicity and computational efficiency and derive analytical results showing the optimality and convergence of the game to a NE. Numerical results not only demonstrate the convergence of the proposed algorithm to a desirable equilibrium maximizing the fairness, but they also demonstrate the correctness of the proposal followed by thorough comparison with random and heuristic approaches.

Contributions

As explained in Section 2.5, although a lot of work for power allocation for NOMA and wireless networks based on game theory has been carried out in the literature, some interesting questions still remain to be answered. How to optimize distributed power control, especially for multicell NOMA networks where multiple BSs compete with each other based on the fairness of achievable data rate among its users so as to achieve overall system fairness for the downlink NOMA systems. Therefore, in Paper Paper IX, we propose distributed power control in a multicell downlink NOMA system based on the joint application of RL and game theory.

The major contributions of Paper IX are as follows:

- We first formulate distributed power control in downlink NOMA as a strategic game and derive the Nash Equilibrium of the game.
- We prove that the distributed power control game we designed is an exact potential game. We then propose a LA based game-theoretic approach for distributed power control that provides a full characterization of the best achievable performance for the potential function of the game.
- We show that our proposed distributed power control algorithm that is designed as a game is guaranteed to converge to an NE.

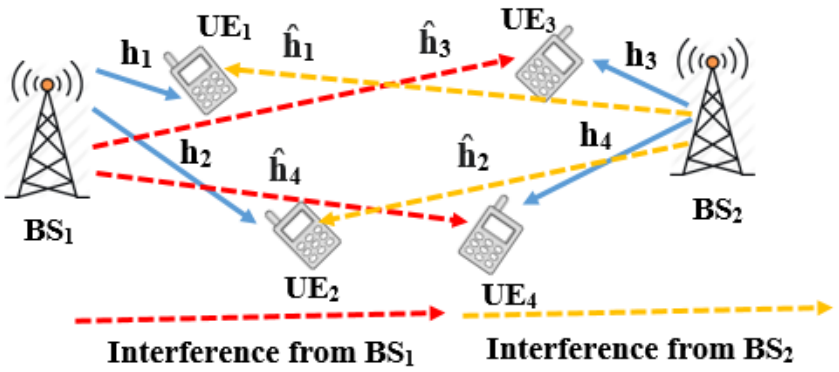

Figure 3.15: Considered System Model Scenario for RL-GT based Distributed Power Control in Downlink NOMA

- We conduct a thorough theoretical analysis that demonstrates the convergence of the proposed algorithm which is maximizing the achievable rate fairness for the respective near users and far users and thus achieving the higher energy efficiency in downlink NOMA systems.

Main Results

Our considered system model scenario for RL-GT based distributed power control in downlink NOMA is shown in Figure 3.15. For simplicity, we assume that there are two BSs (players) in the system and each of the BS is serving its associated NUs and FUs as shown in Figure 3.15. Our work generalises for more than two UEs in a straight forward manner but for the sake of simplicity we content ourselves to two UEs per BS Two UEs per frequency band has been already adopted as a standard by the 3GPP LTE under the name of MUST [1]. Please note that a BS might have a certain number of frequency bands, and thus, more pairs of users can be served in different frequency bands.

In Table 3.3, we present our findings for the overall fairness of the system with different power levels at learning parameter $\lambda = 0.1$. Also, to compensate for the randomness of the probabilities in our experiments, we run all our experiments for 100 number of times and report the average performance of the system together with 95% confidence interval. From Table 3.3, we can observe that, for learning parameter $\lambda = 0.1$, as we increase the power levels from 3 to 9 to 27, the average fairness of the system increases and the average iteration for convergence also increases. The best average fairness of the system 2.9846 is

Table 3.3: Fairness of the System When Learning Parameter $\lambda = 0.1$

Power levels K	Learning Parameter λ	Average Iteration	Average Fairness	95% CI Lower Range	95% CI Upper Range
3	0.1	244	2.9632	2.9467	2.9798
9	0.1	259	2.9770	2.9647	2.9893
27	0.1	276	2.9846	2.9740	2.9952

Table 3.4: Comparison of Fairness of the System

Learning Parameter λ	Power Levels K	Random Method	Exhaustive Method	LA-GT Method
0.1	3	2.5648	3.0195	2.9632
0.1	9	2.7537	3.0248	2.9770
0.1	27	2.8009	3.0249	2.9846

achieved when there are 27 power levels which converges at an average iteration of 276. It should be noted that even with 27 different power levels for each of the player, the average iteration for convergence is 276, which is significant compared to having just three power levels where the average iteration is 244.

In Table 3.4, we present the comparison of the fairness of the system through our LA based Game-Theoretic (LA-GT) approach with the random and exhaustive search method. Unlike our proposed method, in a random method, the players choose the actions randomly with equal probability and no active learning parameters in each iteration. We can see that, at different power levels, the fairness of the LA-GT approach is higher compared to the random method. This signifies the importance of having LA in combination with game theory to improve the fairness of the system by distributed power control over a range of players with different power levels in the system. Also, we can observe that fairness of the LA-GT approach is quite competitive compared to exhaustive search method. It should be noted that exhaustive search method is the heuristics method which finds the best solution by including all power levels. Although exhaustive method gives the best fairness of the system, it is not desirable as it is usually centralized and require large message exchanges between BSs and users. Hence, energy-efficiency of the system cannot be achieved through exhaustive search method. Our LA-GT converges much faster at just an average iteration of 244 to achieve 2.9846 average fairness of the system which is quite competitive compared to exhaustive search method and better than random method.

3.10 Paper X: Summary, Contributions and Main Results

Summary

Paper X studies the performance analysis of RF energy harvesting and information transmission based on NOMA with interfering signal for IoT relay systems. Usually, in the practical environments, IoT networks or systems are subjected to external interference factors which often results in a loss in the system rate. Specifically, in the presence on interfering signals, we study the combination of two popular energy harvesting relaying architectures - TSR and PSR with NOMA protocol for IoT relay systems. Considering the interference from the external entity, we have mathematically derived the outage probability, throughput, and sum-throughput for our proposed system. Extensive simulations are carried out to find the optimal TS and PS factor that maximizes the sum-throughput of the considered system in the presence of an interfering signal. A thorough comparison with the TS and PS protocol with NOMA revealed that the outage performance of the source user and IoT relay user is greatly affected by the interfering signal power in the system which in turn decreases the overall sum-throughput of the system. Therefore, in such interfering conditions, a careful selection of EH parameters such as TS and PS factor is envisaged to achieve higher sum-throughput of the system.

Contributions

As explained in Section 2.5, in the practical environments, IoT networks or systems are subjected to the external interference factors which often results in the loss of the system rate. Moreover, no interference constraint was considered in our work in Paper VII. We extend our work presented in Paper VII by introducing the interference in our considered system model. We investigate the performance analysis of RF EH and information transmission based on the TS, PS and NOMA for IoT relay systems and study the effect of interference in proposed system in Paper X.

The major contributions of Paper X can be outlined as:

- Considering the practical interference constraint and realizing the energy constrained nature of IoT nodes, we have considered and investigated an RF EH-based on the TS, PS and NOMA with interfering signal for IoT relay systems.
- We have mathematically derived the outage probability, throughput and sum-throughput for our considered scenario.
- Our proposed system analytical results for the TS, PS relaying and NOMA with interfering signal are validated by the simulation results. The developed analysis is corroborated through Monte-Carlo simulations to show the correctness of our derived analysis.

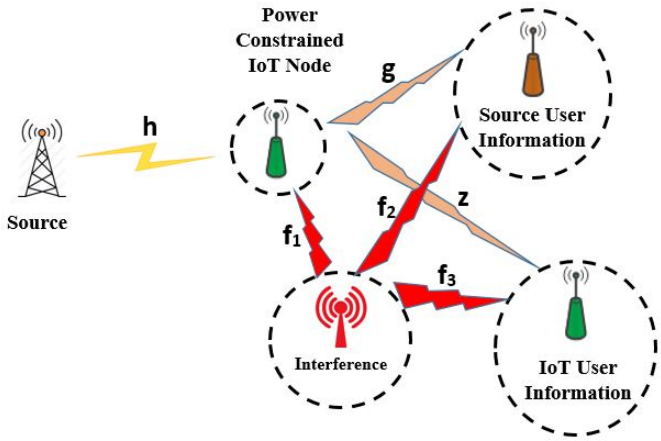

Figure 3.16: Considered System Model with Interfering Signal

- A thorough comparison with the TS and PS protocol with NOMA is made to investigate the impact of interfering signal on the outage and throughput performance of the source and the IoT relay node.

Main Results

Our considered system model is as shown in Figure 3.16. Here, a source node has to transmit its data to the destination i.e. source user information destination node in the presence of an interfering signal from the external source or entity. We have assumed that the source has abundant energy supply. It is also assumed that there are no direct links between the source user node due to deep shadowing or blockage; thus information exchange between them only relies on the relay node. Therefore, it requires the help of the IoT node (IoT_R) for relaying its information data to its intended destination. IoT_R is rather power constrained node that acts as a DF relay and it will first harvest the RF energy from the source signal using the time switching relaying or power splitting relaying protocol in the first stage and then transmits the source information data along with its own data using NOMA protocol in the next stage. Here, IoT_R harvests the energy which is used for transmitting the source user and IoT_R node data to their respective destinations. The destination pair for source and IoT_R node serves as the receiving end for data transmission. Also, in the considered system, the network is subjected to interference from the external entity (marked as red in Figure 3.16) which affects the system performance.

We plot the outage probability of the source user and IoT_R for TS and PS relaying with NOMA against the interfering signal power in Figure 3.17 and Figure 3.18 respectively at 10 dB transmit SNR, at different $\alpha = 0.3, 0.5, \&$

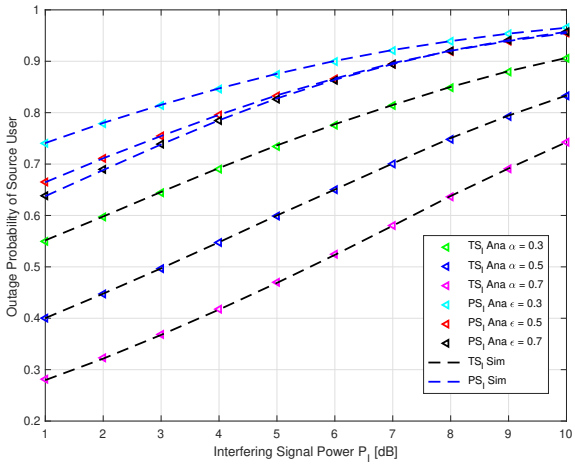

Figure 3.17: Outage probability of the Source User Under Interfering Signal

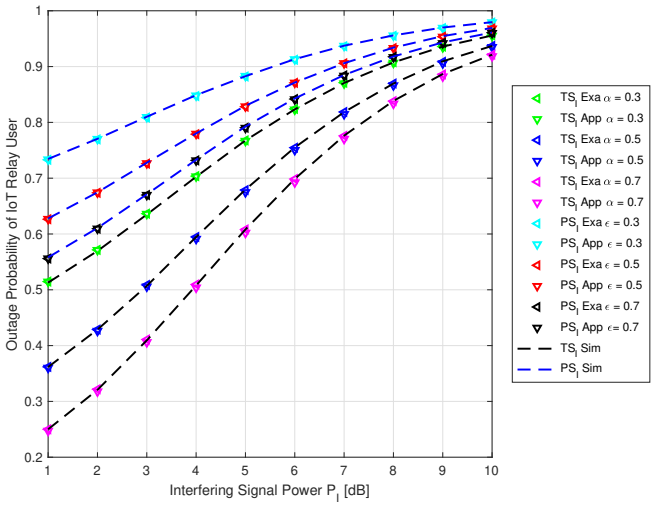

Figure 3.18: Outage probability of the IoT Relay User Under Interfering Signal

0.7 and at different $\varepsilon = 0.3, 0.5, \& 0.7$. We can see that the outage probability for both source and IoT_R is an increasing function with respect to the increase in interfering signal power. Also, the outage probability for PS relaying with NOMA is shown higher than the TS relaying with NOMA against the same amount of time switching factor $\alpha = 0.3, 0.5, \& 0.7$ and power splitting factor $\varepsilon = 0.3, 0.5, \& 0.7$. Also, it can be seen from Figure 3.17, for interfering signal power

greater than 5 dB, the outage probability of the source user for PS relaying with NOMA has almost identical performance at $\varepsilon = 0.5$, & 0.7 unlike TS relaying with NOMA. This indicate that the interfering signal power has a significant role in the outage probability of the source user for PS relaying with NOMA compared to TS relaying with NOMA.

3.11 Paper XI: Summary, Contributions and Main Results

Summary

Paper XI investigates the EC and ESC performance of cooperative NOMA-SWIPT aided IoT relay systems with direct links over the Rayleigh fading channels. To the best of our knowledge, there is no published literature that investigates the EC and ESC of the NOMA-SWIPT aided IoT relay systems with the direct link, in which one source or BS transmits symbol to two destination nodes through the direct link and with the help of EH based relay node. Specifically, we study the TSR, and PSR architecture for increasing the spectral and energy-efficiency of the considered system. Analytical expressions for the EC and the ESC are mathematically derived and validated by the simulation results. Our results provide a thorough comparison of the TS and PS relaying EH architecture for the considered system model. It also demonstrates that the ESC performance could be significantly improved through the optimal choice of the power splitting factor for PS relaying with NOMA compared to TS relaying with NOMA.

Contributions

For a delay-tolerant transmission mode, Ergodic capacity is an appropriate measure for the performance analysis of the system. As explained in Section 2.6, previous works haven't studied the EC and ESC of the system with direct links, in which one source or BS wants to transmit symbols to two destination nodes through the direct links and with the help of EH based relay node. Therefore, for the considered NOMA-SWIPT system, in Paper XI, we investigate EC and ESC for TSR, and PSR relaying architecture with NOMA in the presence of direct links.

The principle contributions of Paper XI are as follows:

- To the best of our knowledge, there is no published literature that investigates the EC and ESC of the NOMA-SWIPT aided IoT relay systems with direct links, in which one source or BS wants to transmit symbols to two destination nodes through the direct links and with the help of EH based relay node.

- Specifically, for the considered NOMA-SWIPT system, we investigate the TSR, PSR relaying architecture.

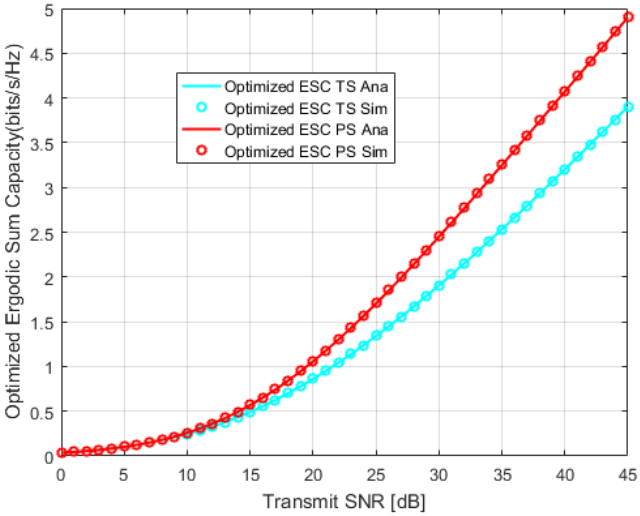

Figure 3.19: Optimized Ergodic Sum Capacity

- We derive the analytical expressions for the EC and the ESC for the considered system model and validate it through the simulation results, which shows that our derived analytical expressions are intact.

- We provide a thorough comparison of TS and PS relaying EH architecture for the considered NOMA-SWIPT system model with direct links.

- Our results demonstrate that the EC performance could be significantly improved through the optimal choice of power splitting ϵ factor for PS relaying with NOMA compared to TS relaying with NOMA.

Main Results

In Figure 3.19, we plot the optimized ESC of the system for both - TS and PS relaying with NOMA at different transmit SNR. We observe that at the lower transmit SNR values, i.e. less than 10 dB, both TS and PS relaying with NOMA almost have the same optimized ESC. After 10 dB and higher transmit SNR, PS relaying with NOMA outperforms the TS relaying with NOMA. This confirms that through the optimal choice of ϵ, it is possible to achieve better optimized ESC for the PS relaying with NOMA than the TS relaying with NOMA.

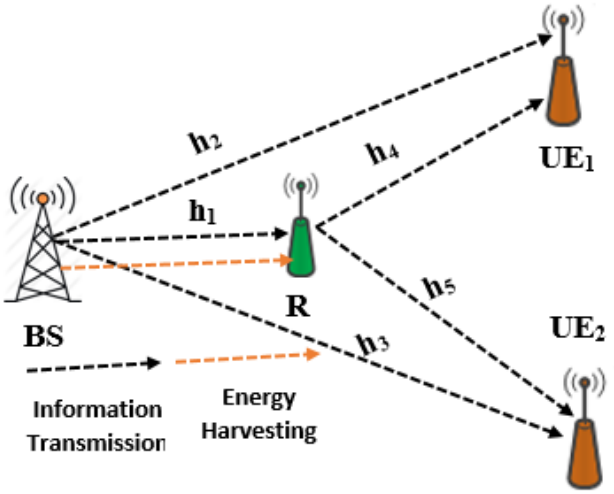

Figure 3.20: Considered System Model for the NOMA-SWIPT with Direct Links

3.12 Paper XII: Summary, Contributions and Main Results

Summary

Paper XII investigates capacity enhancement of NOMA-SWIPT IoT relay system with direct links over Rayleigh fading channels. It is known that when the direct links between the BS and the users exist and are non-negligible, consolidating direct links could significantly enhance the performance of the cooperative relaying systems. Specifically, for the considered NOMA-SWIPT system with direct links, we study a time-switching EH architecture in which a BS transmits two symbols to the two users through the direct links and via an EH-based relay node. On the receiving user node, we employ MRC to show the capacity enhancement of the considered system. Moreover, analytical expressions for the EC and ESC are mathematically derived for the MRC and SDS scheme. The analytical expressions are corroborated with the Monte-Carlo simulation results. This not only reveals the effect of different EH parameters on the system performance, but it also demonstrates the capacity enhancement of the considered NOMA-SWIPT system compared to a similar NOMA-SWIPT system without direct links and to conventional OMA schemes.

Contributions

In wireless communication, it is known that when direct links between the BS and the users exist and are non-negligible, consolidating direct links could

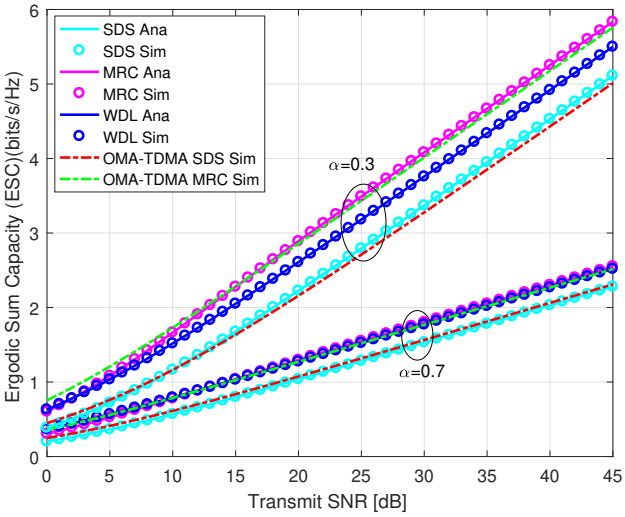

Figure 3.21: Ergodic Sum Capacity of Considered System Model for the NOMA-SWIPT with the Direct Link

significantly enhance the performance of the cooperative relaying systems. As mentioned in the Section 2.6, although a myriad of works have been carried out in the literature for NOMA-SWIPT systems, to the best of our knowledge, there is no published literature investigating the EC and ESC of the NOMA-SWIPT assisted IoT relay systems with the direct link over the Rayleigh fading channels in which one BS transmit two symbols to two destination nodes through the direct link and with the assistance of EH-based relay node. Therefore, in Paper XII, we investigate the capacity enhancement of NOMA-SWIPT IoT relay system with direct links over the Rayleigh fading channels. Since the direct links are involved, we employ the MRC scheme and show the capacity enhancement of the system.

The major contributions of Paper XII are as follows:

- We propose and investigate the capacity enhancement of the NOMA-SWIPT assisted IoT relay systems with the direct link over the Rayleigh fading channels in which one BS wants to transmit two symbols to two destination nodes through the direct link and with the assistance of EH-based relay node using the TS architecture.

- Since the direct links are involved, we employ the MRC scheme and show the capacity enhancement of the system by comparing it with the SDS scheme.

- For the considered NOMA-SWIPT system model with direct links, we derive the analytical expressions for the EC and the ESC for both the

MRC and SDS schemes and validate them by Monte-Carlo simulations, demonstrating that our derived analytical expressions are correct.

- For a fair and logical evaluation of the considered NOMA-SWIPT system with the direct link, we devised a comparable model using OMA. Along with its analytical derivations, a thorough comparison is provided between the NOMA-SWIPT and OMA-SWIPT system models without considering the impact of direct links.

- Our results demonstrate that employing the MRC scheme could significantly enhance the ESC performance of the system compared to using the SDS scheme. Moreover, we also showed that, with proper selection of EH parameters, such as the time switching factor and the power allocation factor for the NOMA, the ESC performance of the system could be further improved as compared to a NOMA-SWIPT system that has no direct links and to a conventional OMA schemes.

Main Results

The considered cooperative NOMA-SWIPT system model with direct links is shown in Figure 3.20. Here, a BS transmits two symbols, x_1 and x_2, to the two destination nodes, UE_1 and UE_2, respectively through the direct link and with the assistance of an EH-based relay node using the TS protocol. As R is a power-constrained node that acts as a DF relay, it first harvests the RF energy from the BS signal using the TS protocol, and then it decodes the symbols x_1 and x_2 transmitted by the BS in the first phase. Also, UE_1 and UE_2 receive the information transmitted by the BS through the direct links in the first phase. Then, R forwards the decoded symbols x_1 and x_2 using the NOMA protocol to the UE_1 and UE_2 in the subsequent phase.

We plot the ESC at $\alpha = 0.3$ and $\alpha = 0.7$ against the transmit SNR for all the schemes for a thorough comparison in 3.21. We observe that the ESC is an increasing function with respect to increase in the transmit SNR for all of the schemes. At low transmit SNR, i.e. less than 10 dB, the OMA-TDMA MRC scheme has higher ESC than our NOMA-SWIPT model with direct links. However, as we increase the transmit SNR, the ESC of our NOMA-SWIPT model gives the overall higher ESC for the system. The reason for OMA-TDMA MRC scheme to have better ESC at low transmit SNR is that the BS transmits the signal for UE_1 and UE_2 with its full power of BS in two time slots whereas, in our considered NOMA-SWIPT model, the power of the BS is divided into two parts for the UE_1 and UE_2 using a single time slot. Also, it is interesting to note that the NOMA-SWIPT model without direct links has higher EC for UE_2 than our considered NOMA-SWIPT model with direct links that is using the SDS scheme. The reason for this is that the EC is dominated by the weakest link. Moreover, as we increase the α factor from 0.3 to 0.7, we see that the ESCs for all the models decrease. This indicates that a small α factor is sufficient for

the system to harvest enough energy and the remaining time can be used for the data transmission.

3.13 Paper XIII: Summary, Contributions and Main Results

Summary

Paper XIII investigates the EC performance of D2D IoT relay NOMA-SWIPT systems where the relayed communication is supported with the direct link communication. A two-user case is considered in which a base station transmits symbols to two NOMA users, and the EH based relay node via a direct link. The EH based relay node harvests the energy from the BS's signal and again transmits a superimposed composite NOMA signal intended for the user with poor channel condition and for its D2D user to offload its data traffic. A D2D user offloading is considered to further enhance the spectral efficiency of the system. We derive the analytical expressions for the EC of each of the user and the ESC of the system and validate them with simulation results. In such settings, our results demonstrate that the EC of a node and the ESC of the system can be improved through the MRC scheme compared to a system with single signal decoding scheme. Our results also indicate that the overall ESC of the NOMA-SWIPT system can be improved by incorporating a direct link communication with a relayed communication for a user in the system.

Contributions

In Paper XIII, we consider a NOMA-SWIPT system in which a BS transmits symbols to two NOMA users and to the EH based relay node via a direct link. The PS EH based relay node harvests the energy from the BS's signal and again transmits a superimposed composite NOMA signal intended for the user with poor channel condition and for its D2D user. The reason we have considered a D2D user in the considered system is to assist the EH based relay node for offloading its data traffic and thereby further enhancing the spectral efficiency of the considered system as explained in the Section 2.6.

The major contributions of Paper XIII are as follows:

- Unlike existing works, our proposed system model is more practical as we have assumed that the UE_2 user has a strong direct link with the BS, and the UE_1 user has a weak direct link from the BS. Therefore, the data of UE_1 has to be re-transmitted again via an EH based relay node UE_3. Further, UE_3 not only forwards the data of UE_1, but it will also transmit the data for its D2D user, i.e. UE_4 to offload its data traffic.
- To show the impact of direct links, we have used the SDS scheme, and the MRC scheme and derive its analytical expressions for the EC and ESC. We show the performance gains in terms of ESC of the system by using MRC scheme.

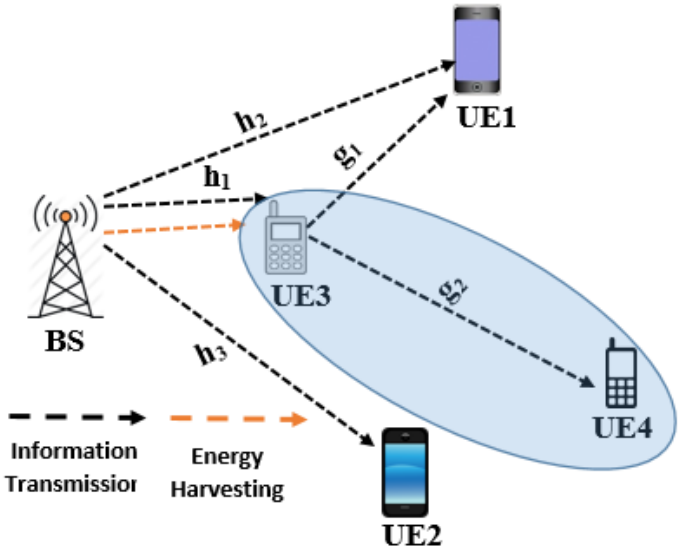

Figure 3.22: Considered System Model for NOMA-SWIPT with Direct Link

- Effect of transmit signal-to-noise ratio (SNR) and other EH parameters on the EC and ESC performance for both the MRC and SDS schemes were investigated to gain further insight into the NOMA-SWIPT system.

Main Results

The considered cooperative NOMA-SWIPT aided D2D IoT relay system model with direct links is shown in Figure 3.22. Here, a BS transmits two symbols, x_1 and x_2 to UE_1 and UE_2, respectively, through the direct links. UE_1 is considered as a distant user with poor channel conditions compared to UE_2. As UE_3 is a power constrained node that acts as a DF relay, it first harvests the RF energy from the signal of BS using the PS protocol and then decodes the symbols x_1 and x_2 transmitted by the BS in the first phase. Also UE_1 and UE_2 receives the information transmitted by the BS through the direct link in the first phase. Since UE_1 is a distant user with poor channel conditions compared to UE_2, the symbol x_1 is re-transmitted via a energy constrained relay node UE_3. Further to improve the spectral efficiency of the considered NOMA-SWIPT system, we have considered that UE_3 will also transmit or offload its data traffic to its D2D user UE_4 to enhance the spectral efficiency of the system. Thus, UE_3 forwards the symbol x_1 and x_r using the NOMA protocol to UE_1 and UE_4 in the subsequent phase.

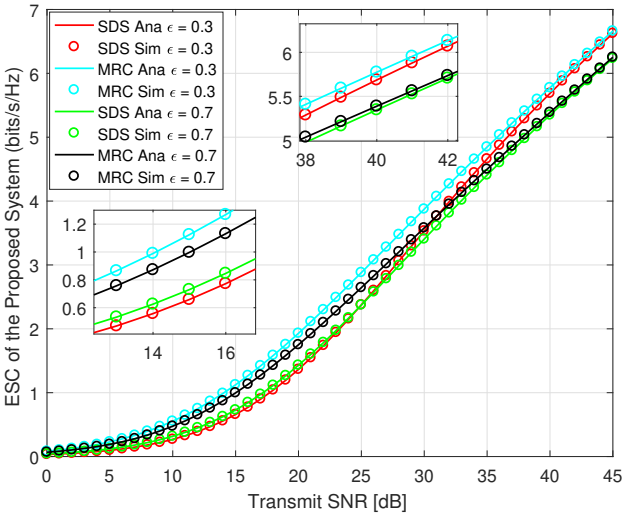

Figure 3.23: Ergodic Sum Capacity of the Proposed System

Taking UE_1, UE_2, and UE_4 as three users in the considered system, we plot the ESC of the system against the transmit SNR at $\epsilon = 0.3$ and 0.7 in Figure 3.23. As expected, we see that the MRC scheme outperforms the SDS scheme. However, the ESC difference between MRC and SDS is clearly seen when the transmit SNR is less than 35 dB. When the transmit SNR is above 35 dB, the ESC difference between the MRC and SDS schemes becomes very small and eventually negligible. The reason for this is that at such high transmit SNR, i.e., above 35 dB, the relay node UE_3 can harvest more energy, which eventually increases the ESC of the SDS scheme. It should be noted that in our considered system, the MRC scheme is only applied to the UE_1 user since it receives data through the direct link and via UE_3. Figure 3.23 clearly shows that by having a direct link and using the MRC scheme for a single user, the ESC of the whole system can be improved.

Chapter 4

Conclusions

With the proliferation of IoT, spectral and energy efficiency are some of the key requirements of 5G and next-generation IoT networks. Therefore, new energy and spectral efficient protocols to ameliorate the capacity and energy demands of the massive IoT networks need to be designed. In this regard, to provide higher data rate, and massive connectivity requirements of the IoT devices, NOMA has been considered as a promising radio access technique for the 5G and next-generation IoT networks to meet their heterogeneous capacity demands. To this end, this dissertation focused on exploring and enhancing the spectral and energy-efficiency of NOMA in next-generation IoT networks.

In Chapter 1, we introduced the background and motivation for our work. We also defined research aims and objectives along with our research questions. State of the knowledge related to these defined research objectives are explained in Chapter 2. This leads us to propose and study new spectral and energy-efficient NOMA system models that advances the state-of-the-art. The defined research aims and objectives are further divided into thirteen different papers, which are briefly explained in Chapter 3 along with their main contributions and results.

The main findings of our work can be listed as follows:

- We demonstrate how bi-directional communications can be achieved in a NOMA-SWIPT enabled IoT relay network through the uplink and downlink NOMA protocol. The effect of user pairing for the exchange of information in different NOMA groups are investigated. We showed how it affects the BR NOMA-SWIPT system capacity under both pSIC and ipSIC scenarios. A thorough comparison of the proposed BR NOMA-SWIPT system with BR OMA-SWIPT system model is devised, which showed the performance enhancement.

- Since efficient user pairing between multiple users is needed to enhance the capacity of NOMA systems, an efficient Adaptive user pairing strategy for uplink NOMA systems is proposed and studied in order to accommodate the unpaired user into formed clusters. We showed how our proposed Adaptive user pairing strategy finds the right paired cluster to serve the unpaired user in a way that increases the overall sum capacity under both pSIC and ipSIC scenarios. A thorough comparison against the state-of-art, such as OMA and C-NOMA pairing techniques, shows the effectiveness of our proposed Adaptive user pairing strategy.

- Moreover, location of the nodes plays an important role for user pairing and energy harvesting. We propose and study a new distributed localization algorithm inspired by nature, which we call social learning based particle swarm optimization for IoT. Our experimental results depict that a

precise localization of deployed IoT sensors nodes can be achieved with reduced computational complexity that further enhances the lifetime of these resource constrained IoT sensor nodes. Experimental results also demonstrate that our proposed SL-PSO algorithm can not only increase convergence rate but it also significantly reduces the average localization error compared to traditional PSO and its other variants.

- A NOMA based diamond relaying network provides an effective strategy to improve the achievable rate of the system compared to a traditional two-relay cooperative communication protocol. Contrary to research objective 1, we show how downlink and then uplink NOMA can be used to achieve higher spectral, energy efficiency and capacity enhancement of the NDR-SWIPT system compared to OMA-SWIPT diamond relaying system.

- Realizing the energy constrained nature of IoT nodes, we consider and investigate an RF EH based on time switching, power splitting and NOMA for IoT relay systems. Unlike several of the previous works, where the participating relay node is used only to transmit source node data successfully, we also consider to send the IoT relay node data along with the source node data to its respective destination. This is particularly important for data offloading by the IoT relay node to its own D2D user or destination node. A thorough comparison between a TS and a PS protocol with NOMA under both delay limited and delay tolerant transmission mode is made to show the effect of EH parameters on the considered system. By the Golden section search method, we find the optimal time switching and power splitting factor that maximizes the sum-throughput of the proposed model. It is revealed that PS with NOMA performs better at higher transmit SNR than TS with NOMA. For a smaller values of transmit SNR, TS with NOMA performs better than PS with NOMA. Moreover, for a higher sum-throughput of the considered system, a higher PS factor is required for PS with NOMA to perform better than a corresponding TS factor for TS with NOMA. Our results demonstrate that PS relaying with NOMA is more energy-efficient than TS relaying with NOMA for the considered system. Our results also confirm that the SIC imperfection only affects the ESC performance, and it does not show any effect on the time switching factor α or power splitting factor ε at which ESC is maximized.

- A simple and energy-efficient distributed power control in downlink NOMA using RL based game theoretic approach is proposed and investigated. Since resources are not used in an orthogonal manner in NOMA, it is important to efficiently manage the interference between multiple users to maximize the system throughput or capacity. The aim of the game is to optimize the achievable rate fairness of the BSs in a distributed manner by appropriately choosing the power levels of the BSs. We prove that the distributed power control game we designed is an exact potential game. We then propose a RL based game-theoretic approach for distributed power control that provides a full characterization of the best achievable

performance for the potential function of the game. We show that our proposed distributed power control algorithm which is designed as a game is guaranteed to converge to a Nash equilibrium. We also conducted a thorough theoretical analysis that demonstrates the convergence of the proposed algorithm that is maximizing the achievable rate fairness for the respective near users and far users and thus achieving higher energy efficiency in downlink NOMA systems.

- Usually, in practical environments, IoT networks or systems are subjected to external interference factors. This often results in a loss in the system rate. To study the effect of interference on the system, specifically, we study the combination of two popular energy harvesting relaying architectures - TSR and PSR with the NOMA protocol for IoT relay systems in the presence of interfering signals. Extensive simulations are carried out to find the optimal TS and PS factors that maximize the sum-throughput of the considered system in the presence of an interfering signal. A thorough comparison of the TS and PS protocols with NOMA revealed that the outage performances of the source user and IoT relay user are greatly affected by the interfering signal power in the system which in turn decreases the overall sum-throughput of the system. Also, the results demonstrate that the interfering signal power has a significant role in the outage probability of the source user for PS relaying with NOMA compared to TS relaying with NOMA. Therefore, in such interfering conditions, a careful selection of EH parameters, such as the TS and PS factors is envisaged to achieve higher sum-throughput of the system.

- It is known that when direct links between the BS and the users exist and are non-negligible, consolidating direct links could significantly enhance the performance of the cooperative relaying systems. Specifically, we investigate the EC and ESC of the NOMA-SWIPT aided IoT relay systems in the presence of direct links. Here, one source or base station transmit symbols to two destination nodes through the direct links and with the help of a EH based relay node. We made a thorough comparison of the TS and PS relaying EH architectures for the considered NOMA-SWIPT system model with direct links. The results demonstrate that the EC performance could be significantly improved through the optimal choice of power splitting factor for the PS relaying with NOMA compared to the TS relaying with NOMA. Our results also demonstrate that, employing the MRC scheme could significantly enhance the ESC performance of the system compared to using the SDS scheme. Moreover, the results also show that, with the proper selection of EH parameters, such as the time switching factor and the power allocation factors for the NOMA, the ESC performance of the considered system with direct links could be further improved compared to a similar NOMA-SWIPT system that has no direct links and to a conventional OMA schemes.

- We further investigate the EC performance of D2D IoT relay NOMA-

SWIPT systems. Here the relayed communication is supported with direct link communications to support the user with poor channel condition. Further, a D2D user offloading is considered to further enhance the spectral efficiency of the system. In such settings, our results demonstrate that the overall ESC of the NOMA-SWIPT system can be improved by incorporating a direct link communication with a relayed communication for a user in the system.

For all our evaluations, we demonstrate the effectiveness of our proposed methods through analytical modeling and validating them through Monte-Carlo simulations. The proof of the analytical model derivations are given in the paper itself or in the appendix of each of the paper.

Finally, we believe that our work presented in this dissertation opens new doors to the design and implementation of spectral and energy efficient NOMA in the next generation IoT networks. We further believe that the study and results presented here will be potentially useful to network operators, researchers and scientists in the wireless networking community from both academia and industry who want to assess the characteristics of NOMA to design next-generation IoT networks.

4.1 Future Research Directions

At this juncture, we discuss the possible future directions that exploit the approaches outlined in this dissertation and stimulate more studies to introduce new and innovative strategies to design spectral and energy-efficient architectures in next-generation IoT networks.

- The use of optimized wireless technologies is essential in the context of IoT and industrial IoT. Bringing intelligence into IoT systems is mostly constrained by the availability of energy. IoT devices should prepare carefully how they use their available energy resources. This includes the tasks they should execute and when in order to make the most of the available energy. This requires the development of policies. However, it is difficult to know which policy will be best for IoT devices as different IoT devices may find themselves in different situations. This is a research challenge. Therefore, it would be useful to automate it with the use of Artificial Intelligence (AI) and Machine Learning (ML) algorithms.

  As a future work, it would be interesting to model the energy harvesting profile for each of the IoT devices taking NOMA-SWIPT into account. Further, various machine-learning methods can be exploited for modeling the input/output of power supplies. This will allow IoT devices to learn more about their current and future states as well as about their energy budget policies to work better and more autonomously. Moreover, the expected energy profiles for each device in its operating environment will be different. To this end, it will be interesting to investigate expected

energy profiles for each devices so that it can learn to decide when to do work and when to wait for recharging. Furthermore, investigating the performance of the designed solutions over a choice of wireless technologies such as WiFi 5, 5G New Radio (NR), WiFi 6, or LoRa would be an interesting research direction.

- Paper I is one of the initial attempts to address and use BR NOMA with SWIPT that support the low data rate requirement of the users. Modeling a system that will also support high data rate requirements of NOMA users according to their Quality of Service (QoS) requirements is interesting. Moreover, extending the BR NOMA-SWIPT system model to study secrecy capacity for secure communication in IoT networks is an interesting research direction. Nevertheless, evaluating the performance of the BR NOMA-SWIPT system with other multipath fading channel models would be also interesting for future research work.

- Paper II proposed an Adaptive user pairing strategy for sum capacity maximization of uplink NOMA systems. As an extension to this, proposing, comparing and investigating the user pairing strategy for the downlink NOMA systems along with the closed-form analytical expressions to gain more insights would be interesting for future research work.

- An extension to Paper IV would be to investigate the outage performance of the proposed NOMA-NDR SWIPT system with a non-linear energy harvesting model. Studying and investigating the secrecy capacity in the presence of eavesdroppers is also interesting for future work.

- In Paper IX, we only consider discrete power levels that used linear discretization for downlink NOMA systems where the power levels are equi-spaced. Nevertheless, for future work, extending our model and study the scenario with non-linear discretization power levels for uplink and downlink NOMA systems would be interesting. Studying and designing a game for distributed power control in multicell NOMA systems in the presence of smart jammers and eavesdroppers is also an interesting research direction for future work.

- As an extension to Paper X, it would also be interesting to apply a game theory approach for power allocation for RF EH under the influence of various interfering signals using a stochastic geometry approach.

- As an extension to Paper XIII, investigating the outage probability and doing a thorough comparison of the considered NOMA-SWIPT aided D2D IoT relay system model with other energy harvesting architectures would be another interesting future research direction. Also, studying the effect of interference and secrecy capacity in the presence of eavesdroppers is an interesting topic for the future work.

Bibliography

[1] (3GPP), 3. G. P. P. "Study on Downlink Multi-user Superposition Transmission for LTE, TSG RAN Meeting 67". In: *Tech. Rep. RP-150496* (Mar. 2015).

[2] 3GPP. "Study on security architecture enhancements to Proximity Services (ProSe) User Equipment (UE)-to-network relay". In: *3GPP Technical report (TR) 33.843* vol. V1.0.0 (2018).

[3] Aldebes, R., Dimyati, K., and Hanafi, E. "Game-theoretic power allocation algorithm for downlink NOMA cellular system". In: *Electronics Letters* vol. 55, no. 25 (2019), pp. 1361–1364.

[4] Atzori, L., Iera, A., and Morabito, G. "The internet of things: A survey". In: *Computer networks* vol. 54, no. 15 (2010), pp. 2787–2805.

[5] Aziz, M., Tayarani-N, M.-H., and Meybodi, M. R. "A two-objective memetic approach for the node localization problem in wireless sensor networks". In: *Genetic Programming and Evolvable Machines* vol. 17, no. 4 (2016), pp. 321–358.

[6] Balanis, C. A. *Antenna Theory Analysis and Design . New York: John Willey & Sons.* 1982.

[7] Balasubramanya, N. M., Gupta, A., and Sellathurai, M. "Combining code-domain and power-domain NOMA for supporting higher number of users". In: *2018 IEEE Global Communications Conference (GLOBECOM)*. IEEE. 2018, pp. 1–6.

[8] Behdad, Z., Mahdavi, M., and Razmi, N. "A new relay policy in RF energy harvesting for IoT networks—A cooperative network approach". In: *IEEE Internet of Things Journal* vol. 5, no. 4 (2018), pp. 2715–2728.

[9] Bockelmann, C. et al. "Towards massive connectivity support for scalable mMTC communications in 5G networks". In: *IEEE access* vol. 6 (2018), pp. 28969–28992.

[10] Céspedes-Mota, A. et al. "Optimization of the distribution and localization of wireless sensor networks based on differential evolution approach". In: *Mathematical Problems in Engineering* vol. 2016 (2016).

[11] Chen, Y.-H. et al. "Low Complexity User Selection and Power Allocation for Uplink NOMA Beamforming Systems". In: *Wireless Personal Communications* vol. 111, no. 3 (2020), pp. 1413–1429.

[12] Chen, Z. et al. "A localization method for the Internet of Things". In: *The Journal of Supercomputing* vol. 63, no. 3 (2013), pp. 657–674.

[13] Cheng, J. and Xia, L. "An Effective Cuckoo Search Algorithm for Node Localization in Wireless Sensor Network". In: *Sensors* vol. 16, no. 9 (2016), p. 1390.

[14] Cheng, M. X. and Wu, W. B. "A model-free localization method for sensor networks with sparse anchors". In: *Communications (ICC), 2016 IEEE International Conference on*. IEEE. 2016, pp. 1–7.

[15] Cheng, R. and Jin, Y. "A social learning particle swarm optimization algorithm for scalable optimization". In: *Information Sciences* vol. 291 (2015), pp. 43–60.

[16] Choi, J. "A game-theoretic approach for NOMA-ALOHA". In: *2018 European Conference on Networks and Communications (EuCNC)*. IEEE. 2018, pp. 54–9.

[17] Choi, M., Han, D.-J., and Moon, J. "Bi-Directional Cooperative NOMA Without Full CSIT". In: *IEEE Transactions on Wireless Communications* vol. 17, no. 11 (2018), pp. 7515–7527.

[18] Cota-Ruiz, J. et al. "A Recursive Shortest Path Routing Algorithm With Application for Wireless Sensor Network Localization". In: *IEEE Sensors Journal* vol. 16, no. 11 (2016), pp. 4631–4637.

[19] Dai, L. et al. "A survey of non-orthogonal multiple access for 5G". In: *IEEE communications surveys & tutorials* vol. 20, no. 3 (2018), pp. 2294–2323.

[20] Dai, L. et al. "Non-orthogonal multiple access for 5G: solutions, challenges, opportunities, and future research trends". In: *IEEE Communications Magazine* vol. 53, no. 9 (2015), pp. 74–81.

[21] Ding, Z., Dai, H., and Poor, H. V. "Relay selection for cooperative NOMA". In: *IEEE Wireless Communications Letters* vol. 5, no. 4 (2016), pp. 416–419.

[22] Ding, Z. et al. "A survey on non-orthogonal multiple access for 5G networks: Research challenges and future trends". In: *IEEE Journal on Selected Areas in Communications* vol. 35, no. 10 (2017), pp. 2181–2195.

[23] Do, D.-T. and Nguyen, H.-S. "A tractable approach to analyzing the energy-aware two-way relaying networks in the presence of co-channel interference". In: *EURASIP Journal on Wireless Communications and Networking* vol. 2016, no. 1 (2016), p. 271.

[24] Do, N. T. et al. "A BNBF user selection scheme for NOMA-based cooperative relaying systems with SWIPT". In: *IEEE Communications Letters* vol. 21, no. 3 (2016), pp. 664–667.

[25] Doan, K. N. et al. "Power allocation in cache-aided NOMA systems: Optimization and deep reinforcement learning approaches". In: *IEEE Transactions on Communications* vol. 68, no. 1 (2019), pp. 630–644.

[26] Du, G., Xiong, K., and Qiu, Z. “Outage analysis of cooperative transmission with energy harvesting relay: Time switching versus power splitting”. In: *Mathematical Problems in Engineering* vol. 2015 (2015).

[27] Elmorshedy, L., Leung, C., and Mousavifar, S. A. “RF energy harvesting in DF relay networks in the presence of an interfering signal”. In: *2016 IEEE International Conference on Communications (ICC)*. IEEE. 2016, pp. 1–6.

[28] Al-Falahy, N. and Alani, O. Y. “Technologies for 5G networks: Challenges and opportunities”. In: *IT Professional* vol. 19, no. 1 (2017), pp. 12–20.

[29] Fu, Y., Chen, Y., and Sung, C. W. “Distributed downlink power control for the non-orthogonal multiple access system with two interfering cells”. In: *2016 IEEE International Conference on Communications (ICC)*. IEEE. 2016, pp. 1–6.

[30] Ge, R. et al. “RF-powered battery-less Wireless Sensor Network in structural monitoring”. In: *2016 IEEE international conference on electro information technology (EIT)*. IEEE. 2016, pp. 0547–0552.

[31] Geng, K. et al. “Relay selection in cooperative communication systems over continuous time-varying fading channel”. In: *Chinese Journal of Aeronautics* vol. 30, no. 1 (2017), pp. 391–398.

[32] Gopakumar, A. and Jacob, L. “Localization in wireless sensor networks using particle swarm optimization”. In: *Wireless, Mobile and Multimedia Networks, 2008. IET International Conference on*. IET. 2008, pp. 227–230.

[33] Gu, Y. and Aissa, S. “RF-based energy harvesting in decode-and-forward relaying systems: Ergodic and outage capacities”. In: *IEEE Transactions on Wireless Communications* vol. 14, no. 11 (2015), pp. 6425–6434.

[34] Guntupalli, L., Gidlund, M., and Li, F. Y. “An on-demand energy requesting scheme for wireless energy harvesting powered IoT networks”. In: *IEEE Internet of Things Journal* vol. 5, no. 4 (2018), pp. 2868–2879.

[35] Guo, W. et al. “Simultaneous information and energy flow for IoT relay systems with crowd harvesting”. In: *IEEE Communications Magazine* vol. 54, no. 11 (2016), pp. 143–149.

[36] Ha, D.-B. and Nguyen, S. Q. “Outage Performance of Energy Harvesting DF Relaying NOMA Networks”. In: *Mobile Networks and Applications* (2017), pp. 1–14.

[37] Ha, D.-B. and Nguyen, S. Q. “Outage performance of energy harvesting DF relaying NOMA networks”. In: *Mobile Networks and Applications* vol. 23, no. 6 (2018), pp. 1572–1585.

[38] Hasan, S. and Curry, E. “Thingsonomy: Tackling variety in internet of things events”. In: *IEEE Internet Computing* vol. 19, no. 2 (2015), pp. 10–18.

[39] He, J., Tang, Z., and Che, Z. “Fast and efficient user pairing and power allocation algorithm for non-orthogonal multiple access in cellular networks”. In: *Electronics letters* vol. 52, no. 25 (2016), pp. 2065–2067.

[40] Huang, B.-Y., Lee, Y., and Sou, S.-I. “Joint Power Allocation for NOMA-Based Diamond Relay Networks With and Without Cooperation”. In: *IEEE Open Journal of the Communications Society* vol. 1 (2020), pp. 428–443.

[41] Ibrahim, A. S. et al. “Cooperative communications with relay-selection: when to cooperate and whom to cooperate with?” In: *IEEE Transactions on wireless communications* vol. 7, no. 7 (2008), pp. 2814–2827.

[42] Islam, S. R. et al. “Nonorthogonal Multiple Access (NOMA): How It Meets 5G and Beyond”. In: *Wiley 5G Ref: The Essential 5G Reference Online* (2019), pp. 1–28.

[43] Jain, N. and Bohara, V. A. “Energy harvesting and spectrum sharing protocol for wireless sensor networks”. In: *IEEE Wireless Communications Letters* vol. 4, no. 6 (2015), pp. 697–700.

[44] Jiao, R. et al. “On the performance of NOMA-based cooperative relaying systems over Rician fading channels”. In: *IEEE Transactions on Vehicular Technology* vol. 66, no. 12 (2017), pp. 11409–11413.

[45] Kader, M. F., Shahab, M. B., and Shin, S. Y. “Cooperative spectrum sharing with energy harvesting best secondary user selection and non-orthogonal multiple access”. In: *2017 International Conference on Computing, Networking and Communications (ICNC)*. IEEE. 2017, pp. 46–51.

[46] Kader, M. F. et al. “Bidirectional relaying using non-orthogonal multiple access”. In: *Physical Communication* (2019).

[47] Kader, M. F. et al. “Capacity and outage analysis of a dual-hop decode-and-forward relay-aided NOMA scheme”. In: *Digital Signal Processing* vol. 88 (2019), pp. 138–148.

[48] Kim, J.-B. and Lee, I.-H. “Non-orthogonal multiple access in coordinated direct and relay transmission”. In: *IEEE Communications Letters* vol. 19, no. 11 (2015), pp. 2037–2040.

[49] Kim, J.-B., Lee, I.-H., and Lee, J. “Capacity scaling for D2D aided cooperative relaying systems using NOMA”. In: *IEEE Wireless Communications Letters* vol. 7, no. 1 (2017), pp. 42–45.

[50] Kulkarni, R. V. and Venayagamoorthy, G. K. “Particle swarm optimization in wireless-sensor networks: A brief survey”. In: *IEEE Transactions on Systems, Man, and Cybernetics, Part C (Applications and Reviews)* vol. 41, no. 2 (2011), pp. 262–267.

[51] Lee, J.-H. et al. “A matched RF charger for wireless RF power harvesting system”. In: *Microwave and Optical Technology Letters* vol. 57, no. 7 (2015), pp. 1622–1625.

[52] Li, X. et al. “Energy consumption optimization for self-powered IoT networks with non-orthogonal multiple access”. In: *International Journal of Communication Systems* vol. 33, no. 1 (2020), e4174.

[53] Li, X. et al. “Smart community: an internet of things application”. In: *IEEE Communications magazine* vol. 49, no. 11 (2011), pp. 68–75.

[54] Liang, X. et al. “Cooperative communications with relay selection for wireless networks: design issues and applications”. In: *Wireless Communications and Mobile Computing* vol. 13, no. 8 (2013), pp. 745–759.

[55] Liu, H. et al. “Decode-and-forward relaying for cooperative NOMA systems with direct links”. In: *IEEE Transactions on Wireless Communications* vol. 17, no. 12 (2018), pp. 8077–8093.

[56] Liu, Y. et al. “Cooperative Non-orthogonal Multiple Access With Simultaneous Wireless Information and Power Transfer”. In: *IEEE Journal on Selected Areas in Communications* vol. 34, no. 4 (2016), pp. 938–953.

[57] Lu, X. et al. “Wireless networks with RF energy harvesting: A contemporary survey”. In: *IEEE Communications Surveys & Tutorials* vol. 17, no. 2 (2014), pp. 757–789.

[58] Mao, G., Fidan, B., and Anderson, B. D. “Wireless sensor network localization techniques”. In: *Computer networks* vol. 51, no. 10 (2007), pp. 2529–2553.

[59] Mateu, L. and Moll, F. “Review of energy harvesting techniques and applications for microelectronics (Keynote Address)”. In: *VLSI Circuits and Systems II*. Vol. 5837. International Society for Optics and Photonics. 2005, pp. 359–374.

[60] Miandoab, F. T. and Tazehkand, B. M. “A user pairing method to improve the channel capacity for multiuser MIMO channels in downlink mode based on NOMA”. In: *Computer Communications* vol. 146 (2019), pp. 15–21.

[61] Moraes, C. and Har, D. “Charging distributed sensor nodes exploiting clustering and energy trading”. In: *IEEE Sensors Journal* vol. 17, no. 2 (2016), pp. 546–555.

[62] Murti, F. W. and Shin, S. Y. “User pairing schemes based on channel quality indicator for uplink non-orthogonal multiple access”. In: *2017 Ninth International Conference on Ubiquitous and Future Networks (ICUFN)*. IEEE. 2017, pp. 225–230.

[63] Nasir, A. A. et al. “Relaying Protocols for Wireless Energy Harvesting and Information Processing”. In: *IEEE Transactions on Wireless Communications* vol. 12, no. 7 (2013), pp. 3622–3636.

[64] Nasir, A. A. et al. “Relaying protocols for wireless energy harvesting and information processing”. In: *IEEE Transactions on Wireless Communications* vol. 12, no. 7 (2013), pp. 3622–3636.

[65] Nikopour, H. and Baligh, H. "Sparse code multiple access". In: *2013 IEEE 24th Annual International Symposium on Personal, Indoor, and Mobile Radio Communications (PIMRC)*. IEEE. 2013, pp. 332–336.

[66] Niyato, D., Hossain, E., and Lu, X. *Basics of Wireless Energy Harvesting and Transfer*. 2016.

[67] Pal, A. "Localization algorithms in wireless sensor networks: Current approaches and future challenges". In: *Network protocols and algorithms* vol. 2, no. 1 (2010), pp. 45–73.

[68] Pandey, S. and Varma, S. "A Range Based Localization System in Multihop Wireless Sensor Networks: A Distributed Cooperative Approach". In: *Wireless Personal Communications* vol. 86, no. 2 (2016), pp. 615–634.

[69] Rankov, B. and Wittneben, A. "Spectral efficient protocols for half-duplex fading relay channels". In: *IEEE Journal on selected Areas in Communications* vol. 25, no. 2 (2007), pp. 379–389.

[70] Razeghi, B., Hodtani, G. A., and Nikazad, T. "Multiple criteria relay selection scheme in cooperative communication networks". In: *Wireless Personal Communications* vol. 96, no. 2 (2017), pp. 2539–2561.

[71] Reinsel, D., Gantz, J., and Rydning, J. "Data age 2025: the digitization of the world from edge to core". In: *IDC White Paper Doc# US44413318* (2018), pp. 1–29.

[72] Riaz, S., Kim, J., and Park, U. "Evolutionary game theory-based power control for uplink NOMA." In: *KSII Transactions on Internet & Information Systems* vol. 12, no. 6 (2018).

[73] Sastry, P., Phansalkar, V., and Thathachar, M. "Decentralized learning of Nash equilibria in multi-person stochastic games with incomplete information". In: *IEEE Transactions on systems, man, and cybernetics* vol. 24, no. 5 (1994), pp. 769–777.

[74] Shahab, M. B., Kader, M. F., and Shin, S. Y. "A virtual user pairing scheme to optimally utilize the spectrum of unpaired users in non-orthogonal multiple access". In: *IEEE Signal Processing Letters* vol. 23, no. 12 (2016), pp. 1766–1770.

[75] Shahab, M. B. et al. "User pairing schemes for capacity maximization in non-orthogonal multiple access systems". In: *Wireless Communications and Mobile Computing* vol. 16, no. 17 (2016), pp. 2884–2894.

[76] Singh, S. et al. "Energy efficiency in wireless networks–a composite review". In: *IETE Technical Review* vol. 32, no. 2 (2015), pp. 84–93.

[77] Su, X. et al. "Power domain NOMA to support group communication in public safety networks". In: *Future Generation Computer Systems* vol. 84 (2018), pp. 228–238.

[78] Sun, L. et al. “Cooperative communications with relay selection in wireless sensor networks”. In: *IEEE Transactions on Consumer Electronics* vol. 55, no. 2 (2009), pp. 513–517.

[79] Sung, C. W. and Fu, Y. “A game-theoretic analysis of uplink power control for a non-orthogonal multiple access system with two interfering cells”. In: *2016 IEEE 83rd Vehicular Technology Conference (VTC Spring)*. IEEE. 2016, pp. 1–5.

[80] Tabassum, H. et al. “Non-orthogonal multiple access (NOMA) in cellular uplink and downlink: Challenges and enabling techniques”. In: *arXiv preprint arXiv:1608.05783* (2016).

[81] Tabassum, H., Hossain, E., and Hossain, J. “Modeling and analysis of uplink non-orthogonal multiple access in large-scale cellular networks using poisson cluster processes”. In: *IEEE Transactions on Communications* vol. 65, no. 8 (2017), pp. 3555–3570.

[82] Tabassum, H. et al. “Uplink vs. downlink NOMA in cellular networks: Challenges and research directions”. In: *2017 IEEE 85th vehicular technology conference (VTC Spring)*. IEEE. 2017, pp. 1–7.

[83] Tang, J. et al. “Energy Efficiency Optimization for NOMA with SWIPT”. In: *IEEE Journal of Selected Topics in Signal Processing* vol. 13, no. 3 (2019), pp. 452–466.

[84] Tao, Y. et al. “A survey: Several technologies of non-orthogonal transmission for 5G”. In: *China communications* vol. 12, no. 10 (2015), pp. 1–15.

[85] Tran, L.-G., Cha, H.-K., and Park, W.-T. “RF power harvesting: a review on designing methodologies and applications”. In: *Micro and Nano Systems Letters* vol. 5, no. 1 (2017), p. 14.

[86] Tsai, C.-W., Lai, C.-F., and Vasilakos, A. V. “Future Internet of Things: open issues and challenges”. In: *Wireless Networks* vol. 20, no. 8 (2014), pp. 2201–2217.

[87] Tsiropoulou, E. E., Vamvakas, P., and Papavassiliou, S. “Joint Customized Price and Power Control for Energy-Efficient Multi-Service Wireless Networks via S-Modular Theory”. In: *IEEE Transactions on Green Communications and Networking* vol. 1, no. 1 (2017), pp. 17–28.

[88] Tsiropoulou, E. E., Vamvakas, P., and Papavassiliou, S. “Joint customized price and power control for energy-efficient multi-service wireless networks via S-modular theory”. In: *IEEE Transactions on Green Communications and Networking* vol. 1, no. 1 (2017), pp. 17–28.

[89] Uddin, M. B., Kader, M. F., and Shin, S. Y. “On the capacity of full-duplex diamond relay networks using NOMA”. In: *2019 7th International Conference on Information and Communication Technology (ICoICT)*. IEEE. 2019, pp. 1–6.

[90] Vaezi, M. et al. “Interplay between NOMA and other emerging technologies: A survey”. In: *IEEE Transactions on Cognitive Communications and Networking* vol. 5, no. 4 (2019), pp. 900–919.

[91] Vafashoar, R. and Meybodi, M. R. “Reinforcement learning in learning automata and cellular learning automata via multiple reinforcement signals”. In: *Knowledge-Based Systems* vol. 169 (2019), pp. 1–27.

[92] Vejlgaard, B. et al. “Interference impact on coverage and capacity for low power wide area IoT networks”. In: *2017 IEEE Wireless Communications and Networking Conference (WCNC)*. IEEE. 2017, pp. 1–6.

[93] Visser, H. J. and Vullers, R. J. “RF energy harvesting and transport for wireless sensor network applications: Principles and requirements”. In: *Proceedings of the IEEE* vol. 101, no. 6 (2013), pp. 1410–1423.

[94] Wan, D. et al. “On the achievable sum-rate of NOMA-based diamond relay networks”. In: *IEEE Transactions on Vehicular Technology* vol. 68, no. 2 (2018), pp. 1472–1486.

[95] Wan, D. et al. “User pairing strategy: A novel scheme for non-orthogonal multiple access systems”. In: *2017 IEEE Globecom Workshops (GC Wkshps)*. IEEE. 2017, pp. 1–6.

[96] Xiao, L. et al. “Reinforcement learning-based NOMA power allocation in the presence of smart jamming”. In: *IEEE Transactions on Vehicular Technology* vol. 67, no. 4 (2017), pp. 3377–3389.

[97] Xu, M. et al. “Novel receiver design for the cooperative relaying system with non-orthogonal multiple access”. In: *IEEE Communications Letters* vol. 20, no. 8 (2016), pp. 1679–1682.

[98] Yang, Z. et al. “Novel relay selection strategies for cooperative NOMA”. In: *IEEE Transactions on Vehicular Technology* vol. 66, no. 11 (2017), pp. 10114–10123.

[99] Yang, Z. et al. “The impact of power allocation on cooperative non-orthogonal multiple access networks with SWIPT”. In: *IEEE Transactions on Wireless Communications* vol. 16, no. 7 (2017), pp. 4332–4343.

[100] Yazidi, A. et al. “Game-Theoretic Learning for Sensor Reliability Evaluation Without Knowledge of the Ground Truth”. In: *IEEE Transactions on Cybernetics* (2020), pp. 1–11.

[101] Yazidi, A. et al. “The hierarchical continuous pursuit learning automation: a novel scheme for environments with large numbers of actions”. In: *IEEE Transactions on Neural Networks and Learning Systems* vol. 31, no. 2 (2019), pp. 512–526.

[102] Yue, X. et al. “Exploiting full/half-duplex user relaying in NOMA systems”. In: *IEEE Transactions on Communications* vol. 66, no. 2 (2017), pp. 560–575.

[103] Yue, X. et al. “Modeling and analysis of two-way relay non-orthogonal multiple access systems”. In: *IEEE Transactions on Communications* vol. 66, no. 9 (2018), pp. 3784–3796.

[104] Zaidi, S. K., Hasan, S. F., and Gui, X. “Evaluating the ergodic rate in SWIPT-aided hybrid NOMA”. In: *IEEE Communications Letters* vol. 22, no. 9 (2018), pp. 1870–1873.

[105] Zaidi, S. K., Hasan, S. F., and Gui, X. “SWIPT-aided uplink in hybrid non-orthogonal multiple access”. In: *2018 IEEE Wireless Communications and Networking Conference (WCNC)*. IEEE. 2018, pp. 1–6.

[106] Zaidi, S. K., Hasan, S. F., and Gui, X. “Two-way SWIPT-aided hybrid NOMA relaying for out-of-coverage devices”. In: *Wireless Networks* vol. 26, no. 3 (2020), pp. 2255–2270.

[107] Zain, I. F. M. and Shin, S. Y. “Distributed localization for wireless sensor networks using binary particle swarm optimization (BPSO)”. In: *2014 IEEE 79th Vehicular Technology Conference (VTC Spring)*. IEEE. 2014, pp. 1–5.

[108] Zeadally, S. et al. “Design architectures for energy harvesting in the Internet of Things”. In: *Renewable and Sustainable Energy Reviews* vol. 128 (2020), p. 109901.

[109] Zhang, H. et al. “User pairing algorithm with SIC in non-orthogonal multiple access system”. In: *2016 IEEE International Conference on Communications (ICC)*. IEEE. 2016, pp. 1–6.

[110] Zhang, R. and Ho, C. K. “MIMO broadcasting for simultaneous wireless information and power transfer”. In: *IEEE Transactions on Wireless Communications* vol. 12, no. 5 (2013), pp. 1989–2001.

[111] Zhang, X. et al. “A novel user pairing in downlink non-orthogonal multiple access”. In: *2018 IEEE International Symposium on Broadband Multimedia Systems and Broadcasting (BMSB)*. IEEE. 2018, pp. 1–5.

[112] Zhang, Z., Sun, H., and Hu, R. Q. “Downlink and uplink non-orthogonal multiple access in a dense wireless network”. In: *IEEE Journal on Selected Areas in Communications* vol. 35, no. 12 (2017), pp. 2771–2784.

[113] Zhao, N. et al. “Simultaneous wireless information and power transfer strategies in relaying network with direct link to maximize throughput”. In: *IEEE Transactions on Vehicular Technology* vol. 67, no. 9 (2018), pp. 8514–8524.

[114] Zhong, C. et al. “Improving the throughput of wireless powered dual-hop systems with full duplex relaying”. In: *2015 IEEE International Conference on Communications (ICC)* (2015), pp. 4253–4258.

[115] Zhou, Z. et al. “Energy-efficient cooperative communication based on power control and selective single-relay in wireless sensor networks”. In: *IEEE transactions on wireless communications* vol. 7, no. 8 (2008).

Papers

Paper I

On the Performance of Bidirectional NOMA-SWIPT Enabled IoT Relay Networks

Ashish Rauniyar, Paal E. Engelstad, Olav N. Østerbø

In: *IEEE Sensors Journal* Vol. 21, no. 2 (2020), pp. 2299 - 2315, DOI: 10.1109/JSEN.2020.3018905.

I

Paper II

An Adaptive User Pairing Strategy for Uplink Non-Orthogonal Multiple Access

Ashish Rauniyar, Paal E. Engelstad, Olav N. Østerbø

In: *2020 IEEE 31st Annual International Symposium on Personal, Indoor and Mobile Radio Communications, London, UK, 31 August - 3 September 2020,* DOI: 10.1109/PIMRC48278.2020.9217383.

II

Paper III

A New Distributed Localization Algorithm Using Social Learning based Particle Swarm Optimization for Internet of Things

Ashish Rauniyar, Paal E. Engelstad, Jonas Moen

In: *2018 IEEE 87th Vehicular Technology Conference (VTC Spring), Porto, Portugal, 3-6 June* (2018), pp. 1–7, DOI: 10.1109/VTCSpring.2018.8417665.

III

Paper IV

Exploiting SWIPT for IoT NOMA-based Diamond Relay Networks

IV

Ashish Rauniyar, Paal E. Engelstad, Olav N. Østerbø

In: *EAI MobiQuitous 2020 - 17th EAI International Conference on Mobile and Ubiquitous Systems: Computing, Networking and Services, Darmstadt, Germany, December 7 - 9* (2020), pp. 1–10, DOI: 10.1145/3448891.3448931.

Paper V

RF Energy Harvesting and Information Transmission Based on Power Splitting and NOMA for IoT Relay Systems

Ashish Rauniyar, Paal E. Engelstad, Olav N. Østerbø

In: *2018 IEEE 17th International Symposium on Network Computing and Applications (NCA), Cambridge, MA, USA, 1-3 November* (2018), pp. 1–8, DOI: 10.1109/NCA.2018.8548068.

Paper VI

RF Energy Harvesting and Information Transmission in IoT Relay Systems based on Time Switching and NOMA

Ashish Rauniyar, Paal E. Engelstad, Olav N. Østerbø

In: *2018 28th International Telecommunication Networks and Applications Conference, Sydney, NSW, Australia, 21-23 November* (2018), pp. 1–7, DOI: 10.1109/ATNAC.2018.8615403.

Paper VII

RF Energy Harvesting and Information Transmission Based on NOMA for Wireless Powered IoT Relay Systems

VII

Ashish Rauniyar, Paal E. Engelstad, Olav N. Østerbø

In: *Sensors Journal, Special Issue: Selected Papers from the 28th International Telecommunication Networks and Applications Conference,* Vol. 18, no. 10 (2018), pp. 3254–3275, DOI: 10.3390/s18103254.

sensors

MDPI

Article

RF Energy Harvesting and Information Transmission Based on NOMA for Wireless Powered IoT Relay Systems

Ashish Rauniyar [1,2,*], Paal Engelstad [1,2] and Olav N. Østerbø [3]

[1] Autonomous System and Networks Research Group, Department of Computer Science, Oslo Metropolitan University, 0130 Oslo, Norway; paalen@oslomet.no
[2] Autonomous Sensor and Technologies Research Group, Department of Technology Systems, University of Oslo, 0316 Oslo, Norway
[3] Telenor Research, 0316 Oslo, Norway; olav.osterbo@getmail.no
* Correspondence: ashish@oslomet.no; Tel.: +47-67-238864

Received: 13 August 2018; Accepted: 20 September 2018; Published: 27 September 2018

Abstract: Amidst the rapid development of the fifth generation (5G) networks, Internet of Things (IoT) is considered as one of the most important part of 5G next generation networks as it can support massive object communications. These massive object communications in the context of IoT is expected to consume a huge power. Furthermore, IoT sensors or devices are rather power constrained and are mostly battery operated. Therefore, energy efficiency of such network of IoT devices is a major concern. On the other hand, energy harvesting (EH) is an emerging paradigm that allows the wireless nodes to recharge themselves through radio frequency (RF) signals directed to them from the source node and then relaying or transmitting the information. Although a myriad of works have been carried out in the literature for EH, the vast majority of those works only consider RF EH at the relay node and successfully transmitting the source node data. Those approaches do not consider the data transmission of the relay node that may be an energy deprived IoT node which needs to transmit its own data along with the source node data to their respective destination nodes. Therefore, in this paper, we envisioned a RF EH and information transmission system based on time switching (TS) relaying, power splitting (PS) relaying and non-orthogonal multiple access (NOMA) which is suitable for wireless powered IoT relay systems. A source node information data is relayed through power constrained IoT relay node IoT_R that first harvests the energy from source node RF signal using either TS and PS relaying protocol and then transmits the source node information along with its information using NOMA protocol to the respective destination nodes. Considering NOMA as a transmission protocol, we have mathematically derived analytical expressions for TS and PS relaying protocol for our proposed system. We have also formulated an algorithm to find out optimal TS and PS factor that maximizes the sum-throughput for our proposed system. Our proposed system analytical results for TS and PS protocol are validated by the simulation results.

Keywords: Internet of Things; time switching; power splitting; NOMA; energy harvesting; radio frequency; relaying; outage probability; sum-throughput

1. Introduction

The Internet of Things (IoT) is a promising technology that aims to provide connectivity solutions. With the expeditious expansion of IoT technology across the globe, it is expected that billions of small sensors or devices will be connected with each other over the next few years [1–3]. The technological development in IoT integrates various sensors, devices, smart objects to be fully operated as autonomous device-to-device (D2D), machine-to machine (M2M) without any human

intervention [4–6]. IoT is considered as one of the most important part of the fifth generation (5G) wireless systems as it can support massive object communications [7,8]. These massive object communications in the context of IoT is expected to consume a huge power. Therefore, energy efficient green communication within the context of 5G and IoT is a challenging problem to be solved [9].

Sensor nodes are the principal components which brings the idea of IoT into reality [10]. These massive IoT sensor nodes and devices are usually battery operated and hence replacement of battery in such small objects is not a feasible option. Moreover, cooperative communication has been widely studied to mitigate wireless impairments such as fading and other environmental factors [11–14]. However, conventional cooperative relaying techniques requires the participating relaying nodes to spend extra energy for data transmission which may prevent the battery operated IoT nodes to take an active part in relaying. Therefore, wireless energy harvesting (EH) from ambient Radio Frequency (RF) signals is considered as a buoyant energy efficient solution to combat the issue of powering massive IoT sensor and devices [15–17].

RF EH is thus considered as an appealing solution in extending the lifetime of these IoT sensors and devices from months to years and even decades, that ultimately enable their self-sustaining operations [18]. In wireless communication systems, simultaneous information and power transfer (SWIPT) is another emerging paradigm that allows the wireless nodes to recharge themselves through RF signals directed to them from the source node and then relaying or transmitting the information [19]. Meanwhile, accommodating multiple users that can be multiplexed in power domain, non-orthogonal multiple access (NOMA) has been proposed as another important candidate for future 5G technology for providing spectral efficiency and power gains [20,21]. The main idea of NOMA is to serve multiple users in the same frequency band, but with different power levels, which is fundamentally different from conventional orthogonal multiple access schemes [22]. In particular, power-domain NOMA allocates more transmit power to users with worse channel conditions and less transmitting power to users with better channel conditions in order to achieve a balanced trade-off between system throughput and user fairness. Therefore, users can be separated by successive interference cancellation (SIC) at the receiver side [23].

An illustration of generic RF EH relay communication system is shown in Figure 1, where a source node selects one of the RF EH relaying node to transmits its information to its intended destination. The harvested energy from RF source signals allows the relay node to power up themselves for simultaneous information processing and transmission (SWIPT) [24]. It is also understood that using more than one relay increases the complexity of the systems greatly [25]. Such cooperative RF EH relay communication systems as depicted by Figure 1, only considers the transmission of source node data successfully. In this paper, we envisioned an ubiquitous IoT relay system where an IoT node that can acts as a relay for transmitting source node information data to its intended destination and at the same time, it also transmits its own data to its destination node based on NOMA protocol. Furthermore, if EH is employed in such IoT relay systems, it has the potential to provide unlimited energy to sensor nodes and thus enabling self-sustainable green communications [26]. Also, in order for small IoT device to communicate and transmit data, M2M relaying has been proposed as a suitable heterogeneous architecture for 802.16p IoT, Third Generation Partnership Project (3GPP) machine type communications (MTC) and European Telecommunications Standards Institute (ETSI) M2M communication [27]. Hence, we believe that our considered scenario for IoT relay EH system fits to the standardization activities of ETSI and 3GPP projects for self-sustainable green communications.

In SWIPT, time splitting (TS) relaying and power splitting (PS) relaying schemes are very popular for energy harvesting and decoding the information separately. In TS relaying scheme, the receiver switches between energy harvesting and information decoding over time. However, in PS relaying scheme, the receiver uses a portion of received power for energy harvesting purpose and then uses the remaining power for information decoding.

Nasir et al. studied amplify-and-forward (AF) relaying network based on TS and PS relaying schemes [28]. They derived the analytical expressions for outage probability and the ergodic capacity

for delay-limited and delay tolerant transmission modes. Du et al. investigated outage analysis of multi-user cooperative transmission network with TS and PS relay receiver architectures [29]. They theoretically analyze the system outage probability based on TS and PS relaying protocols. A cooperative SWIPT NOMA protocol has been studied in [30]. Here, near NOMA users that are close to source node acts as EH-based relay to help far NOMA users. Considering user selection schemes, they derived the closed-form expressions for the outage probability and system throughput. Ha et al. [31] studied the outage performance of EH-based decode-and-forward (DF) relaying NOMA networks by deriving the closed form equation of the outage probability. Two copies of same information from the source node direct link and EH-based relay link were received at the destination nodes. Kader et al. [32] studied TS and PS with EH and NOMA in a spectrum sharing environment. The secondary transmitter acts as an EH-based relay and then transmits the primary transmitter data along with its data using NOMA protocol. Jain et al. [33] also proposed an EH-based spectrum sharing protocol for wireless sensor networks. However, although a myriad of such EH works have been carried out in the literature, EH considering the energy-efficient data transmission of source and IoT relay node together based on TS, PS and NOMA suitable for IoT relay systems has not been considered in the previous works. This motivated us to propose an RF EH and information transmission based on TS, PS and NOMA for IoT relay systems and analyze their performance by deriving the analytical expressions for outage probability, throughput and sum-throughput.

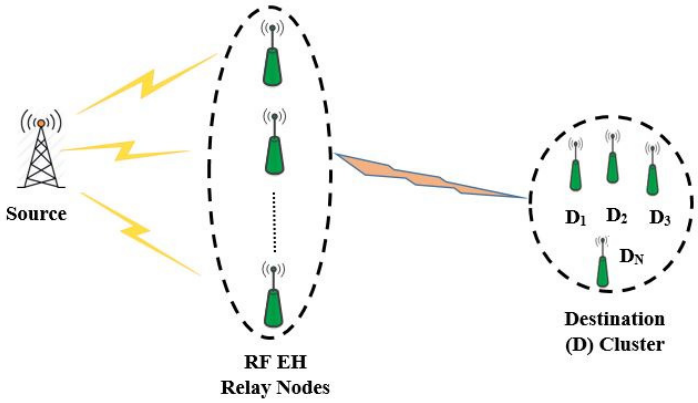

Figure 1. Generic RF EH relay communication system.

In summary, the main contribution of this paper is as follows:

- Realizing the energy constrained nature of IoT nodes, we have considered and investigated an RF EH-based on TS, PS and NOMA for IoT relay systems.
- Although a myriad of works have been carried out in the literature for EH, the absolute vast majority of those works only consider RF EH at relay node and transmission of source node data successfully to its destination node. Those approaches do not consider the data transmission of the relay node that may be an IoT node which needs to transmit its data along with the source node data to their respective destinations. In this paper, we rather focus on RF EH and information transmission based on TS, PS relaying and NOMA for IoT relay systems.
- We have mathematically derived the outage probability, throughput and sum-throughput for our proposed system. We have also formulated an iterative algorithm-Golden Section Search Method to find the optimal time switching and power splitting factor for sum-throughput maximization.
- Our proposed system analytical results for TS and PS are validated by simulation results. The developed analysis is corroborated through Monte-Carlo simulations and some representative performance comparisons are presented.

The rest of the paper is organized as follows. In Section 2, we present the system model for the considered scenario. Section 3 deals with the considered system model based on time switching and NOMA protocol along with outage probability, throughput and sum-throughput derivations. Section 4 deals with the considered system model based on power splitting and NOMA protocol along with outage probability, throughput and sum-throughput derivations. In Section 5, we explain the algorithm—Golden Section Search Method to find out the optimal time switching and power splitting factor that maximizes the sum-throughput for our proposed system. Numerical results and discussions are presented in Section 6. Conclusions and future works are drawn in Section 7.

2. System Model

We have considered a cooperative relaying EH scenario as shown in Figure 2, where a source has to transmit its information data to the destination. Due to fading or weak link between a source-destination pair, the source node seek the help of IoT relay node (IoT_R) for relaying its information data. Here, the source node may be an IoT node which has abundant energy supply from the other sources. Cooperative communication with single relay is a simple but effective communication scheme especially for energy constrained networks such as IoT networks [34]. Furthermore, using more than one relay increases the complexity of the systems greatly [25]. Therefore, we have considered a single IoT_R node for our system model. However, it can be extended to multiple IoT_R node scenario as well.

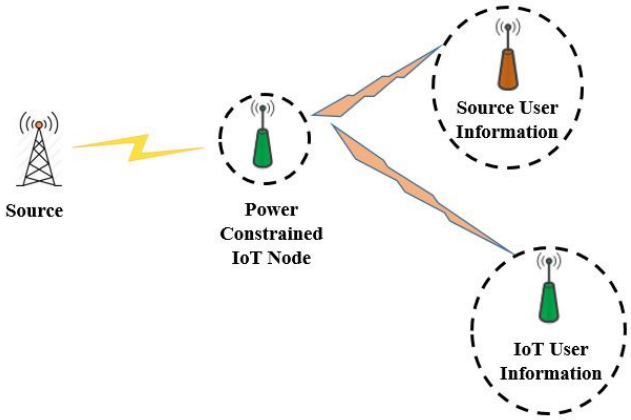

Figure 2. Considered system model scenario.

IoT_R is rather power constrained node that acts as a DF relay. It first harvests the RF energy from source signal using either time switching protocol or power splitting protocol in the first stage and then transmits the source information data along with its own data using NOMA protocol in next subsequent stage. The dual purpose of energy harvesting and forwarding the information data is thus served by IoT_R. The receiving end for source and IoT_R node serves as the destination for data transmission. Unlike several of the previous works, here the information data forwarded by IoT_R node is the source node information data and its own data.

3. System Model Based on Time Switching and NOMA

The proposed system model based on TS and NOMA is shown in Figure 3. In this TS relaying scheme, power constrained IoT_R node first harvests the energy from the source node's RF signal for αT duration and uses the time $\frac{(1-\alpha)T}{2}$ for information processing and $\frac{(1-\alpha)T}{2}$ for information transmission to the source and IoT user using NOMA protocol. We have assumed that all nodes are considered to

be operating in half duplex mode. An independent Rayleigh block fading with channel coefficient $h_i \sim CN(0, \lambda_i = d_i^{-v})$ with zero mean and variance λ_i is assumed between any two nodes where, d_i is the distance between the corresponding link and v is the path loss exponent.The detailed step of our proposed system model based on TS and NOMA is given below.

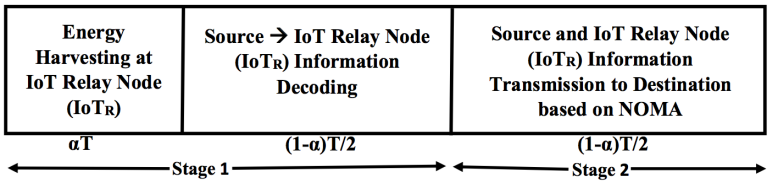

Figure 3. System model based on time switching and NOMA.

3.1. Stage 1

In this stage, the source transmits signal x_s with power P_s to the IoT_R for half of the block time T i.e., $T/2$ period of time. Here, IoT_R node works as TS-based relay. The IoT_R node divide the time block in the ratio αT:$\frac{(1-\alpha)T}{2}$:$\frac{(1-\alpha)T}{2}$. Here αT is for energy harvesting by IoT_R and $\frac{(1-\alpha)T}{2}$ is for information processing by IoT_R respectively, $0 \leq \alpha \leq 1$. The information signal received at IoT_R during this stage is given as:

$$\hat{y}_{IoT_R} = \sqrt{P_s} h_{IoT_R} x_s + n_{IoT_R}, \tag{1}$$

where $n_{IoT_R} \sim CN(0, \sigma^2_{IoT_R})$ is the additive white Gaussian noise at IoT_R with mean zero and variance $\sigma^2_{IoT_R}$. $h_{IoT_R} \sim CN(0, \lambda_h)$ is the channel coefficient between source node and IoT_R node with zero mean and variance λ_h.

The energy harvested at IoT_R in αT duration of time is given as:

$$\hat{E}_{h_{IoT_R}} = \eta P_s |h_{IoT_R}|^2 \alpha T, \tag{2}$$

where $0 \leq \eta \leq 1$ is the energy conversion efficiency. Here, we assume that the pre-processing power for the energy harvesting is negligible in contrast to the transmission power P_s which is in line with the previous works [31–33].

The transmit power of IoT_R i.e., $\hat{P}_{IoT_R}$ in $\frac{(1-\alpha)T}{2}$ block of time can be given as:

$$\hat{P}_{IoT_R} = \frac{\hat{E}_{h_{IoT_R}}}{(1-\alpha)T/2} = \frac{2\eta P_s |h_{IoT_R}|^2 \alpha}{(1-\alpha)}, \tag{3}$$

3.2. Stage 2

In this stage, the IoT_R node transmits a superimposed composite signal $\hat{Z}_{I_{C1}}$ which consists of source information x_s and IoT_R information x_{IoT_R} to the respective destination of source and IoT relay node using NOMA protocol. The superimposed composite signal $\hat{Z}_{I_{C1}}$ following NOMA protocol can be given as:

$$\hat{Z}_{I_{C1}} = \sqrt{\phi_1 \hat{P}_{IoT_R}} x_s + \sqrt{\phi_2 \hat{P}_{IoT_R}} x_{IoT_R} \tag{4}$$

where $\phi_1 + \phi_2 = 1$ and $\phi_2 = 1 - \phi_1$ is the power allocation factor for the NOMA protocol.

Now, the received signals at the receiver of Source user and IoT user can be respectively given as:

$$\hat{y}_{s_{rec}} = \sqrt{\hat{P}_{IoT_R}} h_{s_{rec}} \hat{Z}_{I_{C1}} + n_{s_{rec}}, \tag{5}$$

$$\hat{y}_{IoT_{rec}} = \sqrt{\hat{P}_{IoT_R}} h_{IoT_{rec}} \hat{Z}_{I_{C1}} + n_{IoT_{rec}}, \tag{6}$$

where $n_{s_{rec}}$ and $n_{IoT_{rec}}$ is the additive white Gaussian noise at the receiver of source and IoT user node respectively with mean zero and variance $\sigma^2_{s_{rec}}$ and $\sigma^2_{IoT_{rec}}$. Also, $h_{s_{rec}} \sim CN(0, \lambda_g)$ is the channel coefficient between IoT_R node and receiving source user with zero mean and variance λ_g and $h_{IoT_{rec}} \sim CN(0, \lambda_z)$ is the channel coefficient between IoT_R node and receiving IoT user with zero mean and variance λ_z. We have also assumed that $h_{s_{rec}} > h_{IoT_{rec}}$. Therefore, $\lambda_g > \lambda_z$ and $\phi_1 < \phi_2$.

3.3. Outage Probability, Throughput and Sum-Throughput

According to Equation (1), the received signal to noise ratio (SNR) at IoT_R is given by:

$$\hat{\gamma}_{IoT_R} = \frac{P_s |h_{IoT_R}|^2}{\sigma^2_{IoT_R}} = \hat{\delta} |h_{IoT_R}|^2 \tag{7}$$

where $\hat{\delta} \triangleq \frac{P_s}{\sigma^2_{IoT_R}}$ represents the transmit signal-to-noise ratio (SNR) from the source.

According to Equation (4), the received SNR with x_{IoT_R} and x_s at the receiving source user is given by:

$$\hat{\gamma}^{x_{IoT_R} \to x_s}_{s_{rec}} = \frac{\phi_2 \hat{P}_{IoT_R} |h_{s_{rec}}|^2}{\phi_1 \hat{P}_{IoT_R} |h_{s_{rec}}|^2 + \sigma^2_{s_{rec}}} \tag{8}$$

$$\hat{\gamma}_{s_{rec}} = \frac{\phi_1 \hat{P}_{IoT_R} |h_{s_{rec}}|^2}{\sigma^2_{s_{rec}}} \tag{9}$$

where $\hat{\gamma}^{x_{IoT_R} \to x_s}_{s_{rec}}$ is the SNR required at x_s to decode and cancel x_{IoT_R}.

The received SNR at IoT user associated with symbol x_{IoT_R} is given by:

$$\hat{\gamma}_{IoT_{rec}} = \frac{\phi_2 \hat{P}_{IoT_R} |h_{IoT_{rec}}|^2}{\phi_1 \hat{P}_{IoT_R} |h_{IoT_{rec}}|^2 + \sigma^2_{IoT_{rec}}} \tag{10}$$

As we can see from Figure 2, the data transmission is break down into two separate hops which are independent of each other. Hence, the outage occurs only if source to IoT_R path and IoT_R to corresponding destination path fails to satisfy the SNR constraint. Therefore, the outage probability of the source can be given as:

$$\hat{P}_{Out_S} = Pr(min(\hat{\gamma}_{IoT_R}, \hat{\gamma}_{s_{rec}}) \leq \hat{\psi}) \tag{11}$$

where $\hat{\psi} = 2^R - 1$ is the lower threshold for SNR i.e., outage probability.

Similarly, the outage probability of the IoT relay node IoT_R can be given as:

$$\hat{P}_{Out_{IoT_R}} = Pr(min(\hat{\gamma}^{x_{IoT_R} \to x_s}_{s_{rec}}, \hat{\gamma}_{IoT_{rec}}) \leq \hat{\psi}) \tag{12}$$

The throughput of the source node can be given as:

$$\hat{Thr}_S = \frac{(1 - \hat{P}_{out_S})(1 - \alpha)R}{2} \tag{13}$$

where R is the transmission rate in bits per second per hertz.

The throughput of the IoT relay node IoT_R can be given as:

$$\hat{Thr}_{IoT_R} = \frac{(1 - \hat{P}_{Out_{IoT_R}})(1 - \alpha)R}{2} \tag{14}$$

Therefore, the sum-throughput of the whole system using TS and NOMA can be given as:

$$\hat{Thr} = \hat{Thr}_S + \hat{Thr}_{IoT_R} = \frac{(1 - \hat{P}_{Out_S})(1 - \alpha)R}{2} + \frac{(1 - \hat{P}_{Out_{IoT_R}})(1 - \alpha)R}{2} \tag{15}$$

Theorem 1. *The outage probability and throughput of the source node using TS and NOMA can be expressed as:*

$$\hat{P}_{Out_S} = 1 - 2\sqrt{\frac{\lambda_h \lambda_g x_0}{k}} K_1\left(2\sqrt{\frac{\lambda_h \lambda_g x_0}{k}}\right) + \sum_{n=0}^{\infty} \frac{(-1)^n}{n!} (\lambda_h x_0)^{n+1} E_{n+2}\left(\frac{\lambda_g}{k}\right) \tag{16}$$

$$\hat{Thr}_S = \frac{R(1-\alpha)}{2}\left(2\sqrt{\frac{\lambda_h \lambda_g x_0}{k}} K_1\left(2\sqrt{\frac{\lambda_h \lambda_g x_0}{k}}\right) - \sum_{n=0}^{\infty} \frac{(-1)^n}{n!} (\lambda_h x_0)^{n+1} E_{n+2}\left(\frac{\lambda_g}{k}\right)\right) \tag{17}$$

where, $x_0 = \frac{\hat{\psi}}{\hat{\delta}}$, $k = \frac{2\alpha\eta\phi_1}{(1-\alpha)}$, $K_1(.)$ *is a first-order modified Bessel function of the second kind, and* $E_n(a) = \int_{y=1}^{\infty} y^{-n} e^{-ay} dy$ *is the exponential integral of order n.*

Proof. The detailed proof is given in Appendix A. □

Theorem 2. *The outage probability and throughput of the IoT relay node using TS and NOMA can be expressed as:*

$$\hat{P}_{Out_{IoT_R}} = 1 - 2\sqrt{d\lambda_h(\lambda_g + \lambda_z)} K_1\left(2\sqrt{d\lambda_h(\lambda_g + \lambda_z)}\right) \tag{18}$$

$$\hat{Thr}_{IoT_R} = \frac{R(1-\alpha)}{2}\left(2\sqrt{d\lambda_h(\lambda_g + \lambda_z)} K_1\left(2\sqrt{d\lambda_h(\lambda_g + \lambda_z)}\right)\right) \tag{19}$$

where, $d = \frac{\hat{\psi}}{(\phi_2 - \phi_1\hat{\psi})l}$, $l = \frac{2\alpha\eta P_s}{(1-\alpha)}$

Proof. The detailed proof is given in Appendix B. □

Combining Equations (17) and (19), we finally get the analytical equation for the sum-throughput of the proposed system using TS and NOMA.

4. System Model Based on Power Splitting and NOMA

The proposed system model based on PS and NOMA protocol is shown in Figure 4. In this PS relaying scheme, power constrained (IoT_R) node first harvests the energy from the source node signal using ϵP_s where P_s is the power of the source transmit signal. IoT_R uses remaining power $(1-\epsilon)P_s$ for information processing.

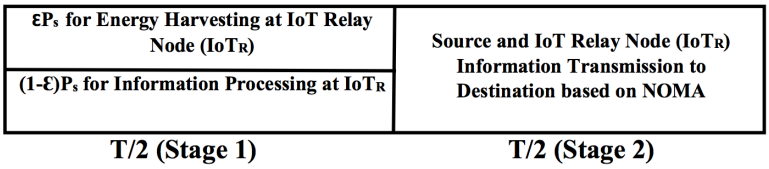

Figure 4. System model based on power splitting and NOMA.

4.1. Stage 1

During this stage, a source node signal x_s with P_s power is transmitted to the IoT_R node for half of the block time T i.e., $T/2$ period of time. The IoT_R node divide the received power P_s in the ratio εP_s:$(1-\varepsilon)P_s$. Accordingly here, εP_s is for energy harvesting and $(1-\varepsilon)P_s$ is for information processing by IoT_R respectively, $0 \leq \varepsilon \leq 1$. The information signal received at IoT_R during this stage is given as:

$$y_{IoT_R} = \sqrt{P_s} h_{IoT_R} x_s + n_{IoT_R}, \tag{20}$$

The energy harvested at IoT_R in $T/2$ period of time is given as:

$$E_{h_{IoT_R}} = \frac{\eta \varepsilon P_s |h_{IoT_R}|^2 T}{2}, \tag{21}$$

The signal received at the information receiver of the IoT_R is given as:

$$\sqrt{(1-\varepsilon)} y_{IoT_R} = \sqrt{(1-\varepsilon) P_s} h_{IoT_R} x_s + n_{IoT_R}, \tag{22}$$

The transmit power of IoT_R i.e., P_{IoT_R} in $T/2$ block of time is given as:

$$P_{IoT_R} = \frac{E_{h_{IoT_R}}}{T/2} = \eta \varepsilon P_s |h_{IoT_R}|^2, \tag{23}$$

4.2. Stage 2

In this stage, the IoT_R node transmits a superimposed composite signal $Z_{I_{C1}}$ which consists of source information x_s and IoT_R information x_{IoT_R} to the respective destination node i.e., source user and IoT user using NOMA protocol. The superimposed composite signal $Z_{I_{C1}}$ following NOMA protocol is given as:

$$Z_{I_{C1}} = \sqrt{\phi_1 P_{IoT_R}} x_s + \sqrt{\phi_2 P_{IoT_R}} x_{IoT_R} \tag{24}$$

where $\phi_1 + \phi_2 = 1$ and $\phi_2 = 1 - \phi_1$.

Now, the received signals at the respective source user and IoT user can be given as:

$$y_{s_{rec}} = \sqrt{P_{IoT_R}} h_{s_{rec}} Z_{I_{C1}} + n_{s_{rec}}, \tag{25}$$

$$y_{IoT_{rec}} = \sqrt{P_{IoT_R}} h_{IoT_{rec}} Z_{I_{C1}} + n_{IoT_{rec}}, \tag{26}$$

4.3. Outage Probability, Throughput and Sum-Throughput

According to Equation (22), the received signal to noise ratio (SNR) at IoT_R node is given by:

$$\gamma_{IoT_R} = \frac{(1-\varepsilon) P_s |h_{IoT_R}|^2}{\sigma^2_{IoT_R}} = (1-\varepsilon) \delta |h_{IoT_R}|^2 \tag{27}$$

where $\delta \triangleq \frac{P_s}{\sigma^2_{IoT_R}}$ represents the transmit signal-to-noise ratio (SNR) from the source.

According to Equation (25), the received SNR with x_{IoT_R} and x_s at the receiving source user is given by:

$$\gamma_{s_{rec}}^{x_{IoT_R} \to x_s} = \frac{\phi_2 P_{IoT_R} |h_{s_{rec}}|^2}{\phi_1 P_{IoT_R} |h_{s_{rec}}|^2 + \sigma^2_{s_{rec}}} \tag{28}$$

$$\gamma_{s_{rec}} = \frac{\phi_1 P_{IoT_R} |h_{s_{rec}}|^2}{\sigma^2_{s_{rec}}} \tag{29}$$

where $\gamma_{s_{rec}}^{x_{IoT_R} \to x_s}$ is the SNR required at the receiving source user to decode and cancel IoT_R information i.e., x_{IoT_R}.

The received SNR at the receiving IoT user node associated with symbol x_{IoT_R} is given by:

$$\gamma_{IoT_{rec}} = \frac{\phi_2 P_{IoT_R} |h_{IoT_{rec}}|^2}{\phi_1 P_{IoT_R} |h_{IoT_{rec}}|^2 + \sigma^2_{IoT_{rec}}} \tag{30}$$

As we can see from Figure 2, the data transmission is break down into two separate hops which are independent of each other. Hence, the outage occurs only if source to IoT_R path and IoT_R to corresponding destination path fails to satisfy the SNR constraint. Therefore, the outage probability of the source node can be given as:

$$P_{Out_S} = Pr(min(\gamma_{IoT_R}, \gamma_{s_{rec}}) \leq \psi) \tag{31}$$

where $\psi = 2^R - 1$ is the lower threshold for SNR i.e., outage probability, R being the target data rate.

Similarly, the outage probability of the IoT_R node can be given as:

$$P_{Out_{IoT_R}} = Pr(min(\gamma_{s_{rec}}^{x_{IoT_R} \to x_s}, \gamma_{IoT_{rec}}) \leq \psi) \tag{32}$$

The throughput of the source node can be given as:

$$Thr_S = \frac{(1 - P_{Out_S})R}{2} \tag{33}$$

where R is measured in bits per second per hertz.

The throughput of the IoT relay node can be given as:

$$Thr_{IoT_R} = \frac{(1 - P_{Out_{IoT_R}})R}{2} \tag{34}$$

The factor $1/2$ in Equations (33) and (34) is originated by the predicament that the two transmission phases are involved in the system.

Therefore, the sum-throughput of the whole system can be given as:

$$Thr = Thr_S + Thr_{IoT_R} = (1 - P_{Out_S})\frac{R}{2} + (1 - P_{Out_{IoT_R}})\frac{R}{2} \tag{35}$$

Theorem 3. *The outage probability and throughput of the source node using PS and NOMA can be expressed as:*

$$P_{Out_S} = 1 - 2\sqrt{\frac{\lambda_h \lambda_g (1-\varepsilon) x_0}{a}} K_1\left(2\sqrt{\frac{\lambda_h \lambda_g (1-\varepsilon) x_0}{a}}\right) + \sum_{n=0}^{\infty} \frac{(-1)^n}{n!} (\lambda_h x_0)^{n+1} E_{n+2}\left(\frac{(1-\varepsilon)\lambda_g}{a}\right) \tag{36}$$

$$Thr_S = \frac{R}{2}\left(2\sqrt{\frac{\lambda_h \lambda_g (1-\varepsilon) x_0}{a}} K_1\left(2\sqrt{\frac{\lambda_h \lambda_g (1-\varepsilon) x_0}{a}}\right) - \sum_{n=0}^{\infty} \frac{(-1)^n}{n!} (\lambda_h x_0)^{n+1} E_{n+2}\left(\frac{(1-\varepsilon)\lambda_g}{a}\right)\right) \tag{37}$$

where $x_0 = \frac{\psi}{(1-\varepsilon)\delta}$, $a = \varepsilon\eta\phi_1$, $K_1(.)$ *is a first-order modified Bessel function of the second kind, and* $E_n(a) = \int_{y=1}^{\infty} y^{-n} e^{-ay} dy$ *is the exponential integral of order n.*

Proof. The detailed proof is formulated in Appendix C. □

Theorem 4. *The outage probability and throughput of the IoT node using PS and NOMA can be expressed as:*

$$P_{Out_{IoT_R}} = 1 - 2\sqrt{c\lambda_h(\lambda_g + \lambda_z)} K_1\left(2\sqrt{c\lambda_h(\lambda_g + \lambda_z)}\right) \tag{38}$$

$$Thr_{IoT_R} = \frac{R}{2}\left(2\sqrt{c\lambda_h(\lambda_g + \lambda_z)} K_1\left(2\sqrt{c\lambda_h(\lambda_g + \lambda_z)}\right)\right) \tag{39}$$

where $c = \frac{\psi}{(\phi_2 - \phi_1\psi)b}$, $b = \eta\delta\varepsilon$.

Proof. The detailed proof is formulated in Appendix D. □

Combining Equations (37) and (39), we finally get the analytical equation for the sum-throughput of the proposed system using PS and NOMA.

5. Optimal Time Switching α^* and Optimal Power Splitting Factor ε^* for Sum-Throughput Maximization

To find out optimal time switching factor α^* and power splitting factor ε^* that gives the best performance for sum-throughput maximization for our proposed system using TS, PS and NOMA, we evaluate $\left(\frac{d\hat{Thr}(\alpha)}{d\alpha}\right)_{TS} = 0$ and $\left(\frac{dThr(\varepsilon)}{d\varepsilon}\right)_{PS} = 0$, where $\hat{Thr}(\alpha)$ is the sum-throughput function with respect to time switching factor α and $Thr(\varepsilon)$ is the sum-throughput function with respect to power splitting factor ε respectively. By analyzing the sum-throughput function for source and IoT node versus α and ε, we determine that this is concave function which has a unique maxima α^*, ε^* on the interval $[0, 1]$. Therefore, we resort to Golden section search method [35] which is simple yet compelling iterative process to find out the optimal α^* and ε^* that maximizes the sum-throughput of the proposed system using TS and PS respectively. The Golden section search method for determining optimal α^* and ε^* is shown in Algorithm 1.

Algorithm 1 Golden Section Search Method for Finding Optimal Time Switching Factor α^* and Optimal Power Splitting Factor ε^*

Input: η, δ, R, ϕ_1, ϕ_2

Initialization: Set the start interval $a = 0.001$, end interval $b = 0.99$, golden proportion coefficient $\tau = 0.618$, the iteration index, accuracy value $\mu = 0.000001$, choose starting points $x_1 = a + (1 - \tau) * (b - a)$ and $x_2 = a + \tau * (b - a)$

Output: Optimal α^* and ε^*

do function evaluation for respective TS and PS protocol i.e., $\left(\frac{d\hat{Thr}(\alpha)}{d\alpha}\right)_{TS}$, $\left(\frac{dThr(\varepsilon)}{d\varepsilon}\right)_{PS}$ at point x_1 and x_2

repeat

if evaluated function $\left(\frac{d\hat{Thr}(\alpha)}{d\alpha}\right)_{x_1} < \left(\frac{d\hat{Thr}(\alpha)}{d\alpha}\right)_{x_2}$, $\left(\frac{dThr(\varepsilon)}{d\varepsilon}\right)_{x_1} < \left(\frac{dThr(\varepsilon)}{d\varepsilon}\right)_{x_2}$ then

choose $b = x_2$, $x_2 = x_1$ and find new point x_1 for both TS and PS

do function evaluation as step 1

else

$a = x_1$, $x_1 = x_2$ and find new point x_2 for both TS and PS

do function evaluation as step 1

end if

until $|b - a| > \mu$ and iteration index = max

Choosing Optimal α^* for TS

if evaluated function $\left(\frac{d\hat{Thr}(\alpha)}{d\alpha}\right)_{x_1} < \left(\frac{d\hat{Thr}(\alpha)}{d\alpha}\right)_{x_2}$ then

$\alpha^* = x_1$

else

$\alpha^* = x_2$

Choosing Optimal ε^* for PS

if evaluated function $\left(\frac{dThr(\varepsilon)}{d\varepsilon}\right)_{x_1} < \left(\frac{dThr(\varepsilon)}{d\varepsilon}\right)_{x_2}$ then

$\varepsilon^* = x_1$

else

$\varepsilon^* = x_2$

end of Algorithm 1

6. Numerical Results and Discussion

In this section, we present Monte-Carlo simulation results to verify our analysis for the proposed system as explained in the previous section for both TS and PS protocol. The simulation parameters are given in Table 1. We use MATLAB to run the Monte-Carlo simulation by averaging over 10^5 random realizations of Rayleigh block fading channels h_{IoT_R}, $h_{s_{rec}}$, $h_{IoT_{rec}}$ and get the simulation results. In Figures 5 and 6, the outage probability of the source user and IoT relay user are plotted against the transmit SNR at different time switching factor α = 0.3, 0.5, & 0.7 for TS relaying and different power splitting factor ε = 0.3, 0.5, & 0.7 for PS relaying. It can be observed that outage probability is a decreasing function with respect to increase in transmit SNR and α for TS protocol. It can also be observed that outage probability is also a decreasing function with respect to increase in transmit SNR and ε for PS protocol. Furthermore, our analysis exactly matched with the simulation results as depicted in Figures 5 and 6. From Figures 5 and 6, it should be noted that the outage probability of the source and IoT relay user using PS is higher than the TS protocol for our proposed system.

Table 1. Simulation Parameters.

Parameter	Symbol	Values
Mean of $\|h_{IoT_R}\|^2 \rightarrow X$	λ_h	1
Mean of $\|h_{s_{rec}}\|^2 \rightarrow Y$	λ_g	1
Mean of $\|h_{IoT_{rec}}\|^2 \rightarrow Z$	λ_z	0.5
Source Node Transmit SNR	δ	0–20 dB
Energy Harvesting Efficiency	η	1
Source and IoT Node Rate	R	1 bps/Hz
Power Factor for NOMA	ϕ_1	0.2
Power Factor for NOMA	ϕ_2	0.8
Noise Variance	$\sigma^2_{IoT_{rec}}, \sigma^2_{s_{rec}}$	1

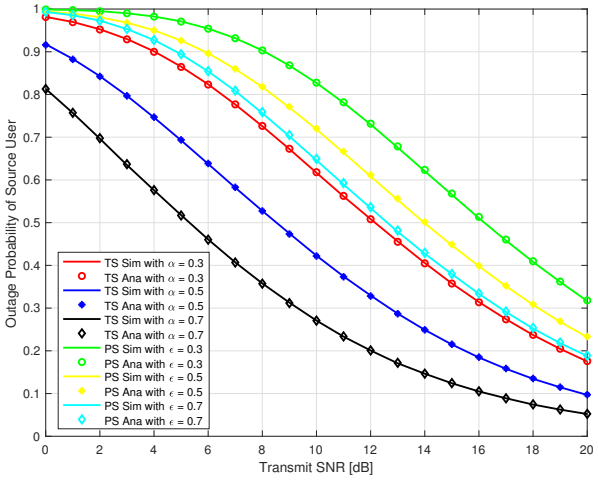

Figure 5. Outage Probability of Source User.

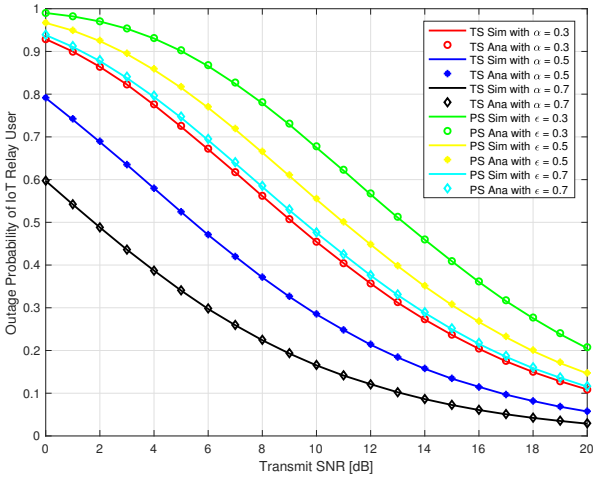

Figure 6. Outage Probability of IoT Relay User.

Considering, source user and IoT relay user as two user in the system for our proposed system, in Figure 7, we plotted the sum-throughput against the transmit SNR at time switching α = 0.3, 0.5, & 0.7 for TS and different power splitting factor ε = 0.3, 0.5, & 0.7 for PS. It can be observed that sum-throughput is a increasing function with respect to increase in transmit SNR and α for TS. Also, it is observed that sum-throughput is a increasing function with respect to increase in δ and ε for PS. Moreover, sum-throughput is higher for PS as compared to TS with the same varying amount of α and ε respectively for transmit SNR greater than 10 dB. At transmit SNR less than 6 dB, TS outperforms the PS protocol.

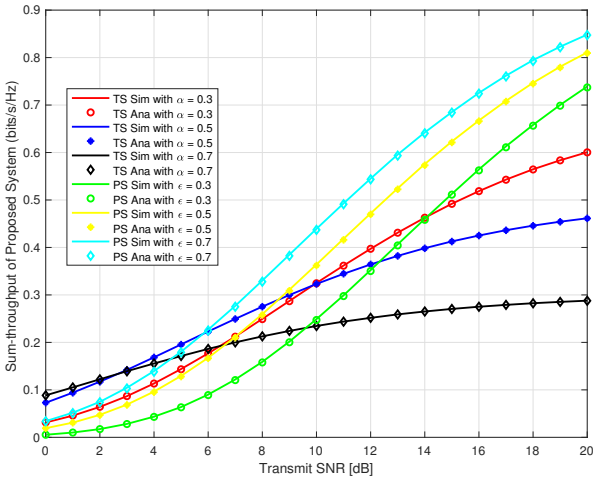

Figure 7. Sum-throughput of proposed system.

Next, we wanted to verify our analysis for the proposed system at different time switching factor α and power splitting factor ε for both TS and PS protocol. We plotted the sum-throughput against

the α and ε varying from 0 to 1 and at δ = 5, 10, & 15. In Figure 8, we can observe the trend that, the sum-throughput first increases with the increase in α, ε, and δ, reaches to the maximum and then decreases. Similarly, in Figure 9, we plotted the sum-throughput for our proposed system with $\delta = 10$ at varying energy harvesting efficiency factor η = 0.6, 0.8, & 1.0 for both TS and PS. We can observe a similar trend as in Figure 8. The sum-throughput of the system first increases with the increase in α, ε, and η, reaches to the maximum and then decreases. This confirms that the sum-throughput is maximum at some optimal time switching factor α^* and optimal power splitting factor ε^*. In reality, we cannot have high α and ε as there will be less time and power allocated for information processing. Hence, there will be an outage in the system as no communication data will be transferred to the respective destinations.

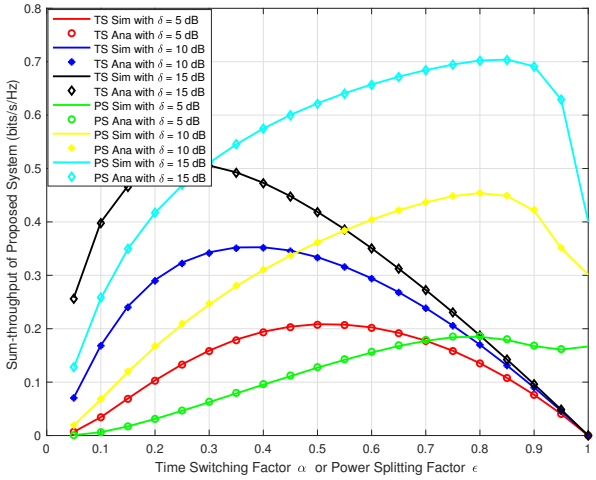

Figure 8. Sum-throughput of proposed system v/s α or ϵ with different δ.

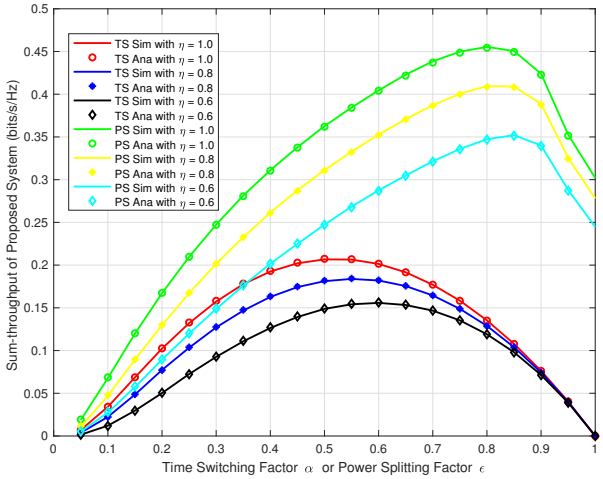

Figure 9. Sum-throughput of proposed system v/s α or ϵ with different η.

Therefore, we need to find optimal α^* and ε^* that maximizes the sum-throughput for the proposed system for TS and PS respectively. In Figures 10 and 11, we found out optimal α^* for TS and optimal ε^* for PS respectively that maximizes the sum-throughput of the proposed system through Golden section search method as explained in Algorithm 1 and plotted it against the transmit SNR. In Figure 10, we can observe that optimal α^* linearly decreases with increase in transmit SNR. Also, in Figure 11, we can see that optimal ε^* first decrease and then slightly tends to increase with increase in transmit SNR. Finding optimal α^* and ε^* is important to avoid an outage in the proposed system and maximizing the sum-throughput.

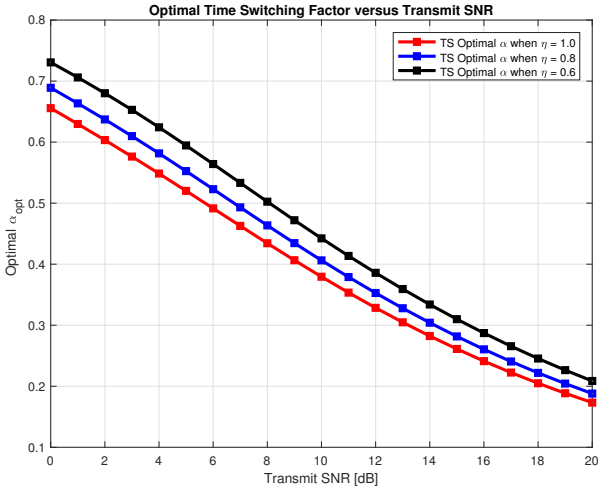

Figure 10. Optimal α for sum-throughput maximization.

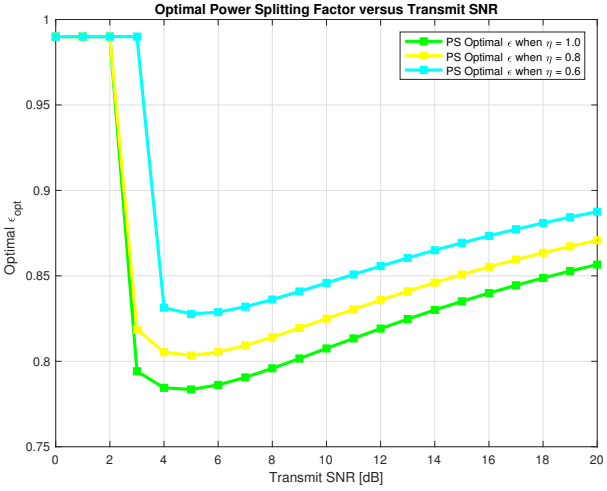

Figure 11. Optimal ϵ for sum-throughput maximization.

7. Conclusions and Future Works

In this paper, we presented our model on RF energy harvesting and information transmission in IoT relay systems based on time switching, power splitting and NOMA. Considering the energy constrained nature of the IoT nodes, here a power constrained IoT relay node first harvests the energy from the source node RF signal to power up themselves. The IoT relay node can harvests the energy using either time switching relaying or power splitting relaying protocol. Then in the next subsequent stage, IoT relay node transmits the source node information along with its information data using NOMA protocol. We have mathematically derived the outage probability, throughput and sum-throughput for our proposed system based on TS, PS and NOMA. Furthermore, we verified our derived analysis with the simulation results and some representative performance comparisons were presented. We showed that our analytical results for TS and PS relaying protocol exactly matched with the simulation results. We also found out the optimal time switching factor α^* and optimal power splitting factor ε^* that maximizes the sum-throughput of the proposed system through the formulated Golden section search algorithm as shown in Algorithm 1.

For future work, we would like to investigate the ergodic capacity of the proposed system and derive the exact-forms of outage probability and sum-throughput for the proposed system. We would also like to study the performance of our proposed system by introducing interference from other nodes.

Author Contributions: A.R. and P.E. conceived the idea; A.R. designed the experiments, performed the simulation experiments and analyzed the data; O.N.Ø. contributed to developing some mathematical analysis part; A.R. wrote the paper; P.E. and O.N.Ø. critically reviewed the paper.

Funding: This research is supported through KD funding from Norwegian Ministry of Education.

Conflicts of Interest: The authors declare no conflict of interest.

Abbreviations

The following abbreviations are used in this manuscript:

Symbol	Meaning
IoT_R	IoT relay node
P_s	Power of source node transmit signal
RF	Radio Frequency
EH	Energy Harvesting
SNR	Signal-to-noise ratio
NOMA	Non-orthogonal multiple access
PS	Power splitting
DF	Decode and Forward
ϵ	Power splitting factor
x_s	Source node information data
T	Time period
y_{IoT_R}, $\hat{y}_{IoT_R}$	Information signal received at IoT_R
n_{IoT_R}	Additive White Gaussian Nosie at IoT_R
$\sigma^2_{IoT_R}$	Noise variance at IoT_R
h_{IoT_R}	Channel co-efficient between source node and IoT_R node
λ_h	Mean variance of h_{IoT_R}
$h_{s_{rec}}$	Channel co-efficient between IoT_R and source user
λ_g	Mean variance of $h_{s_{rec}}$
$h_{IoT_{rec}}$	Channel co-efficient between IoT_R and IoT user
λ_z	Mean variance of $h_{IoT_{rec}}$
η	Energy conversion efficiency

$E_{h_{IoT_R}}$, $\hat{E}_{h_{IoT_R}}$	Energy harvested at IoT_R node
P_{IoT_R}, $\hat{P}_{IoT_R}$	Transmit power of IoT_R node
$Z_{I_{C1}}$,$\hat{Z}_{I_{C1}}$	Superimposed composite signal for NOMA protocol
ϕ_1,ϕ_2	Power allocation factors for NOMA protocol
x_{IoT_R}	IoT_R node information data
$y_{s_{rec}}$, $\hat{y}_{s_{rec}}$	Received signal at destination source user
$y_{IoT_{rec}}$, $\hat{y}_{IoT_{rec}}$	Received signal at destination IoT user
$n_{s_{rec}}$, $\hat{y}_{IoT_{rec}}$	Additive White Gaussian Nosie at destination source user
$n_{IoT_{rec}}$	Additive White Gaussian Nosie at destination IoT user
γ_{IoT_R}, $\hat{\gamma}_{IoT_R}$	Received SNR at IoT_R node
δ, $\hat{\delta}$	Transmit SNR
$\gamma_{s_{rec}}^{x_{IoT_R}\to x_s}$, $\hat{\gamma}_{s_{rec}}^{x_{IoT_R}\to x_s}$	SNR required at the destination source user to decode and cancel IoT_R information data
$\gamma_{s_{rec}}$, $\hat{\gamma}_{s_{rec}}$	Received SNR at destination source user node
$\gamma_{IoT_{rec}}$, $\hat{\gamma}_{IoT_{rec}}$	Received SNR at destination IoT_R user node
$\sigma^2_{s_{rec}}$	Noise variance at destination source user node
$\sigma^2_{IoT_{rec}}$	Noise variance at destination IoT_R user node
ψ, $\hat{\psi}$	Outage probability
P_{Out_S}, $\hat{P}_{Out_S}$	Outage probability of source node
$P_{Out_{IoT_R}}$, $\hat{P}_{Out_{IoT_R}}$	Outage probability of IoT_R node
R	Rate in bits per second per hertz
Thr_S, $\hat{Thr}_S$	Throughput of source node
Thr_{IoT_R}, $\hat{Thr}_{IoT_R}$	Throughput of IoT_R node
Thr, $\hat{Thr}$	Sum-throughput of whole system
α^*	Optimal time switching factor
ε^*	Optimal power splitting factor
$K_1(.)$	First-order modified Bessel function of the second kind
$E_n(a)$	Exponential integral of order n

Appendix A. Proof of Theorem 1 in (16) and (17)

From Equation (7) we have,

$$\hat{\gamma}_{IoT_R} = \hat{\delta}X \text{ where, } |h_{IoT_R}|^2 = X$$

Also, from Equation (9), we have,

$$\hat{\gamma}_{s_{rec}} = \frac{\phi_1 \hat{P}_{IoT_R}|h_{s_{rec}}|^2}{\sigma^2_{s_{rec}}} \triangleq \delta XYk$$

where

$$Y = |h_{s_{rec}}|^2, \sigma^2_{s_{rec}} = 1, k = \frac{2\alpha\eta P_s}{(1-\alpha)}$$

From Equation (11), the outage probability of the source is:

$$\begin{aligned}\hat{P}_{Out_S} &= Pr(min(\hat{\gamma}_{IoT_R}, \hat{\gamma}_{s_{rec}}) < \hat{\psi})\\ &= 1 - Pr(min(\hat{\gamma}_{IoT_R}, \hat{\gamma}_{s_{rec}}) \geq \hat{\psi})\\ &= 1 - Pr(\hat{\delta}X \geq \hat{\psi}, \hat{\delta}kXY \geq \hat{\psi})\\ &= 1 - Pr\left(X \geq \frac{\hat{\psi}}{\hat{\delta}}, Y \geq \frac{\hat{\psi}}{\hat{\delta}kX}\right)\end{aligned}$$

Let

$$\begin{aligned}
x_0 &= \frac{\hat{\psi}}{\delta}, \\
&= 1 - Pr\left(X \geq x_0, Y \geq \frac{x_0}{kX}\right) \\
&= 1 - \int_{x_0}^{\infty} f_X(x)\left(\int_{\frac{x_0}{kx}}^{\infty} f_Y(y)dy\right)dx \\
&= 1 - \int_{x_0}^{\infty} \lambda_h e^{-\lambda_h x}\left(\int_{\frac{x_0}{kx}}^{\infty} \lambda_g e^{-\lambda_g y}dy\right)dx \\
&= 1 - \int_{x_0}^{\infty} \lambda_h e^{-\lambda_h x}\left(e^{-\lambda_g \frac{x_0}{kx}}\right)dx \\
&= 1 - \int_{x_0}^{\infty} \lambda_h \left(e^{-\lambda_h x - \lambda_g \frac{x_0}{kx}}\right)dx \\
&= 1 - \left(\underbrace{\lambda_h \int_{x=0}^{\infty} \left(e^{-4\lambda_g \frac{x_0}{k4x} - \lambda_h x}\right)dx}_{I_1} - \underbrace{\lambda_h \int_{x=0}^{x_0} \left(e^{-\lambda_g \frac{x_0}{kx} - \lambda_h x}\right)dx}_{I_2}\right)
\end{aligned}$$

Let us first evaluate the integral I_1 by using the formula [36], Equation 3.324.1)

$$\begin{aligned}
\int_0^{\infty} e^{-\frac{\beta}{4x} - \gamma x}dx &= \sqrt{\frac{\beta}{\gamma}} K_1 \sqrt{\beta\gamma} \\
I_1 &= \lambda_h \sqrt{\frac{4\lambda_g x_0}{k\lambda_h}} K_1\left(\sqrt{\frac{4\lambda_g x_0 \lambda_h}{k}}\right) \\
I_1 &= 2\sqrt{\frac{\lambda_h \lambda_g x_0}{k}} K_1\left(2\sqrt{\frac{\lambda_h \lambda_g x_0}{k}}\right)
\end{aligned}$$

Now, let us evaluate the integral I_2

$$I_2 = \lambda_h \int_{x=0}^{x_0} \left(e^{-\lambda_h x - \frac{\lambda_g x_0}{kx}}\right)dx$$

Expanding the term $e^{-\lambda_h x}$ in Taylor series

$$= \lambda_h \sum_{n=0}^{\infty} \frac{(-1)}{n\,!}(\lambda_h)^n \int_{x=0}^{x_0} x^n e^{-\frac{\lambda_g x_0}{kx}}dx$$

Substituting $y = \frac{1}{x} \rightarrow dx = -\frac{1}{y^2}dy$

$$= \sum_{n=0}^{\infty} \frac{(-1)}{n\,!}(\lambda_h)^{n+1} \int_{y=\frac{1}{x_0}}^{\infty} y^{-n-2} e^{-\frac{\lambda_g x_0 y}{k}}dy$$

Now, substituting further $t = x_0 y \rightarrow dt = x_0 dy$

$$= \sum_{n=0}^{\infty} \frac{(-1)}{n\,!}(\lambda_h x_0)^{n+1} \int_{t=1}^{\infty} t^{-n-2} e^{-\frac{\lambda_g t}{k}}dt$$

Now, by definition of exponential integral of order n, we have,

$$\begin{aligned}
E_n(a) &= \int_{y=1}^{\infty} y^{-n} e^{-ay}dy \\
I_2 &= \sum_{n=0}^{\infty} \frac{(-1)}{n\,!}(\lambda_h x_0)^{n+1} E_{n+2}\left(\frac{\lambda_g}{k}\right)
\end{aligned}$$

Therefore,

$$\begin{aligned}
\hat{P}_{Out_S} &= 1 - I_1 + I_2 \\
\hat{P}_{Out_S} &= 1 - 2\sqrt{\frac{\lambda_h \lambda_g x_0}{k}} K_1\left(2\sqrt{\frac{\lambda_h \lambda_g x_0}{k}}\right) + \sum_{n=0}^{\infty} \frac{(-1)^n}{n\,!}(\lambda_h x_0)^{n+1} E_{n+2}\left(\frac{\lambda_g}{k}\right)
\end{aligned}$$

Putting the value of $\hat{P}_{Out_S}$ in Equation (13), we get,

$$\hat{Thr}_S = \frac{R(1-\alpha)}{2}\left(2\sqrt{\frac{\lambda_h\lambda_g x_0}{k}}K_1\left(2\sqrt{\frac{\lambda_h\lambda_g x_0}{k}}\right) - \sum_{n=0}^{\infty}\frac{(-1)^n}{n!}(\lambda_h x_0)^{n+1}E_{n+2}\left(\frac{\lambda_g}{k}\right)\right)$$

This ends the proof of Theorem 1.

Appendix B. Proof of Theorem 1 in (18) and (19)

From Equation (12), the outage probability of IoT relay node is:

$$\hat{P}_{Out_{IoT_R}} = Pr(min(\hat{\gamma}_{S_{rec}}^{x_{IoT_R}\to x_s}, \hat{\gamma}_{IoT_{rec}}) < \hat{\psi})$$
$$\hat{P}_{Out_{IoT_R}} = 1 - Pr(\tfrac{\phi_2 lXY}{\phi_1 lXY+1} \geq \hat{\psi}, \tfrac{\phi_2 lXZ}{\phi_1 lXZ+1} \geq \hat{\psi})$$

where

$$\hat{P}_{IoT_R} = \frac{2\alpha\eta P_s|h_{IoT_R}|^2}{(1-\alpha)} \triangleq \frac{2\alpha\eta\hat{\delta}X}{(1-\alpha)}, l = \frac{2\alpha\eta\hat{\delta}}{(1-\alpha)}$$

$$X = |h_{IoT_R}|^2, Y = |h_{S_{rec}}|^2, Z = |h_{IoT_{rec}}|^2, \sigma^2_{IoT_{rec}} = 1, \sigma^2_{S_{rec}} = 1$$
$$= 1 - Pr(Y \geq \tfrac{\hat{\psi}}{(\phi_2-\phi_1\hat{\psi})lX}, Z \geq \tfrac{\hat{\psi}}{(\phi_2-\phi_1\hat{\psi})lX})$$

Conditioning on X, we have,

$$= 1 - \int_0^\infty Pr(Y \geq \frac{\hat{\psi}}{(\phi_2-\phi_1\hat{\psi})lx}) \times Pr(Z \geq \frac{\hat{\psi}}{(\phi_2-\phi_1\hat{\psi})lx}) f_X(x)dx$$

put

$$\tfrac{\hat{\psi}}{(\phi_2-\phi_1\hat{\psi})lx} = T$$
$$= 1 - \int_0^\infty Pr(Y \geq T)Pr(Z \geq T)f_X(x)dx$$
$$= 1 - \int_0^\infty \left(\int_T^\infty \lambda_g e^{-\lambda_g y}dy\right)\left(\int_T^\infty \lambda_z e^{-\lambda_z z}dz\right)\lambda_h e^{-\lambda_h x}dx$$
$$= 1 - \int_0^\infty e^{-\lambda_g T}e^{-\lambda_z T}\lambda_h e^{-\lambda_h x}dx$$
$$= 1 - \int_0^\infty e^{-\lambda_g T}e^{-\lambda_z T}\lambda_h e^{-\lambda_h x}dx$$

substituting the value of T above

$$= 1 - \int_0^\infty e^{-\lambda_g \frac{\hat{\psi}}{(\phi_2-\phi_1\hat{\psi})lx}} e^{-\lambda_z \frac{\hat{\psi}}{(\phi_2-\phi_1\hat{\psi})lx}} \lambda_h e^{-\lambda_h x}dx$$

let

$$d = \tfrac{\hat{\psi}}{(\phi_2-\phi_1\hat{\psi})l}$$
$$= 1 - \int_0^\infty e^{-\lambda_g \frac{d}{x}} e^{-\lambda_z \frac{d}{x}} \lambda_h e^{-\lambda_h x}dx$$
$$= 1 - \lambda_h \int_0^\infty e^{-4(\lambda_g+\lambda_z)\frac{c}{4x} - \lambda_h x}dx$$

Now, using the formula

$$\int_0^\infty e^{-\frac{\beta}{4x}-\gamma x}dx = \sqrt{\frac{\beta}{\gamma}}K_1\sqrt{\beta\gamma}$$
$$= 1 - \lambda_h\sqrt{\tfrac{4(\lambda_g+\lambda_z)d}{\lambda_h}}K_1\left(\sqrt{4(\lambda_g+\lambda_z)d\lambda_h}\right)$$
$$\hat{P}_{Out_{IoT_R}} = 1 - 2\sqrt{d\lambda_h(\lambda_g+\lambda_z)}K_1\left(2\sqrt{d\lambda_h(\lambda_g+\lambda_z)}\right)$$

Putting the value of $\hat{P}_{Out_{IoT_R}}$ in Equation (14), we get,

$$\hat{Thr}_{IoT_R} = \frac{R(1-\alpha)}{2}\left(2\sqrt{d\lambda_h(\lambda_g+\lambda_z)}K_1\left(2\sqrt{d\lambda_h(\lambda_g+\lambda_z)}\right)\right)$$

This ends the proof of Theorem 2.

Appendix C. Proof of Theorem 1 in (36) and (37)

From Equation (27), we have,

$$\gamma_{IoT_R} = (1-\varepsilon)\delta X \text{ where } |h_{IoT_R}|^2 = X$$

Also, from Equation (29), we have,

$$\gamma_{s_{rec}} = \frac{\phi_1 P_{IoT_R}|h_{s_{rec}}|^2}{\sigma^2_{s_{rec}}} \triangleq \delta XYa$$

where

$$Y = |h_{s_{rec}}|^2, \sigma^2_{s_{rec}} = 1, a = \eta\varepsilon\phi_1$$

From Equation (31), the outage probability of the source is:

$$\begin{aligned} P_{Out_S} &= Pr(min(\gamma_{IoT_R}, \gamma_{s_{rec}}) < \psi) \\ &= 1 - Pr(min(\gamma_{IoT_R}, \gamma_{s_{rec}}) \geq \psi) \\ &= 1 - Pr((1-\varepsilon)\delta X \geq \psi, \delta aXY \geq \psi) \\ &= 1 - Pr\big(X \geq \tfrac{\psi}{(1-\varepsilon)\delta}, Y \geq \tfrac{\psi}{\delta aX}\big) \end{aligned}$$

Let

$$\begin{aligned} x_0 &= \tfrac{\psi}{(1-\varepsilon)\delta} \\ &= 1 - Pr\big(X \geq x_0, Y \geq \tfrac{(1-\varepsilon)x_0}{aX}\big) \\ &= 1 - \int_{x_0}^{\infty} f_X(x)\big(\int_{\frac{(1-\varepsilon)x_0}{ax}}^{\infty} f_Y(y)dy\big)dx \\ &= 1 - \int_{x_0}^{\infty} \lambda_h e^{-\lambda_h x}\big(\int_{\frac{(1-\varepsilon)x_0}{ax}}^{\infty} \lambda_g e^{-\lambda_g y}dy\big)dx \\ &= 1 - \int_{x_0}^{\infty} \lambda_h e^{-\lambda_h x}\big(e^{-\lambda_g \frac{(1-\varepsilon)x_0}{ax}}\big)dx \\ &= 1 - \int_{x_0}^{\infty} \lambda_h \big(e^{-\lambda_h x - \lambda_g \frac{(1-\varepsilon)x_0}{ax}}\big)dx \\ &= 1 - \Bigg(\underbrace{\lambda_h \int_{x=0}^{\infty} \big(e^{-4\lambda_g \frac{(1-\varepsilon)x_0}{a4x} - \lambda_h x}\big)dx}_{I_1} - \underbrace{\lambda_h \int_{x=0}^{x_0} \big(e^{-\lambda_g \frac{(1-\varepsilon)x_0}{ax} - \lambda_h x}\big)dx}_{I_2}\Bigg) \end{aligned}$$

Let us first evaluate the integral I_1 by using the formula [36], Equation 3.324.1)

$$\begin{aligned} &\int_0^{\infty} e^{-\frac{\beta}{4x} - \gamma x}dx = \sqrt{\frac{\beta}{\gamma}}K_1\big(\sqrt{\beta\gamma}\big) \\ &I_1 = \lambda_h \sqrt{\frac{4\lambda_g(1-\varepsilon)x_0}{a\lambda_h}} K_1\Bigg(\sqrt{\frac{4\lambda_g(1-\varepsilon)x_0\lambda_h}{a}}\Bigg) \\ &I_1 = 2\sqrt{\frac{\lambda_h\lambda_g(1-\varepsilon)x_0}{a}} K_1\Bigg(2\sqrt{\frac{\lambda_h\lambda_g(1-\varepsilon)x_0}{a}}\Bigg) \end{aligned}$$

Now, let us evaluate the integral I_2

$$I_2 = \lambda_h \int_{x=0}^{x_0} \big(e^{-\lambda_h x - \frac{(1-\varepsilon)\lambda_g x_0}{ax}}\big)dx$$

Expanding the term $e^{-\lambda_h x}$ in Taylor series

$$= \lambda_h \sum_{n=0}^{\infty} \frac{(-1)}{n!}(\lambda_h)^n \int_{x=0}^{x_0} x^n e^{-\frac{(1-\varepsilon)\lambda_g x_0}{ax}}dx$$

Substituting $y = \frac{1}{x}$, and further $t = x_0 y$, we get,

$$= \sum_{n=0}^{\infty} \frac{(-1)}{n!} (\lambda_h x_0)^{n+1} \int_{t=1}^{\infty} t^{-n-2} e^{-\frac{(1-\varepsilon)\lambda_g t}{a}} dt$$

Now, by definition of exponential integral of order n, we have

$$E_n(a) = \int_{y=1}^{\infty} y^{-n} e^{-ay} dy$$
$$I_2 = \sum_{n=0}^{\infty} \frac{(-1)}{n!} (\lambda_h x_0)^{n+1} E_{n+2}\Big(\frac{(1-\varepsilon)\lambda_g}{a}\Big)$$

Therefore,

$$P_{Out_S} = 1 - 2\sqrt{\frac{\lambda_h \lambda_g (1-\varepsilon) x_0}{a}} K_1\left(2\sqrt{\frac{\lambda_h \lambda_g (1-\varepsilon) x_0}{a}}\right) + \sum_{n=0}^{\infty} \frac{(-1)^n}{n!} (\lambda_h x_0)^{n+1} E_{n+2}\Big(\frac{(1-\varepsilon)\lambda_g}{a}\Big)$$

Putting the value of P_{Out_S} in Equation (33), we get,

$$Thr_S = \frac{R}{2}\left(2\sqrt{\frac{\lambda_h \lambda_g (1-\varepsilon) x_0}{a}} K_1\left(2\sqrt{\frac{\lambda_h \lambda_g (1-\varepsilon) x_0}{a}}\right) - \sum_{n=0}^{\infty} \frac{(-1)^n}{n!} (\lambda_h x_0)^{n+1} E_{n+2}\Big(\frac{(1-\varepsilon)\lambda_g}{a}\Big)\right)$$

This ends the proof of Theorem 3.

Appendix D. Proof of Theorem 1 in (38) and (39)

From Equation (32), the outage probability of IoT relay node is:

$$P_{Out_{IoT_R}} = Pr(min(\gamma_{s_{rec}}^{x_{IoT_R} \to x_s}, \gamma_{IoT_{rec}}) < \psi)$$
$$P_{Out_{IoT_R}} = 1 - Pr\big(\tfrac{\phi_2 bXY}{\phi_1 bXY+1} \geq \psi, \tfrac{\phi_2 bXZ}{\phi_1 bXZ+1} \geq \psi\big)$$

where

$$P_{IoT_R} = \eta \varepsilon P_s |h_{IoT_R}|^2 \triangleq \eta \varepsilon \delta X, b = \eta \delta \varepsilon$$
$$X = |h_{IoT_R}|^2, Y = |h_{s_{rec}}|^2, Z = |h_{IoT_{rec}}|^2, \sigma^2_{IoT_{rec}} = 1, \sigma^2_{s_{rec}} = 1$$
$$= 1 - Pr\big(Y \geq \tfrac{\psi}{(\phi_2 - \phi_1\psi)bX}, Z \geq \tfrac{\psi}{(\phi_2 - \phi_1\psi)bX}\big)$$

Conditioning on X, we have,

$$= 1 - \int_0^{\infty} Pr\big(Y \geq \frac{\psi}{(\phi_2 - \phi_1\psi)bx}\big) \times Pr\big(Z \geq \frac{\psi}{(\phi_2 - \phi_1\psi)bx}\big) f_X(x) dx$$

putting,

$$\tfrac{\psi}{(\phi_2 - \phi_1\psi)bx} = U$$
$$= 1 - \int_0^{\infty} Pr(Y \geq U) Pr(Z \geq U) f_X(x) dx$$
$$= 1 - \int_0^{\infty} \big(\int_U^{\infty} \lambda_g e^{-\lambda_g y} dy\big)\big(\int_U^{\infty} \lambda_z e^{-\lambda_z z} dz\big) \lambda_h e^{-\lambda_h x} dx$$
$$= 1 - \int_0^{\infty} e^{-\lambda_g U} e^{-\lambda_z U} \lambda_h e^{-\lambda_h x} dx$$

substituting the value of U above

$$= 1 - \int_0^{\infty} e^{-\lambda_g \frac{\psi}{(\phi_2 - \phi_1\psi)bx}} e^{-\lambda_z \frac{\psi}{(\phi_2 - \phi_1\psi)bx}} \lambda_h e^{-\lambda_h x} dx$$

let

$$c = \tfrac{\psi}{(\phi_2 - \phi_1\psi)b}$$
$$= 1 - \int_0^{\infty} e^{-\lambda_g \frac{c}{x}} e^{-\lambda_z \frac{c}{x}} \lambda_h e^{-\lambda_h x} dx$$
$$= 1 - \lambda_h \int_0^{\infty} e^{-4(\lambda_g + \lambda_z)\frac{c}{4x} - \lambda_h x} dx$$

Now, using the formula,

$$\int_0^\infty e^{-\frac{\beta}{4x}-\gamma x}dx = \sqrt{\frac{\beta}{\gamma}}K_1\left(\sqrt{\beta\gamma}\right)$$
$$= 1 - \lambda_h\sqrt{\frac{4(\lambda_g+\lambda_z)c}{\lambda_h}}K_1\left(\sqrt{4(\lambda_g+\lambda_z)c\lambda_h}\right)$$
$$P_{Out_{IoT_R}} = 1 - 2\sqrt{c\lambda_h(\lambda_g+\lambda_z)}K_1\left(2\sqrt{c\lambda_h(\lambda_g+\lambda_z)}\right)$$

Putting the value of $P_{Out_{IoT_R}}$ in Equation (34), we get,

$$Thr_{IoT_R} = \frac{R}{2}\left(2\sqrt{c\lambda_h(\lambda_g+\lambda_z)}K_1\left(2\sqrt{c\lambda_h(\lambda_g+\lambda_z)}\right)\right)$$

This ends the proof of Theorem 4.

References

1. Ericsson, L. More Than 50 Billion Connected Devices. 2011. Available online: https://www.akos-rs.si/files/Telekomunikacije/Digitalna_agenda/Internetni_protokol_Ipv6/More-than-50-billion-connected-devices.pdf (accessed on 26 September 2018)
2. Mumtaz, S.; Alsohaily, A.; Pang, Z.; Rayes, A.; Tsang, K.F.; Rodriguez, J. Massive Internet of Things for industrial applications: Addressing wireless IIoT connectivity challenges and ecosystem fragmentation. *IEEE Ind. Electron. Mag.* **2017**, *11*, 28–33. [CrossRef]
3. Molina, B.; Palau, C.E.; Fortino, G.; Guerrieri, A.; Savaglio, C. Empowering smart cities through interoperable Sensor Network Enablers. In Proceedings of the 2014 IEEE International Conference on Systems, Man and Cybernetics (SMC), San Diego, CA, USA, 5–8 October 2014; pp. 7–12.
4. Rauniyar, A.; Hagos, D.H.; Shrestha, M. A Crowd-Based Intelligence Approach for Measurable Security, Privacy, and Dependability in Internet of Automated Vehicles with Vehicular Fog. *Mob. Inf. Syst.* **2018**, *2018*, 7905960. [CrossRef]
5. Savaglio, C.; Fortino, G. Autonomic and cognitive architectures for the Internet of Things. In Proceedings of the International Conference on Internet and Distributed Computing Systems, Windsor, UK, 2–4 September 2015; pp. 39–47.
6. Ambrosin, M.; Anzanpour, A.; Conti, M.; Dargahi, T.; Moosavi, S.R.; Rahmani, A.M.; Liljeberg, P. On the Feasibility of Attribute-Based Encryption on Internet of Things Devices. *IEEE Micro* **2016**, *36*, 25–35. [CrossRef]
7. Li, S.; Xu, L.D.; Zhao, S. 5G internet of things: A survey. *J. Ind. Inf. Integr.* **2018**, *10*, 1–9. [CrossRef]
8. Atzori, L.; Iera, A.; Morabito, G. The internet of things: A survey. *Comput. Netw.* **2010**, *54*, 2787–2805. [CrossRef]
9. Guo, W.; Deng, Y.; Yilmaz, H.B.; Farsad, N.; Elkashlan, M.; Eckford, A.; Nallanathan, A.; Chae, C.B. SMIET: Simultaneous molecular information and energy transfer. *IEEE Wirel. Commun.* **2018**, *25*, 106–113. [CrossRef]
10. Rauniyar, A.; Engelstad, P.; Moen, J. A New Distributed Localization Algorithm Using Social Learning Based Particle Swarm Optimization for Internet of Things. In Proceedings of the 2018 IEEE 87th Vehicular Technology Conference (VTC Spring), Porto, Portugal, 3–6 June 2018; pp. 1–7.
11. Liang, X.; Chen, M.; Balasingham, I.; Leung, V.C. Cooperative communications with relay selection for wireless networks: Design issues and applications. *Wirel. Commun. Mob. Comput.* **2013**, *13*, 745–759. [CrossRef]
12. Razeghi, B.; Hodtani, G.A.; Nikazad, T. Multiple Criteria Relay Selection Scheme in Cooperative Communication Networks. *Wirel. Pers. Commun.* **2017**, *96*, 2539–2561. [CrossRef]
13. Ibrahim, A.S.; Sadek, A.K.; Su, W.; Liu, K.R. Cooperative communications with relay-selection: When to cooperate and whom to cooperate with? *IEEE Trans. Wirel. Commun.* **2008**, *7*, 2814–2827. [CrossRef]
14. Geng, K.; Gao, Q.; Fei, L.; Xiong, H. Relay selection in cooperative communication systems over continuous time-varying fading channel. *Chin. J. Aeronaut.* **2017**, *30*, 391–398. [CrossRef]

15. Lu, X.; Wang, P.; Niyato, D.; Kim, D.I.; Han, Z. Wireless networks with RF energy harvesting: A contemporary survey. *IEEE Commun. Surv. Tutor.* **2015**, *17*, 757–789. [CrossRef]
16. Zhou, X.; Zhang, R.; Ho, C.K. Wireless information and power transfer: Architecture design and rate-energy tradeoff. *IEEE Trans. Commun.* **2013**, *61*, 4754–4767. [CrossRef]
17. Liu, P.; Gazor, S.; Kim, I.M.; Kim, D.I. Noncoherent relaying in energy harvesting communication systems. *IEEE Trans. Wirel. Commun.* **2015**, *14*, 6940–6954. [CrossRef]
18. Mateu, L.; Moll, F. Review of energy harvesting techniques and applications for microelectronics (Keynote Address). *Pro. SPIE* **2005**, *5837*, 359–374.
19. Zhang, R.; Ho, C.K. MIMO broadcasting for simultaneous wireless information and power transfer. *IEEE Trans. Wirel. Commun.* **2013**, *12*, 1989–2001. [CrossRef]
20. Wu, Q.; Chen, W.; Ng, D.W.K.; Schober, R. Spectral and energy efficient wireless powered IoT networks: NOMA or TDMA? *IEEE Trans. Veh. Technol.* **2018**, *67*, 6663–6667. [CrossRef]
21. Islam, S.R.; Avazov, N.; Dobre, O.A.; Kwak, K.S. Power-domain non-orthogonal multiple access (NOMA) in 5G systems: Potentials and challenges. *IEEE Commun. Surv. Tutor.* **2017**, *19*, 721–742. [CrossRef]
22. Ding, Z.; Yang, Z.; Fan, P.; Poor, H.V. On the performance of non-orthogonal multiple access in 5G systems with randomly deployed users. *arXiv* **2014**, arXiv:1406.1516.
23. Saito, Y.; Kishiyama, Y.; Benjebbour, A.; Nakamura, T.; Li, A.; Higuchi, K. Non-orthogonal multiple access (NOMA) for cellular future radio access. In Proceedings of the 2013 IEEE 77th Vehicular Technology Conference (VTC Spring), Dresden, Germany, 2–5 June 2013; pp. 1–5.
24. Varshney, L.R. Transporting information and energy simultaneously. In Proceedings of the 2008 IEEE International Symposium on Information Theory, Toronto, ON, Canada, 6–11 July 2008; pp. 1612–1616. [CrossRef]
25. Sun, L.; Zhang, T.; Lu, L.; Niu, H. Cooperative communications with relay selection in wireless sensor networks. *IEEE Trans. Consum. Electron.* **2009**, *55*, 513–517. [CrossRef]
26. Sudevalayam, S.; Kulkarni, P. Energy harvesting sensor nodes: Survey and implications. *IEEE Commun. Surv. Tutor.* **2011**, *13*, 443–461. [CrossRef]
27. Lo, A.; Law, Y.; Jacobsson, M. A cellular-centric service architecture for machine-to-machine (M2M) communications. *IEEE Wirel. Commun.* **2013**, *20*, 143–151. [CrossRef]
28. Nasir, A.A.; Zhou, X.; Durrani, S.; Kennedy, R.A. Relaying Protocols for Wireless Energy Harvesting and Information Processing. *IEEE Trans. Wirel. Commun.* **2013**, *12*, 3622–3636. [CrossRef]
29. Du, G.; Xiong, K.; Qiu, Z. Outage analysis of cooperative transmission with energy harvesting relay: Time switching versus power splitting. *Math. Probl. Eng.* **2015**, *2015*, 598290. [CrossRef]
30. Liu, Y.; Ding, Z.; Elkashlan, M.; Poor, H.V. Cooperative Non-orthogonal Multiple Access with Simultaneous Wireless Information and Power Transfer. *IEEE J. Sel. Areas Commun.* **2016**, *34*, 938–953. [CrossRef]
31. Ha, D.B.; Nguyen, S.Q. Outage Performance of Energy Harvesting DF Relaying NOMA Networks. *Mob. Netw. Appl.* **2017**, 1–14. [CrossRef]
32. Kader, M.F.; Shahab, M.B.; Shin, S.Y. Cooperative spectrum sharing with energy harvesting best secondary user selection and non-orthogonal multiple access. In Proceedings of the 2017 International Conference on Computing, Networking and Communications (ICNC), Santa Clara, CA, USA, 26–29 January 2017; pp. 46–51.
33. Jain, N.; Bohara, V.A. Energy harvesting and spectrum sharing protocol for wireless sensor networks. *IEEE Wirel. Commun. Lett.* **2015**, *4*, 697–700. [CrossRef]
34. Zhou, Z.; Zhou, S.; Cui, J.H.; Cui, S. Energy-efficient cooperative communication based on power control and selective single-relay in wireless sensor networks. *IEEE Trans. Wirel. Commun.* **2008**, *7*. [CrossRef]
35. Chong, E.K.P.; Zak, S.H. *An Introduction to Optimization*, 4th ed.; John Wiley & Sons: Hoboken, NJ, USA, 2013.
36. Gradshteyn, I.S.; Ryzhik, I.M. *Table of Integrals, Series, and Products*; Academic Press: Cambridge, MA, USA, 2007.

© 2018 by the authors. Licensee MDPI, Basel, Switzerland. This article is an open access article distributed under the terms and conditions of the Creative Commons Attribution (CC BY) license (http://creativecommons.org/licenses/by/4.0/).

Paper VIII

Ergodic Sum Capacity Analysis of NOMA-SWIPT Enabled IoT Relay Systems

Ashish Rauniyar, Paal E. Engelstad, Olav N. Østerbø

In: *Internet Technology Letters, Wiley* Vol. 00, no. 00 (2020), pp. 1–6, DOI: 10.1002/itl2.218.

VIII

Received: 7 February 2020 | Revised: 23 June 2020 | Accepted: 5 August 2020

DOI: 10.1002/itl2.218

Check for updates

LETTER

WILEY

Ergodic sum capacity analysis of NOMA-SWIPT enabled IoT relay systems

Ashish Rauniyar[1,2] | **Paal Engelstad**[1,2] | **Olav N. Østerbø**[3]

[1]Department of Technology Systems, University of Oslo, Oslo, Norway

[2]Department of Computer Science, Oslo Metropolitan University, Oslo, Norway

[3]Telenor Reserach, Telenor, Oslo, Norway

Correspondence
Ashish Rauniyar, OsloMet, Pilestredet 52, 0167, Oslo, Norway.
Email: ashishr@ifi.uio.no

Present address
Ashish Rauniyar, OsloMet, Pilestredet 52, 0167, Oslo, Norway.

Instead of using the participating relay node only for relaying the data of the source node, in this letter, we have also considered transmitting the data of the IoT relay node (IoT_R) along with the source node data based on time switching (TS), power splitting (PS) relaying and NOMA. Therefore, in this context, we investigate the ergodic sum capacity (ESC) analysis of simultaneous wireless information and power transfer (SWIPT) based non-orthogonal multiple access (NOMA) for the Internet of Things (IoT) relay systems. Furthermore, we also study the effect of both perfect successive interference cancellation (pSIC) and imperfect SIC (ipSIC) on the proposed system. Analytical expressions for the ESC under both pSIC and ipSIC scenarios are mathematically derived and corroborated through Monte-Carlo simulations. Our result demonstrates that the PS relaying with NOMA is more energy-efficient than TS relaying with NOMA for the proposed system.

KEYWORDS

energy harvesting, ergodic capacity, internet of things, NOMA, power splitting, radio frequency, relaying, time switching

1 | INTRODUCTION

The exponential growth of mobile data traffic resulting from the rapid proliferation of the Internet of Things (IoT) is expected to consume a huge power. Therefore Simultaneous wireless information and power transfer (SWIPT) and radio frequency (RF) energy harvesting (EH) has been contemplated as self-sustainable energy efficient solution for realizing next generation of wireless networks to fulfill the energy requirements of Internet of Things (IoT) sensor nodes. Time switching (TS) and power splitting (PS) relaying are two popular EH architecture extensively considered in the literature for EH and information processing separately.[1] The receiver alternatively switches between EH and information decoding (ID) over time in TS relaying while in PS relaying, the receiver splits the incoming signal into two parts, where one part is used for EH and another part is used for ID.[1]

Meanwhile, non-orthogonal multiple access (NOMA) is a key technique considered for fifth generation (5G) networks where multiple users can be accommodated in the same frequency, time and code.[2] Specifically, in power domain NOMA, multiple users can be multiplexed with different power levels based on the channel gain and then the users can be separated through successive interference cancellation (SIC) at the receiver side.[3,4]

Nasir et al.[5] studied the achievable throughput and ergodic capacity (EC) of a decode-and-forward (DF) relaying network for both TS and PS schemes. Yang et al.[6] studied the impact of power allocation on cooperative NOMA with SWIPT. They investigated fixed and cognitive radios (CR) inspired power allocation policies for cooperative NOMA network where a source node communicates with two users through an EH based relay. Similar to,[6] Do et al.[7] studied EH

 © 2020 John Wiley & Sons, Ltd.

protocol based on time power switching-based relaying (TPSR) architecture for amplify-and-forward (AF) mode. They confirmed that the optimal outage and EC performance can be obtained through the right selection of power allocation for NOMA users. Zaidi et al.[8] evaluated the ergodic rate in SWIPT-aided hybrid NOMA in which the users transmits on the uplink by utilizing the harvested energy on the downlink. Jain et al.[9] studied the dual problem of power and spectrum issues in wireless sensor networks (WSN) by utilizing cooperative spectrum sharing and RF EH under the Nakagami fading channel.

Among several research directions of NOMA, NOMA-SWIPT is being considered as the most promising active research area by researchers for the development of next-generation wireless networks.[6,10,11] Unlike most of the previous work in this domain where the participating relay node is only used for relaying the source node data, in our earlier work,[12] we proposed an RF EH and information transmission system based on TS, PS relaying and NOMA where we studied and derived the analytical expressions for the outage, throughput and sum-throughput of the proposed system in delay limited transmission mode. In delay-limited transmission mode, the system throughput is limited by a fixed rate. However, for the delay tolerant transmission mode, the source transmits at any constant rate upper bounded by the EC.[13] Moreover, the impact of imperfect SIC (ipSIC), energy efficiency and effect of NOMA power coefficient was also not studied in.[12] Considering the EC as a fundamental performance indicator, specifically, in this letter, we study and analyze the ergodic sum capacity (ESC) of the NOMA-SWIPT enabled IoT relay systems in the delay tolerant transmission mode under both pSIC and ipSIC scenario.

The principal contribution of this letter are outlined as follows:

- We investigate and propose to use IoT node for the dual role of relaying the source node data and offloading data to its own destination based on TS and PS relaying with NOMA under both pSIC and ipSIC scenario.
- We derive the analytical expressions for the ESC of the proposed system and verified with the Monte-Carlo simulations.
- Our results demonstrate that PS relaying with NOMA is more energy-efficient than TS relaying with NOMA for the proposed system. Our results also confirmed that the SIC imperfection only affect the ESC performance and it does not show any effect on the α or ε at which ESC is maximized.

2 | SYSTEM MODEL BASED ON TS AND NOMA

We have considered a scenario as shown in Figure 1 where a source node has to transmits its data to its destination node. We have assumed that there is no direct link between the source user and its destination node due to deep fading or blockage.[7] Therefore, it will seek the help of a IoT relay node (IoT_R) for transmitting its data to its destination node. We have also assumed that IoT_R has its own data to send to its destination node. IoT_R is rather power constrained and hence it will first harvest the energy from the RF signal of the source node using either TS or PS relaying and then transmits the source data and its own data by using the NOMA protocol to respective destination nodes. We have also assumed that channel state information is perfectly known to the receiver.[4] The nodes are assumed to be operating in a half duplex mode. The channel between any two nodes is subjected to the independent Rayleigh block fading plus additive white Gaussian noise. Also, $h \sim CN(0, \lambda_h)$ is the complex channel co-efficient between source node and IoT_R with zero mean and variance λ_h. Similarly, $g \sim CN(0, \lambda_g)$ and $z \sim CN(0, \lambda_z)$ is the complex channel coefficient between IoT_R and the receiving source and IoT_R destination node respectively. In the first stage, the source node transmits signal x_s with power P_s to the IoT_R. The IoT_R node divide the time block into three parts: $\alpha T, \frac{(1-\alpha)T}{2}$, and $\frac{(1-\alpha)T}{2}$ where αT is used for energy harvesting and $\frac{(1-\alpha)T}{2}$ is used for information processing by IoT_R, and $\frac{(1-\alpha)T}{2}$ is used for the data transmission by the IoT_R node to the respective destination nodes, $0 \leq \alpha \leq 1$. The information signal received at IoT_R during this stage is given as $y_R = \sqrt{P_s}hx_s + n_R$, where $n_R \sim CN(0, \sigma_R^2)$ is the additive white Gaussian noise at IoT_R with mean zero and variance σ_R^2. The energy harvested at IoT_R in αT time interval is given as $E_H = \eta P_s |h|^2 \alpha T$, where $0 \leq \eta \leq 1$ is the energy conversion efficiency. The pre-processing power for the energy harvesting is assumed to be negligible in contrast to the transmission power of IoT_R.

The transmit power of IoT_R ie, P_R in $\frac{(1-\alpha)T}{2}$ period of time can be given as: $P_R = \frac{E_H}{(1-\alpha)T/2} = \frac{2\eta P_s |h|^2 \alpha}{(1-\alpha)} = \frac{2\eta P_s \alpha X}{(1-\alpha)}$.

In the next stage, by following NOMA protocol, the IoT_R node transmits a superimposed composite signal Z consisting source node and IoT_R data that can be given as: $Z = \sqrt{\phi_1 P_R} x_s + \sqrt{\phi_2 P_R} x_R$, where $\phi_1 + \phi_2 = 1$ and $\phi_2 = 1 - \phi_1$.

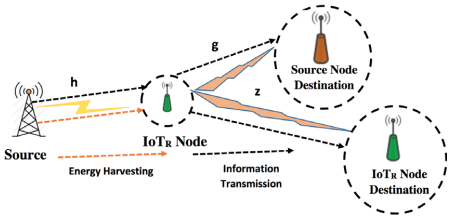

FIGURE 1 Considered system model scenario

3 | ERGODIC SUM CAPACITY ANALYSIS UNDER IPSIC AND PSIC

The received SNR at IoT_R node is given as:

$$\gamma_R = \frac{P_s|h|^2}{\sigma_R^2} = \delta|h|^2 = \delta X \tag{1}$$

where $\delta \triangleq \frac{P_s}{\sigma_R^2}$ represents the transmit SNR and $|h|^2 = X$.

Similarly, the received SINR with x_R and x_s at the receiving destination node of the source can be given as:

$$\gamma_{SR}^{x_R \to x_s} = \frac{\phi_2 P_R |g|^2}{\phi_1 P_R |g|^2 + \sigma_{SR}^2} = \frac{\phi_2 P_R Y}{\phi_1 P_R Y + 1} \tag{2}$$

$$\gamma_{SR} = \frac{\phi_1 P_R |g|^2}{\phi_2 P_R \xi |\widehat{g}|^2 + \sigma_{SR}^2} = \frac{\phi_1 P_R Y}{\phi_2 P_R \xi Y + 1} \tag{3}$$

where $\gamma_{SR}^{x_R \to x_s}$ is the SINR required at x_s to decode and cancel x_R, $\widehat{g} \sim CN(0, \xi\lambda_g)$ and $|g|^2 = Y$, $\sigma_{SR}^2 = 1$.

Here, the parameter ξ, $0 \le \xi \le 1$ denotes the residual interference signal caused by the SIC imperfection.

The received SINR at destination node of IoT_R associated with symbol x_R is given by:

$$\gamma_{RR} = \frac{\phi_2 P_R |z|^2}{\phi_1 P_R |z|^2 + \sigma_{RR}^2} = \frac{\phi_2 P_R Z}{\phi_1 P_R Z + 1} \tag{4}$$

where $|z|^2 = Z$ and $\sigma_{RR}^2 = 1$.

By using Equation (1)–(4), the achievable data rate of source node and IoT_R node based on TS and NOMA can be respectively given as:

$$C_S = \frac{1}{2}(1-\alpha)\log_2(1 + min(\gamma_R, \gamma_{SR})) \tag{5}$$

$$C_{IoT_R} = \frac{1}{2}(1-\alpha)\log_2(1 + min(\gamma_{SR}^{x_R \to x_s}, \gamma_{RR})) \tag{6}$$

The ergodic capacity equation of the source node and IoT_R node in terms of CDF can be given as: $C = \frac{(1-\alpha)}{2\ln 2}\int_0^\infty \frac{1}{1+\gamma}[1 - F_{\gamma_{min}}(\gamma)]d\gamma$.

Theorem 1. The EC of the source node using TS and NOMA with ipSIC can be expressed as:

$$C_S^{ipSIC} = \frac{(1-\alpha)}{2\ln 2}\int_{y=0}^{\frac{\delta}{C\phi_1}} \lambda_g e^{-\lambda_g y}\left(e^{\frac{\lambda_h}{Cy(\phi_1+\xi\phi_2)}} E_1\left(\frac{\lambda_h}{Cy(\phi_1+\xi\phi_2)}\right) - e^{\frac{\lambda_h}{Cy\xi\phi_2}} E_1\left(\frac{\lambda_h}{Cy\xi\phi_2}\right)\right) dy$$

$$+\frac{(1-\alpha)}{2\ln 2}\int_{y=\frac{\delta}{C\phi_1}}^{\infty}\lambda_g e^{-\lambda_g y}\left(e^{\frac{\lambda_h}{Cy(\phi_1+\xi\phi_2)}}E_1\left(\frac{\lambda_h(Cy\phi_1(\phi_1+\xi\phi_2)-\phi_1\delta)}{Cy(\phi_1+\xi\phi_2)(\xi\phi_2\delta)}\right)-e^{\frac{\lambda_h}{Cy\xi\phi_2}}E_1\left(\frac{\phi_1\lambda_h}{\xi\phi_2}\right)\right)dy$$

$$+\frac{(1-\alpha)}{2\ln 2}\int_{\gamma=0}^{\frac{\phi_1}{\phi_2\xi}}\frac{1}{1+\gamma}e^{-\frac{\gamma\lambda_h}{\delta}}e^{-\frac{\lambda_g\delta}{C(\phi_1-\gamma\phi_2\xi)}}d\gamma \tag{7}$$

where $C=\frac{2\alpha\eta\delta}{(1-\alpha)}$ and $E_1()$ is exponential integral function of order 1.

Proof: The proof is given in the Supporting Information.

Due to the involvement of the integral term, it is difficult to obtain a closed form solution from Equation 7. However, it can be evaluated through numerical approaches.

Corollary 1. When $\xi=0$, the EC of the source node using TS and NOMA with pSIC can be expressed as:

$$C_S^{pSIC}=\frac{(1-\alpha)}{2\ln 2}\left(G_{1,3}^{3,1}\left(AB\middle|\begin{matrix}0\\0,0,1\end{matrix}\right)-E_1(B)+\sum_{m=1}^{\infty}\frac{A^m}{(m-1)!}\left((\Psi(m)-\ln A)E_{m+1}(B)+B^m G_{2,3}^{3,0}\left(AB\middle|\begin{matrix}1,1\\0,0,-m\end{matrix}\right)\right)\right) \tag{8}$$

where $A=\frac{\lambda_h}{\delta}$, $B=\frac{\lambda_g}{k}$ and $k=\frac{2\alpha\eta\phi_1}{1-\alpha}$.

Proof: The proof is given in the Supporting Information.

Theorem 2. The EC of the IoT_R node using TS and NOMA can be expressed as:

$$C_{IoT_R}=\frac{(1-\alpha)}{2\ln 2}\left(G_{1,3}^{3,1}\left(C\middle|\begin{matrix}0\\0,0,1\end{matrix}\right)-G_{1,3}^{3,1}\left(\frac{C}{\phi_1}\middle|\begin{matrix}0\\0,0,1\end{matrix}\right)\right) \tag{9}$$

where $C=\frac{\lambda_h(\lambda_g+\lambda_z)}{l}$, $l=\frac{2\alpha\eta P_s}{(1-\alpha)}$ and $G_{1,3}^{3,1}$ is Meijer G function with parameters {0} and {0,0,1}.

Proof: The proof is given in the Supporting Information.

By combining Equations 7 and 9, and combining Equations 8 and 9, we finally get the ESC with ipSIC and pSIC respectively of the proposed system.

4 | SYSTEM MODEL BASED ON PS AND NOMA

In PS relaying scheme, a power-constrained IoT_R node first harvests the energy from the signal of the source node using εP_s where P_s is the power of the transmit signal. IoT_R uses remaining power $(1-\varepsilon)P_s$ for information processing. IoT_R then transmits the respective information signal to source and IoT user destination node using NOMA protocol in $T/2$ remaining period of time. The energy harvested at IoT_R in $\frac{T}{2}$ time interval is given as: $E_H=\frac{\eta\varepsilon P_s|h|^2T}{2}$. The transmit power of IoT_R ie, P_{IoT_R} in $\frac{T}{2}$ period of time can be given as: $P_R=\frac{E_H}{T/2}=\eta\varepsilon P_s|h|^2$.

Now, following the NOMA protocol, IoT_R transmits a superimposed composite signal consisting of the information of the source and IoT_R to respective destination nodes using the power P_{IoT_R} in the next stage. The detailed procedure of the considered system model based on PS and NOMA follows the same steps as of TS and NOMA as explained in Section II and III. The derivations of the EC of the considered system based on PS and NOMA under ipSic and pSIC, is straight forward and it can be derived by following the same steps as in Theorem 1, Corollary 1 and Theorem 2.

Therefore, the EC of the source node using PS and NOMA with ipSIC can be expressed as in Equation 7 by replacing C with $\varepsilon\eta\delta$ and δ with $(1-\varepsilon)\delta$ and removing the $(1-\alpha)$ term. Similarly, the EC of the source node using PS and NOMA with pSIC can be expressed as in Equation 8 by replacing A with $\frac{\lambda_h}{(1-\varepsilon)\delta}$, and k with $\frac{\varepsilon\eta\phi_1}{(1-\varepsilon)}$ and removing the $(1-\alpha)$ term. Finally, the EC of IoT_R node using PS and NOMA can be expressed as in Equation 9 by replacing l with $\varepsilon\eta\delta$ and removing the $(1-\alpha)$ term.

5 | NUMERICAL RESULTS

In this section, we present the simulation results to verify our analysis for the proposed system. We let, distance between source node and IoT_R to 2 m, distance between IoT_R and source destination node to 1 m and distance between IoT_R and IoT_R destination node to 2 m, path loss factor v = 3, $\phi_1 = 0.1$, $\phi_2 = 0.9$, $\xi = 0.03$ and $\eta = 0.9$.

From Figure 2A, we can observe that for TS relaying with NOMA under both pSIC and ipSIC, at $\alpha = 0.3$ outperforms the ESC at $\alpha = 0.7$ for δ greater than 3 dB. The ESC at such high value of $\alpha = 0.7$ gives the worst performance at all δ greater than 3 dB as compared to $\alpha = 0.3$. However, for PS relaying with NOMA, the ESC clearly increases with increases in ε and δ under both pSIC and ipSIC. Moreover, the ESC of PS relaying with NOMA is apparently higher than the TS relaying with NOMA. It is interesting to note the difference in the ESC performance due to pSIC and iPSIC increases especially at high transmit SNR values for both TS and PS relaying with NOMA which implies that ipSIC has a significant effect on the ESC performance. This further demonstrates the need of proper SIC technique that could enhance the ESC performance of the system. Also, our analysis exactly matched with the Monte-Carlo simulation results for both protocols under pSIC and ipSIC as shown in Figures 2 and 3, which verifies that our derived mathematical analysis is correct.

In Figure 2B, we plot the energy efficiency (EE) of the proposed system for both TS and PS relaying with NOMA under pSIC and ipSIC. The EE can be calculated as the ratio of total achievable data rate to the total power consumption in the entire network.[14] From Figure 2B, we can see that PS with NOMA under both pSIC and ipSIC is more energy efficient than TS with NOMA for the same value of EH parameters, that is, $\alpha = 0.3$ and $\varepsilon = 0.3$ especially at transmit SNR less than 25 dB. Same observation can be depicted at higher $\alpha = 0.7$ and $\varepsilon = 0.7$. However, it is omitted for the sake of brevity. For transmit SNR greater than 35 dB, the EE performance gap of the proposed system reduces because at such high transmit SNR, the IoT_R node can harvest more energy for both TS and PS relaying with NOMA.

Since, ϕ_2 is the NOMA power coefficient factor which determines the maximum amount of harvested energy used by the IoT_R node to transmits its data, in Figure 3A, we plot the ESC against the NOMA power allocation factor ϕ_2 at $\delta = 30$ dB. We find that the ESC of both TS and PS with NOMA under pSIC shows an increasing trend with the increase in ϕ_2. However the increase in ESC performance after $\phi_2 = 0.6$ is not much. In addition, the ipSIC case for both TS, and PS with NOMA shows a decreasing trend in the ESC performance. With the increase in ϕ_2, the ESC for both TS, and PS with NOMA under ipSIC decreases rapidly and it remains saturated for ϕ_2 greater than 0.2. This indicates that, with the proper selection of ϕ_2, ESC can be enhanced.

Figure 3B depicts the ESC performance with respect to α or ε at $\delta = 15$ dB and $\xi = 0.02$ and $\xi = 0.03$. It is worthwhile to note that the ESC of PS relaying with NOMA outperforms the TS relaying with NOMA for higher values of α or ε while at smaller values of α or ε TS relaying with NOMA outperforms the PS relaying with NOMA under both pSIC and ipSIC case. Moreover, it can be seen from Figure 2B that for both TS and PS relaying with NOMA protocol under both pSIC and ipSIC case, there lies an optimum value of α or ε that maximizes the ESC of the proposed system. We cannot have high value for EH parameter α for TS with NOMA as less time will be allocated for information decoding and processing at IoT_R node. Similarly, we cannot have high value for EH parameter ε for PS with NOMA as less power will be allocated for information decoding and processing at IoT_R node. Thus, the optimum ESC at α or ε as shown in Figure 3B can be easily found out through iterative search methods such as Golden section search method as in our previous work.[12] Further, we also observe that increasing the ξ value from 0.02 to 0.03, the optimum value of α or ε remains the same at which ESC is maximum for both TS and PS relaying with NOMA under ipSIC scenario. This implies that the SIC imperfection only affects the ESC performance and it does not show any effect on the optimal α or ε for both TS and PS relaying with NOMA under ipSIC scenario.

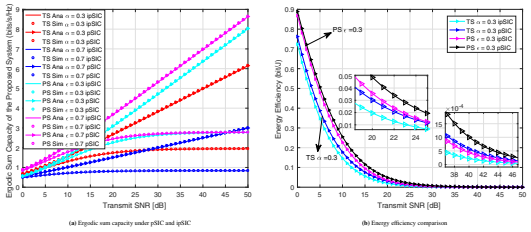

FIGURE 2 Ergodic Sum Capacity of the proposed system

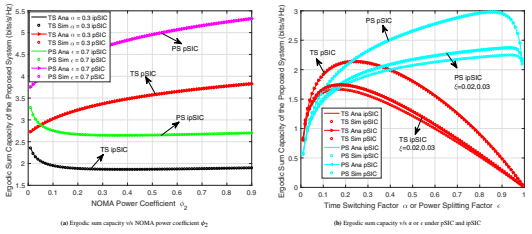

FIGURE 3 Effect of different parameters on the proposed system

6 | CONCLUSIONS

Unlike most of the previous work, we proposed to use IoT node for the dual role of relaying the source node data and offloading data to its own destination based on TS and PS relaying with NOMA. Specifically, in this letter, we investigated the ESC analysis of the NOMA-SWIPT enabled IoT relay systems under the both pSIC and ipSIC scenarios. The impact of parameters such as α, ε, ξ, ϕ_2 and δ are studied to get an insight of the ESC on the system performance. It is confirmed that except for some smaller values of α and δ, increasing the α value for the TS relaying with NOMA gives inferior ESC performance than the corresponding increment in the ε at higher δ value for the PS relaying with NOMA under both pSIC and ipSIC scenario. Our results demonstrate that the PS relaying with NOMA is more energy-efficient than the TS relaying with NOMA for the proposed system. Our results also confirmed that the SIC imperfection only affect the ESC performance and it does not show any positive effect on the α or ε at which ESC is maximized. Also, our results confirmed that the ipSIC has a significant impact on the ESC performance of the proposed system.

ORCID

Ashish Rauniyar https://orcid.org/0000-0002-2142-9522

REFERENCES

1. Zhang R, Ho CK. MIMO broadcasting for simultaneous wireless information and power transfer. *IEEE Trans Wirel Commun*. 2013;12(5):1989-2001.
2. Wu Q, Chen W, Ng DWK, Schober R. Spectral and energy-efficient wireless powered IoT networks: NOMA or TDMA? *IEEE Trans Veh Technol*. 2018;67(7):6663-6667.
3. Ding Z, Lei X, Karagiannidis GK, Schober R, Yuan J, Bhargava VKA. Survey on non-orthogonal multiple access for 5G networks: research challenges and future trends. *IEEE J Sel Areas Commun*. 2017;35(10):2181-2195. https://doi.org/10.1109/JSAC.2017.2725519.
4. Kader MF, Uddin MB, Islam A, Shin SY. Cooperative non-orthogonal multiple access with SWIPT over Nakagami-m fading channels. *Trans Emerg Telecommun Technol*. 2019;30(5):e3571.
5. Nasir AA, Zhou X, Durrani S, Kennedy RA. Throughput and ergodic capacity of wireless energy harvesting based DF relaying network. In 2014 IEEE International Conference on Communications (ICC). IEEE; 2014;4066-4071.
6. Yang Z, Ding Z, Fan P, Al-Dhahir N. The impact of power allocation on cooperative non-orthogonal multiple access networks with SWIPT. *IEEE Trans Wirel Commun*. 2017;16(7):4332-4343. https://doi.org/10.1109/TWC.2017.2697380.
7. Do DT, Le CB. Application of NOMA in wireless system with wireless power transfer scheme: outage and Ergodic capacity performance analysis. *Sensors*. 2018;18(10):3501.
8. Zaidi SK, Hasan SF, Gui X. Evaluating the ergodic rate in SWIPT-aided hybrid NOMA. *IEEE Commun Lett*. 2018;22(9):1870-1873.
9. Jain N, Bohara VA. Energy harvesting and Spectrum sharing protocol for wireless sensor networks. *IEEE Wireless Commun Lett*. 2015;4(6):697-700. https://doi.org/10.1109/LWC.2015.2484341.
10. Rauniyar A, Engelstad PE, Østerbø ON. Performance analysis of RF energy harvesting and information transmission based on NOMA with interfering signal for IoT relay systems. *IEEE Sensors J*. 2019;19(17):7668-7682. https://doi.org/10.1109/JSEN.2019.2914796.
11. Song M, Zheng M. Energy efficiency optimization for wireless powered sensor networks with nonorthogonal multiple access. *IEEE Sens Lett*. 2018;2(1):1-4.
12. Rauniyar A, Engelstad P, Østerbø O. RF energy harvesting and information transmission based on NOMA for wireless powered IoT relay systems. *Sensors*. 2018;18(10):3254.
13. Zhong C, Suraweera HA, Zheng G, Krikidis I, Zhang Z. Improving the throughput of wireless powered dual-hop systems with full duplex relaying. *IEEE Int Conf Commun*. 2015;2015:4253-4258.
14. Yue X, Liu Y, Kang S, Nallanathan A, Ding Z. Exploiting full/half-duplex user relaying in NOMA systems. *IEEE Trans Commun*. 2017;66(2):560-575.

SUPPORTING INFORMATION

Additional supporting information may be found online in the Supporting Information section at the end of this article.

How to cite this article: Rauniyar A, Engelstad P, Østerbø ON. Ergodic sum capacity analysis of NOMA-SWIPT enabled IoT relay systems. *Internet Technology Letters*. 2020;e218. https://doi.org/10.1002/itl2.218

SUPPLEMENTARY MATERIAL - PROOF OF THEOREM 1

Theorem 1: The EC of the source node using TS and NOMA with ipSIC can be expressed as:

$$C_S^{ipSIC} = \frac{(1-\alpha)}{2\ln 2}\int_{y=0}^{\frac{\delta}{C\phi_1}} \lambda_g e^{-\lambda_g y}\left(e^{\frac{\lambda_h}{Cy(\phi_1+\xi\phi_2)}}E_1\left(\frac{\lambda_h}{Cy(\phi_1+\xi\phi_2)}\right) - e^{\frac{\lambda_h}{Cy\xi\phi_2}}E_1\left(\frac{\lambda_h}{Cy\xi\phi_2}\right)\right)dy + \frac{(1-\alpha)}{2\ln 2}\int_{y=\frac{\delta}{C\phi_1}}^{\infty} \lambda_g e^{-\lambda_g y}\left(e^{\frac{\lambda_h}{Cy(\phi_1+\xi\phi_2)}}\right.$$

$$\left.E_1\left(\frac{\lambda_h\left(Cy\phi_1(\phi_1+\xi\phi_2)-\phi_1\delta\right)}{Cy(\phi_1+\xi\phi_2)(\xi\phi_2\delta)}\right) - e^{\frac{\lambda_h}{Cy\xi\phi_2}}E_1\left(\frac{\phi_1\lambda_h}{\xi\phi_2}\right)\right)dy + \frac{(1-\alpha)}{2\ln 2}\int_{\gamma=0}^{\frac{\phi_1}{\phi_2\xi}}\frac{1}{1+\gamma}e^{-\frac{\gamma\lambda_h}{\delta}}e^{-\frac{\lambda_g\delta}{C(\phi_1-\gamma\phi_2\xi)}}d\gamma$$

where $C = \frac{2\alpha\eta\delta}{(1-\alpha)}$ and $E_1()$ is exponential integral function of order 1.

Proof : The CDF of $min\left(\gamma_R, \gamma_{SR}\right)$ can be given as: $F_{\gamma_{min}}(\gamma) = 1 - \Pr((\gamma_R, \gamma_{SR}) > \gamma) = 1 - \Pr(X > \frac{\gamma}{\delta}, XY > \frac{\gamma}{C(\phi_1 - \gamma\phi_2\xi)})$

where $C = \frac{2\alpha\eta\delta}{(1-\alpha)}$, Now, conditioning on Y, we get

$$= 1 - \int_{y=0}^{\infty}\Pr\left(X > \max\left(\frac{\gamma}{\delta}, \frac{\gamma}{Cy(\phi_1-\gamma\phi_2\xi)}\right)\right)f_Y(y)dy = 1 - \int_{y=0}^{\frac{\delta}{C(\phi_1-\gamma\phi_2\xi)}}\lambda_g e^{-\left(\frac{\gamma\lambda_h}{C(\phi_1-\gamma\phi_2\xi)y}\right)-\lambda_g y}dy - e^{-\frac{\gamma\lambda_h}{\delta}}e^{-\frac{\lambda_g\delta}{C(\phi_1-\gamma\phi_2\xi)}}$$

Now, substituting the $F_{\gamma_{min}}(\gamma)$ expression in EC equation,

$$C_S^{ipSIC} = \underbrace{\frac{(1-\alpha)}{2\ln 2}\int_{\gamma=0}^{\frac{\phi_1}{\phi_2\xi}}\frac{1}{1+\gamma}\int_{y=0}^{\frac{\delta}{C(\phi_1-\gamma\phi_2\xi)}}\lambda_g e^{-\left(\frac{\gamma\lambda_h}{C(\phi_1-\gamma\phi_2\xi)y}\right)-\lambda_g y}dyd\gamma}_{I_1} + \underbrace{\frac{(1-\alpha)}{2\ln 2}\int_{\gamma=0}^{\frac{\phi_1}{\phi_2\xi}}\frac{1}{1+\gamma}e^{-\frac{\gamma\lambda_h}{\delta}}e^{-\frac{\lambda_g\delta}{C(\phi_1-\gamma\phi_2\xi)}}d\gamma}_{I_2}$$

First, we will evaluate I_1, Now, let $z = \frac{\gamma}{\phi_1 - \gamma\phi_2\xi} \rightarrow \gamma = \frac{\phi_1 z}{1+z\xi\phi_2} \rightarrow d\gamma = \frac{\phi_1}{(1+z\xi\phi_2)^2}dz$

$$I_1 = \frac{(1-\alpha)}{2\ln 2}\int_{z=0}^{\infty}\frac{\phi_1}{\left(1+z(\phi_1+\xi\phi_2)\right)(1+z\xi\phi_2)}\int_{y=0}^{\frac{\delta(1+z\xi\phi_2)}{C\phi_1}}\lambda_g e^{-\frac{\lambda_h z}{Cy}-\lambda_g y}dyd z$$

Now, decomposing $\frac{\phi_1}{\left(1+z(\phi_1+\xi\phi_2)\right)(1+z\xi\phi_2)}$ by partial fractions,

$$I_1 = \underbrace{\frac{(1-\alpha)}{2\ln 2}\int_{z=0}^{\infty}\frac{\phi_1+\xi\phi_2}{1+z(\phi_1+\xi\phi_2)}\int_{y=0}^{\frac{\delta(1+z\xi\phi_2)}{C\phi_1}}\lambda_g e^{-\frac{\lambda_h z}{Cy}-\lambda_g y}dyd z}_{J_1} - \underbrace{\frac{(1-\alpha)}{2\ln 2}\int_{z=0}^{\infty}\frac{\xi\phi_2}{(1+z\xi\phi_2)}\int_{y=0}^{\frac{\delta(1+z\xi\phi_2)}{C\phi_1}}\lambda_g e^{-\frac{\lambda_h z}{Cy}-\lambda_g y}dyd z}_{J_2}$$

After some algebraic calculations, we can find,

$$J_1 = \frac{(1-\alpha)}{2\ln 2}\left(\int_{y=0}^{\frac{\delta}{C\phi_1}}\lambda_g e^{-\lambda_g y}e^{\frac{\lambda_h}{Cy(\phi_1+\xi\phi_2)}}E_1\left(\frac{\lambda_h}{Cy(\phi_1+\xi\phi_2)}\right)dy + \int_{y=\frac{\delta}{C\phi_1}}^{\infty}\lambda_g e^{-\lambda_g y}e^{\frac{\lambda_h}{Cy(\phi_1+\xi\phi_2)}}E_1\left(\frac{\lambda_h\left(Cy\phi_1(\phi_1+\xi\phi_2)-\phi_1\delta\right)}{Cy(\phi_1+\xi\phi_2)(\xi\phi_2\delta)}\right)dy\right)$$

Similarly, $J_2 = \frac{(1-\alpha)}{2\ln 2}\left(\int_{y=0}^{\frac{\delta}{C\phi_1}}\lambda_g e^{-\lambda_g y}e^{\frac{\lambda_h}{Cy\xi\phi_2}}E_1\left(\frac{\lambda_h}{Cy\xi\phi_2}\right)dy + \int_{y=\frac{\delta}{C\phi_1}}^{\infty}\lambda_g e^{-\lambda_g y}e^{\frac{\lambda_h}{Cy\xi\phi_2}}E_1\left(\frac{\phi_1\lambda_h}{\xi\phi_2}\right)dy\right)$

Therefore, $C_S^{ipSIC} = I_1 + I_2 = J_1 - J_2 + I_2$

By substituting the value of $I_1 = J_1 - J_2$ and I_2, we get the ECequation with ipSIC as in Equation 7 and hence the proof.

PROOF OF COROLLARY 1

Corollary 1: When $\xi = 0$, the EC of the source node using TS and NOMA with pSIC can be expressed as:

$$C_S^{pSIC} = \frac{(1-\alpha)}{2\ln 2}\left(G_{1,3}^{3,1}\left(AB\middle|\begin{matrix}0\\0,0,1\end{matrix}\right) - E_1(B) + \sum_{m=1}^{\infty}\frac{A^m}{(m-1)!}\left(\left(\Psi(m) - \ln A\right)E_{m+1}(B) + B^m G_{2,3}^{3,0}\left(AB\middle|\begin{matrix}1,1\\0,0,-m\end{matrix}\right)\right)\right)$$

where $A = \frac{\lambda_h}{\delta}$, $B = \frac{\lambda_g}{k}$ and $k = \frac{2\alpha\eta\phi_1}{1-\alpha}$.

Proof : The CDF of $min\left(\gamma_R, \gamma_{SR}\right)$ can be given as:

$F_{\gamma_{min}}(\gamma) = 1 - \Pr((\gamma_R, \gamma_{SR}) > \gamma)$

$F_{\gamma_{min}}(\gamma) = 1 - \Pr(X > \frac{\gamma}{\delta}, Y > \frac{\gamma}{\delta k X})$

where k $= \frac{2\alpha\eta\phi_1}{1-\alpha}$and let $\frac{\gamma}{\delta} = x_0$

$= 1 - Pr(X > x_0, Y > \frac{x_0}{kX})$

$= 1 - \int_{x_0}^{\infty} \lambda_h e^{-\lambda_h x - \frac{\lambda_g x_0}{kx}} dx,$

Now, changing the integration variable, we get,

$= 1 - \int_{x=1}^{\infty} A\gamma e^{-A\gamma x - \frac{B}{x}} dx$ where $A = \frac{\lambda_h}{\delta}$and $B = \frac{\lambda_g}{k}$

$= 1 - \left(\int_{x=0}^{\infty} A\gamma e^{-A\gamma x - \frac{B}{x}} dx - \int_{x=0}^{1} A\gamma e^{-A\gamma x - \frac{B}{x}} dx\right)$

$= 1 - 2\sqrt{AB\gamma}K_1(2\sqrt{AB\gamma}) + \int_{x=0}^{1} A\gamma e^{-A\gamma x - \frac{B}{x}} dx$

Now, substituting the $F_{\gamma_{min}}(\gamma)$ expression in EC equation,

$$= \frac{(1-\alpha)}{2\ln 2}\left(\int_0^{\infty}\frac{2\sqrt{AB\gamma}K_1(2\sqrt{AB\gamma})}{1+\gamma}d\gamma - \underbrace{\int_0^{\infty}\int_{x=0}^{1}\frac{A\gamma e^{-A\gamma x - \frac{B}{x}}}{1+\gamma}dx d\gamma}_{I_1}\right)$$

$$= \frac{(1-\alpha)}{2\ln 2}\left(G_{1,3}^{3,1}\left(AB\middle|\begin{matrix}0\\0,0,1\end{matrix}\right) - I_1\right)$$

where $G_{1,3}^{3,1}$ is Meijer G function with parameters $\{0\}$ and $\{0,0,1\}$

Since, $\int_{\gamma=0}^{\infty}\frac{A\gamma e^{-Ax\gamma}}{1+\gamma}d\gamma = \frac{1}{x} - Ae^{Ax}E_1(Ax)$where $E_1(.)$ is exponential integral of order 1

$$I_1 = \int_{x=0}^{1} \left(\frac{1}{x} - Ae^{Ax} E_1(Ax) \right) e^{-\frac{B}{x}} dx = E_1(B) - \underbrace{\int_{x=0}^{A} e^{x - \frac{AB}{x}} E_1(x) dx}_{I(A,B)}$$

Through some algebraic manipulation, we can find I(A,B) $= \sum_{m=1}^{\infty} \frac{A^m}{(m-1)!} \left(\left(\Psi(m) - \ln A \right) E_{m+1}(B) + B^m G_{2,3}^{3,0} \left(AB \middle| \begin{matrix} 1, 1 \\ 0, 0, -m \end{matrix} \right) \right)$

where $\Psi(m)$ is Digamma function and $\Psi(m) = -\gamma + \sum_{i=1}^{m-1} \frac{1}{i}$

By substituting I_1 and I(A,B), we get the EC equation with pSIC as in Equation 8 and hence the proof.

PROOF OF THEOREM 2

Theorem 2: The EC of the IoT_R node using TS and NOMA can be expressed as:

$$C_{IoT_R} = \frac{(1-\alpha)}{2 \ln 2} \left(G_{1,3}^{3,1} \left(C \middle| \begin{matrix} 0 \\ 0, 0, 1 \end{matrix} \right) - G_{1,3}^{3,1} \left(\frac{C}{\phi_1} \middle| \begin{matrix} 0 \\ 0, 0, 1 \end{matrix} \right) \right)$$

where $C = \frac{\lambda_h(\lambda_g + \lambda_z)}{l}$ and $l = \frac{2\alpha\eta P_s}{(1-\alpha)}$.

Proof : The CDF of $min(\gamma_{SR}^{x_R \to x_s}, \gamma_{RR})$ can be given as: $F_{\gamma_{min}}(\gamma) = 1 - \Pr((\gamma_{SR}^{x_R \to x_s}, \gamma_{RR}) > \gamma)$

$= 1 - \Pr\left(\frac{\phi_2 lXY}{\phi_1 lXY + 1} \geq \gamma, \frac{\phi_2 lXZ}{\phi_1 lXZ + 1} \geq \gamma \right)$ where $P_{IoT_R} = \frac{2\alpha\eta P_s X}{(1-\alpha)}, l = \frac{2\alpha\eta P_s}{(1-\alpha)}$

$= 1 - Pr\left(Y \geq \frac{\gamma}{(\phi_2 - \phi_1\gamma) lX}, Z \geq \frac{\gamma}{(\phi_2 - \phi_1\gamma) lX} \right)$

Through some algebraic manipulation,

$F_{\gamma_{min}}(\gamma) = 1 - 2\sqrt{d\lambda_h(\lambda_g + \lambda_z)} K_1\left(2\sqrt{d\lambda_h(\lambda_g + \lambda_z)} \right)$ where $d = \frac{\gamma}{(\phi_2 - \phi_1\gamma) l}$

It can be rewritten with parameter $C = \frac{\lambda_h(\lambda_g + \lambda_z)}{l}$ as, $1 - 2\sqrt{C\frac{\gamma}{\phi_2 - \phi_1\gamma}} K_1\left(2\sqrt{C\frac{\gamma}{\phi_2 - \phi_1\gamma}} \right)$

Now, substituting the $F_{\gamma_{min}}(\gamma)$ expression in EC equation, $= \frac{(1-\alpha)}{2 \ln 2} \int_{\gamma=0}^{\frac{\phi_2}{\phi_1}} \frac{2\sqrt{C\frac{\gamma}{\phi_2 - \phi_1\gamma}} K_1\left(2\sqrt{C\frac{\gamma}{\phi_2 - \phi_1\gamma}} \right)}{1 + \gamma} d\gamma$

Changing the integration variable by $u = \frac{\gamma}{\phi_2 - \phi_1\gamma}$ gives, $\frac{(1-\alpha)\phi_2}{2 \ln 2} \int_{u=0}^{\infty} \frac{2\sqrt{Cu} K_1(\sqrt{Cu})}{(1+u)(1+\phi_1 u)}$

By partial fraction method, we can rewrite it as:

$$= \frac{(1-\alpha)}{2 \ln 2} \left(\int_{u=0}^{\infty} \frac{2\sqrt{Cu} K_1(\sqrt{Cu})}{(1+u)} - \int_{u=0}^{\infty} \frac{2\sqrt{\frac{Cu}{\phi_1}} K_1(\sqrt{\frac{Cu}{\phi_1}})}{(1+u)} \right) = \frac{(1-\alpha)}{2 \ln 2} \left(G_{1,3}^{3,1} \left(C \middle| \begin{matrix} 0 \\ 0, 0, 1 \end{matrix} \right) - G_{1,3}^{3,1} \left(\frac{C}{\phi_1} \middle| \begin{matrix} 0 \\ 0, 0, 1 \end{matrix} \right) \right)$$

where $G_{1,3}^{3,1}$ is Meijer G function with parameters $\{0\}$ and $\{0, 0, 1\}$

Hence the proof of EC for IoT_R node as in Equation 9.

□

Paper IX

A Reinforcement Learning based Game Theoretic Approach for Distributed Power Control in Downlink NOMA

Ashish Rauniyar, Anis Yazidi, Paal E. Engelstad, Olav N. Østerbø

In: *2020 IEEE 19th International Symposium on Network Computing and Applications (NCA), Cambridge, MA, USA, 26-28 November*. (2020) pp. 1–10, DOI: 10.1109/NCA51143.2020.9306737

Paper X

Performance Analysis of RF Energy Harvesting and Information Transmission based on NOMA with Interfering Signal for IoT Relay Systems

Ashish Rauniyar, Paal E. Engelstad, Olav N. Østerbø

In: *IEEE Sensors Journal* Vol. 19, no. 17 (2019), pp. 7668–7682, DOI: 10.1109/JSEN.2019.2914796.

Paper XI

Ergodic Capacity Performance of NOMA-SWIPT Aided IoT Relay Systems with Direct Link

Ashish Rauniyar, Paal E. Engelstad, Olav N. Østerbø

In: *IEEE 18th International Symposium on Modeling and Optimization in Mobile, Ad Hoc and Wireless Networks (WiOpT 2020), Volos, Greece, 15-19 June* (2020), pp. 1–8.

Paper XII

Capacity Enhancement of NOMA-SWIPT IoT Relay System with Direct Links over Rayleigh Fading Channels

Ashish Rauniyar, Paal E. Engelstad, Olav N. Østerbø

In: *Transactions on Emerging Telecommunications Technologies, Wiley, Special Issue: Cross-layer Innovations in Internet of Things,* Vol. 00, no. 00 (2020), pp. 1–18, DOI: 10.1002/ett.3913.

Received: 10 December 2019 | Revised: 25 January 2020 | Accepted: 8 February 2020

DOI: 10.1002/ett.3913

Check for updates

SPECIAL ISSUE ARTICLE

WILEY

Capacity enhancement of NOMA-SWIPT IoT relay system with direct links over rayleigh fading channels

Ashish Rauniyar[1,2] | **Paal Engelstad**[1,2] | **Olav N. Østerbø**[3]

[1]Department of Technology Systems, University of Oslo, Oslo, Norway

[2]Department of Computer Science, Oslo Metropolitan University, Oslo, Norway

[3]Telenor Research, Telenor, Oslo, Norway

Correspondence
Ashish Rauniyar, Pilestredet 52, 0167 Oslo, Norway.
Email: ashishr@ifi.uio.no

Abstract

It is known that when the direct links between the base station (BS) and the users exist and are nonnegligible, consolidating direct links could significantly enhance the performance of the cooperative relaying systems. Therefore, taking the impact of direct link into account, in this article, we investigate the capacity enhancement of the nonorthogonal multiple access (NOMA) with simultaneous wireless information and power transfer (SWIPT) for the Internet of Things (IoT) relay systems over the Rayleigh fading channels. Specifically, for the considered NOMA-SWIPT system with direct links, we study a time-switching energy harvesting (EH) architecture in which a BS transmits two symbols to the two users through the direct links and via an EH-based relay node. On the receiving user node, we employ maximum ratio combining (MRC) to show the capacity enhancement of the considered system. Moreover, analytical expressions for the Ergodic capacity and Ergodic Sum Capacity are mathematically derived for the MRC and single signal decoding scheme, and the analytical expressions are corroborated with the Monte-Carlo simulation results. This not only reveals the effect of different EH parameters on the system performance, but it also demonstrates the capacity enhancement of the considered NOMA-SWIPT system compared to a similar system without direct links and to conventional OMA schemes.

1 | INTRODUCTION

Due to the proliferation of technologies like the Internet of Things (IoT), it has been predicted that by 2025, 80 billion IoT devices will be connected to the Internet, and the global data traffic will reach up to 175 trillion gigabytes.[1] Therefore, the upcoming fifth generation (5G) and next generation networks are expected to support these massive connectivity requirements of the IoT devices.[2,3] Meeting the capacity and energy demands at the same time is a challenge that needs to be resolved.[4] The two key requirements are spectral efficiency and energy efficiency among the various challenging requirements of the 5G and the next-generation networks. Therefore, new, energy and spectral efficient protocols to ameliorate the capacity and energy demands of the massive IoT networks need to be designed. To this end, nonorthogonal multiple access (NOMA) has been contemplated as an efficient multiple access solution to support the massive connectivity of IoT and fulfill the demand of global data traffic.[5-7] Specifically, in power domain NOMA, signals of the multiple users are superposed on each other by allocating different power levels based on the perceived channel conditions. In the downlink power domain NOMA, the users with good channel conditions are allocated less power,

 © 2020 John Wiley & Sons, Ltd.

while the users with poor channel conditions are allocated more power.[8,9] Finally, through the process of successive interference cancellation (SIC), the users can be separated at the receiver side.[10] On the other hand, simultaneous wireless information and power transfer (SWIPT) has been considered as a promising solution to combat the issue of powering up the devices through radio frequency (RF) signals.[11-13] Thus, NOMA and SWIPT can be integrated to serve the purpose of both key requirements—spectral and energy-efficiency for the 5G and the next generation networks.[14,15] Integrating NOMA and SWIPT can also be seen as a sustainable approach for green communication in the IoT networks.

Since RF signals are abundant in nature because of the vast amount of coexisting wireless technologies, these RF signals can actually be exploited to harvest the energy.[16] This harvested energy from the RF signals can be used to power up the small IoT devices for data transmission and prolong the lifetime of such IoT networks. In this regard, through SWIPT, a device or node can harvest the energy from the RF signal and do the data transmission simultaneously.[17,18] However, considering the practical considerations of the energy harvesting (EH) circuits of the receivers, SWIPT cannot be applied directly for the information decoding (ID) at the same time. Therefore, time switching (TS) and power splitting (PS) are two popular EH architectures widely considered for SWIPT. In the TS architecture, a fraction of time is used for EH and ID separately, while in the PS architecture, the receiver splits the incoming signal into two parts by following the signal partition method for EH and ID.[19] In this article, we have used the TS architecture at the relay node because of its low complexity and ease of implementation compared to the PS architecture. However, the analysis in this article can be applied easily to other EH architectures as well.

In Reference 20, TS relaying and PS relaying protocols are proposed for the relay node to harvest the energy and ID. The authors showed that the TS relaying protocol outperformed the PS relaying protocol at relatively low signal-to-noise ratios and at high transmission rates. NOMA has been successively applied in conjugation with several technologies, such as cooperative networks and SWIPT. In Reference 21, a relay selection for the cooperative NOMA networks was studied where a two-stage relay selection strategy was proposed to achieve a minimal outage probability. In Reference 22, a best-near best-far termed as BNBF user selection scheme for NOMA-based cooperative NOMA systems with SWIPT was proposed. Here, the authors investigated the outage performance, and closed-form analytical expressions of the outage probability were derived to evaluate the system performance. Different from most of the works on cooperative NOMA with SWIPT, the work in Reference 23 proposed an RF EH and information transmission based on TS, PS, and NOMA. Here, a power-constrained IoT node operated in the dual-mode of EH and transmitted its own data along with the source node data using the NOMA protocol. The NOMA-SWIPT model was extended to include the interfering signals and further studied in Reference 24.

In cooperative communications research, a general assumption is often that a direct link to the node is not available, and the communication of data is only possible through relaying. However, in wireless communication it is known that when direct links between the base station (BS) and the users exist and are nonnegligible, consolidating direct links could significantly enhance the performance of the cooperative relaying systems.[25,26] The performance analysis of the SWIPT relaying network in the presence of a direct link was carried out in Reference 27. The authors analyzed the optimal throughput performance by considering a simple system model with a source node, a relay node, and a destination node in the presence of a direct link. A Decode-and-Forward (DF) relay was analyzed in Reference 28 for a cooperative NOMA system with direct links. Although three different relay schemes were analyzed by the authors, EH was not considered in their system model. Analyzing and studying the impact of EH in the cooperative NOMA-SWIPT systems is important for increasing the spectral and energy-efficiency demands of IoT networks. The spectral and energy efficiency of the next generation IoT networks is possible through the combined approach of NOMA with SWIPT. Thus, the authors in Reference 29 studied the outage probability of a NOMA-SWIPT network in the presence of direct links. However, the authors only studied and analyzed the outage probability for the NOMA-SWIPT network with the direct link, while the Ergodic capacity (EC) and Ergodic sum capacity (ESC) were not studied. The reason for the necessity of studying the system's EC and ESC is obvious. For the delay-tolerant transmission mode, the source transmits at any constant rate upper bounded by the EC.[30] Since the codeword length is sufficiently large compared to the block time, the codeword could experience all possible realizations of the channel. Therefore, the EC becomes an appropriate measure for the performance analysis of the system.

Motivated by the works in References 28 and 29 and taking the EC as a fundamental performance indicator, in this article, we investigate the EC performance of cooperative NOMA-SWIPT aided IoT relay systems in which one BS sends two symbols to users UE_1 and UE_2 through the direct link and via an EH-based relay node using the TS architecture. In summary, the major contributions of this article are as follows:

- Although a myriad of works have been carried out in the literature for NOMA-SWIPT systems, to the best of our knowledge, there is no published literature investigating the EC and ESC of the NOMA-SWIPT-assisted IoT relay systems with the direct link over the Rayleigh fading channels in which one BS wants to transmit two symbols to two destination nodes through the direct link and with the assistance of EH-based relay node using the TS architecture.
- Since the direct links are involved, we employ the maximum ratio combining (MRC) scheme and show the capacity enhancement of the system, by comparing it with the single signal decoding scheme (SDS).
- For the considered NOMA-SWIPT system model with direct links, we derive the analytical expressions for the EC and the ESC for both the MRC and SDS schemes and validate them by Monte-Carlo simulations, demonstrating that our derived analytical expressions are correct.
- For a fair and logical evaluation of the considered NOMA-SWIPT system with the direct link, we devised a comparable model using OMA. Along with its analytical derivations, a thorough comparison is provided between the NOMA-SWIPT and OMA-SWIPT system models without considering the impact of direct links.
- Our results demonstrate that employing the MRC scheme could significantly enhance the ESC performance of the system compared to using the SDS scheme. Moreover, we also showed that, with proper selection of EH parameters, such as the TS factor and the power allocation factor for the NOMA, the ESC performance of the system could be further improved as compared to a NOMA-SWIPT system that has no direct links and to a conventional OMA schemes.

The rest of the article is organized as follows. In Section 2, we explain the considered NOMA-SWIPT system model with the direct link scenario. Section 3, describes the system model based on TS and NOMA. In Section 4, we explain the single SDS along with its EC and ESC derivations. The MRC scheme along with its EC and ESC derivations are carried out in Section 5. EC and ESC of the OMA system model for benchmarking of results are carried out in Section 6. The performance demonstrated through the simulations is presented in Section 7. Finally, the conclusions of the article are drawn in Section 8.

2 | SYSTEM MODEL SCENARIO

The considered cooperative NOMA-SWIPT system model with direct links is shown in Figure 1. Here, a BS will transmit two symbols, x_1 and x_2, to the two destination nodes, UE_1 and UE_2, respectively, through the direct link and with the assistance of an EH-based relay node using the TS protocol. As R is a power-constrained node that acts as a DF relay, it first harvests the RF energy from the BS signal using the TS protocol, and then it decodes the symbols x_1 and x_2 transmitted by the BS in the first phase. Also, UE_1 and UE_2 receive the information transmitted by the BS through the direct links in the first phase. Then, R forwards the decoded symbols x_1 and x_2 using the NOMA protocol to the UE_1 and UE_2 in the subsequent phase. We have assumed that all nodes are considered to be operating in a half-duplex mode. Each of the communication channels faces an independent Rayleigh flat fading with additive white Gaussian noise (AWGN) with zero mean and variance σ^2. The complex channel coefficient between any two nodes is denoted by $h_i \sim CN(0, \lambda_{h_i} = d_i^{-v})$ where $i \in \{1, 2, 3, 4, 5\}$. $\text{CN}(0, \lambda_{h_i} = d_i^{-v})$ is complex normal distribution to model the Rayleigh flat fading channel with zero mean and variance λ_{h_i}, d_i is the distance between the corresponding link, and v is the path loss exponent. The channel state information is assumed to be known at all nodes. As there exists direct links from the BS to R and UEs in our considered system model, therefore, the scenario in this article can be also depicted as the worst-case scenario of the Rician fading.

3 | SYSTEM MODEL BASED ON TS AND NOMA

In the TS relaying scheme, a power-constrained R node first harvests the energy from the BS signal for the duration of αT and then uses the time $\frac{(1-\alpha)T}{2}$ for the ID and finally $\frac{(1-\alpha)T}{2}$ for the information transmission to the UE_1 and UE_2 by following the NOMA protocol. The working of the system model based on the TS and NOMA can be explained in two phases as follows:

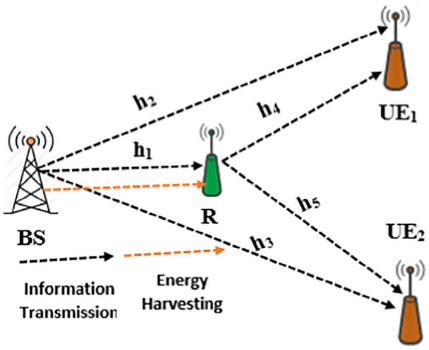

FIGURE 1 Considered System Model for the NOMA-SWIPT with Direct Links

3.1 | First phase

In the first phase, the BS broadcasts the following signal to R, UE_1 and UE_2:

$$x = \sqrt{a_1 P} x_1 + \sqrt{a_2 P} x_2 \tag{1}$$

where a_1 and a_2 are the NOMA power allocation coefficients and $a_1 > a_2$, and $a_1 + a_2 = 1$.

The received signal at R, UE_1 and UE_2 can be given, respectively, as:

$$y_{\mathrm{R}} = h_1 \left(\sqrt{a_1 P} x_1 + \sqrt{a_2 P} x_2 \right) + n_{\mathrm{R}} \tag{2}$$

$$y_{\mathrm{UE}_1} = h_2 \left(\sqrt{a_1 P} x_1 + \sqrt{a_2 P} x_2 \right) + n_{\mathrm{UE}_1} \tag{3}$$

$$y_{\mathrm{UE}_2} = h_3 \left(\sqrt{a_1 P} x_1 + \sqrt{a_2 P} x_2 \right) + n_{\mathrm{UE}_2} \tag{4}$$

where n_R, n_{UE_1}, and $n_{\mathrm{UE}_2} \sim \mathrm{CN}(0, \sigma^2 = 1)$ denote the AWGN at R, UE_1, and UE_2, respectively.

The energy harvested at R in the αT period of time is given as:

$$E_{h_{\mathrm{IoT_R}}} = \eta P |h_1|^2 \alpha T, \tag{5}$$

where $0 \leq \eta \leq 1$ is the energy conversion efficiency. We let P_{R} denote the transmit power of R in the $\frac{(1-\alpha)T}{2}$ time interval. P_{R} is given as:

$$P_{\mathrm{R}} = \frac{E_{h_{\mathrm{IoT_R}}}}{(1-\alpha)T/2} = \frac{2\eta P |h_1|^2 \alpha}{(1-\alpha)} = k\eta P |h_1|^2 \tag{6}$$

where $k = \frac{2\alpha}{1-\alpha}$.

Now, the SINR for x_1 at R, UE_1 and UE_2 can be given, respectively, as:

$$\gamma_{\mathrm{R}}^{x_1} = \frac{a_1 P |h_1|^2}{a_2 P |h_1|^2 + 1} = \frac{a_1 P X_1}{a_2 P X_1 + 1} \tag{7}$$

$$\gamma_{\mathrm{UE}_1}^{x_1} = \frac{a_1 P |h_2|^2}{a_2 P |h_2|^2 + 1} = \frac{a_1 P X_2}{a_2 P X_2 + 1} \tag{8}$$

$$\gamma_{\mathrm{UE}_2}^{x_1} = \frac{a_1 P |h_3|^2}{a_2 P |h_3|^2 + 1} = \frac{a_1 P X_3}{a_2 P X_3 + 1}. \tag{9}$$

Now, R and UE_2 decode the symbol x_2 by cancelling x_1 symbol with SIC. Therefore, the received SINR for x_2 at R and UE_2 can be given, respectively, as:

$$\gamma_{\mathrm{R}}^{x_2} = a_2 P|h_1|^2 = a_2 P X_1 \tag{10}$$

$$\gamma_{\mathrm{UE}_2}^{x_2} = a_2 P|h_3|^2 = a_2 P X_3. \tag{11}$$

It should be noted that in Equations (10) and (11), we have taken noise variance $\sigma^2 = 1$.

3.2 | Second phase

In this phase, R now uses the harvested energy (Equation (6)) to forward the successfully decoded symbols x_1 and x_2 to UE_1 and UE_2. R broadcasts the signal $\left(\sqrt{b_1 P_{\mathrm{R}}} x_1 + \sqrt{b_2 P_{\mathrm{R}}} x_2\right)$ to UE_1 and UE_2 with b_1 and b_2 as the power allocation coefficients for the decoded symbols x_1 and x_2, respectively, and $b_1 + b_2 = 1$, $b_1 > b_2$.

The received signal at UE_1 and UE_2 in the second phase can be given, respectively, as:

$$y_{\mathrm{UE}_1}^{II} = h_4 \left(\sqrt{b_1 P_{\mathrm{R}}} x_1 + \sqrt{b_2 P_{\mathrm{R}}} x_2\right) + n_{\mathrm{UE}_1}^{II} \tag{12}$$

$$y_{\mathrm{UE}_2}^{II} = h_5 \left(\sqrt{b_1 P_{\mathrm{R}}} x_1 + \sqrt{b_2 P_{\mathrm{R}}} x_2\right) + n_{\mathrm{UE}_2}^{II} \tag{13}$$

Now, UE_1 decodes x_1 by treating x_2 as noise.

$$\gamma_{\mathrm{UE}_1}^{x_1,II} = \frac{b_1 P_{\mathrm{R}}|h_4|^2}{b_2 P_{\mathrm{R}}|h_4|^2 + 1} = \frac{b_1 k\eta P X_1 X_4}{b_2 k\eta P X_1 X_4 + 1}. \tag{14}$$

UE_2 decodes x_2 after decoding x_1 and cancelling it by SIC.

$$\gamma_{\mathrm{UE}_2}^{x_1,II} = \frac{b_1 P_{\mathrm{R}}|h_5|^2}{b_2 P_{\mathrm{R}}|h_5|^2 + 1} = \frac{b_1 k\eta P X_1 X_5}{b_2 k\eta P X_1 X_5 + 1} \tag{15}$$

$$\gamma_{\mathrm{UE}_2}^{x_2,II} = b_2 P_{\mathrm{R}}|h_5|^2 = b_2 P_{\mathrm{R}} X_5 = b_2 k\eta P X_1 X_5. \tag{16}$$

In Equation (16), we have taken noise variance $\sigma^2 = 1$.

4 | SDS SCHEME

In the first phase of the SDS scheme, R, UE_1, and UE_2 immediately decode the symbol x_1 with the corresponding received SINR as shown in Equations (7), (8), and (9). Similarly, R, and UE_2 decode the symbol x_2 by cancelling the symbol x_1 with SIC. The corresponding received SINR for decoding the symbol x_2 at R, and UE_2 can be given by Equations (10), (11). During the second phase, UE_1 and UE_2 decode the symbols x_1 and x_2 retransmitted from the R with the received SINR as shown in Equations (14), (15), (16). Thus, during the first and second phase of the SDS scheme, a single signal or symbol 'x_1' and 'x_2' is detected at UE_1 and UE_2, respectively.

4.1 | EC and ESC Analysis for the Single SDS

By using Equations (7), (8), (9), (14) and (15), the achievable data rate of UE_1 associated with the symbol x_1 based on TS and NOMA for the SDS scheme is given as:

$$C_{\mathrm{SDS}}^{x_1} = \frac{(1-\alpha)}{2} \log_2 \left(1 + \min\left(\gamma_R^{x_1}, \gamma_{UE_1}^{x_1,II}, \gamma_{UE_2}^{x_1,II}, \gamma_{UE_1}^{x_1}, \gamma_{UE_2}^{x_1}\right)\right) \tag{17}$$

Theorem 1. *The EC of* UE_1 *using TS and NOMA for the single SDS can be expressed as:*

$$C^{x_1}_{\text{SDS-Ana}} = \frac{(1-\alpha)}{2\ln 2}\int_{\gamma=0}^{\frac{a_1}{a_2}} \frac{\lambda_{h_1}}{1+\gamma} e^{-\frac{(\lambda_{h_2}+\lambda_{h_3})\gamma}{P(a_1-\gamma a_2)}} \left(2\sqrt{\frac{(\lambda_{h_4}+\lambda_{h_5})\gamma}{k\eta P\lambda_{h_1}(b_1-\gamma b_2)}}K_1\left(2\sqrt{\frac{(\lambda_{h_4}+\lambda_{h_5})\gamma\lambda_{h_1}}{k\eta P(b_1-\gamma b_2)}}\right)\right.$$
$$\left. - \sum_{n=0}^{\infty}\frac{(-1)^n}{n!}\lambda_{h_1}^n\left(\frac{\gamma}{P(a_1-\gamma a_2)}\right)^{n+1} E_{n+2}\left(\frac{(\lambda_{h_4}+\lambda_{h_5})(a_1-\gamma a_2)}{k\eta(b_1-\gamma b_2)}\right)\right) d\gamma \tag{18}$$

Proof. The proof is given in Appendix A1. ∎

Corollary 1. *In Theorem* 1*, when* $\lambda_{h_2}=0$ *and* $\lambda_{h_3}=0$*, the analytical expression for EC of* UE_1 *using TS and NOMA without direct links (WDLs) can be expressed as:*

$$C^{x_1}_{\text{WDL-Ana}} = \frac{(1-\alpha)}{2\ln 2}\int_{\gamma=0}^{\frac{a_1}{a_2}} \frac{\lambda_{h_1}}{1+\gamma} \left(2\sqrt{\frac{(\lambda_{h_4}+\lambda_{h_5})\gamma}{k\eta P\lambda_{h_1}(b_1-\gamma b_2)}}K_1\left(2\sqrt{\frac{(\lambda_{h_4}+\lambda_{h_5})\gamma\lambda_{h_1}}{k\eta P(b_1-\gamma b_2)}}\right)\right.$$
$$\left. - \sum_{n=0}^{\infty}\frac{(-1)^n}{n!}\lambda_{h_1}^n\left(\frac{\gamma}{P(a_1-\gamma a_2)}\right)^{n+1} E_{n+2}\left(\frac{(\lambda_{h_4}+\lambda_{h_5})(a_1-\gamma a_2)}{k\eta(b_1-\gamma b_2)}\right)\right) d\gamma \tag{19}$$

Proof. Substituting $\lambda_{h_2}=0$ and $\lambda_{h_3}=0$, the proof can be derived by following the same steps as in Theorem 1. ∎

Now, by using Equations (10), (11), and (16), the achievable data rate of UE_2 associated with the symbol x_2 based on TS and NOMA for the SDS scheme is given as:

$$C^{x_2}_{\text{SDS}} = \frac{1}{2}\log_2\left(1+\min\left(\gamma_R^{x_2}, \gamma_{\mathrm{UE}_2}^{x_2,II}, \gamma_{\mathrm{UE}_2}^{x_2}\right)\right) \tag{20}$$

Theorem 2. *The EC of* UE_2 *using TS and NOMA for the single SDS can be expressed as:*

$$C^{x_2}_{\text{SDS-Ana}} = \frac{(1-\alpha)}{2\ln 2}\int_{\gamma=0}^{\infty} \frac{\lambda_{h_1}}{1+\gamma} e^{-\frac{\lambda_{h_3}\gamma}{a_2 P}} \left(2\sqrt{\frac{\lambda_{h_5}\gamma}{b_2 k\eta P\lambda_{h_1}}}K_1\left(2\sqrt{\frac{\lambda_{h_1}\lambda_{h_5}\gamma}{b_2 k\eta P}}\right) - \sum_{n=0}^{\infty}\frac{(-1)^n}{n!}\lambda_{h_1}^n\left(\frac{\gamma}{a_2 P}\right)^{n+1} E_{n+2}\left(\frac{\lambda_{h_5}a_2}{b_2 k\eta}\right)\right) d\gamma \tag{21}$$

Proof. The proof is given in Appendix B1. ∎

Corollary 2. *In Theorem* 2*, when* $\lambda_{h_2}=0$ *and* $\lambda_{h_3}=0$*, the analytical expression for EC of* UE_2 *using TS and NOMA WDL can be expressed as:*

$$C^{x_2}_{\text{WDL-Ana}} = \frac{(1-\alpha)}{2\ln 2}\int_{\gamma=0}^{\infty} \frac{\lambda_{h_1}}{1+\gamma} \left(2\sqrt{\frac{\lambda_{h_5}\gamma}{b_2 k\eta P\lambda_{h_1}}}K_1\left(2\sqrt{\frac{\lambda_{h_1}\lambda_{h_5}\gamma}{b_2 k\eta P}}\right) - \sum_{n=0}^{\infty}\frac{(-1)^n}{n!}\lambda_{h_1}^n\left(\frac{\gamma}{a_2 P}\right)^{n+1} E_{n+2}\left(\frac{\lambda_{h_5}a_2}{b_2 k\eta}\right)\right) d\gamma \tag{22}$$

Proof. Substituting $\lambda_{h_2}=0$ and $\lambda_{h_3}=0$, the proof can be derived by following the same steps as in Theorem 2. ∎

Now, by combining Equations (18) and (20), the analytical expression for the ESC of the considered system based on TS and NOMA with direct links for the SDS scheme is given by:

$$C^{\text{SDS}}_{\text{ESum}} = C^{x_1}_{\text{SDS-Ana}} + C^{x_2}_{\text{SDS-Ana}} \tag{23}$$

Similarly, by combining Equations (19) and (22), the analytical expression for the ESC of the considered system based on TS and NOMA WDL is given by:

$$C^{\text{WDL}}_{\text{ESum}} = C^{x_1}_{\text{WDL-Ana}} + C^{x_2}_{\text{WDL-Ana}} \tag{24}$$

It should be noted that the final analytical expression of $C^{x_1}_{\text{SDS-Ana}}$, $C^{x_2}_{\text{SDS-Ana}}$, $C^{x_1}_{\text{WDL-Ana}}$ and $C^{x_1}_{\text{WDL-Ana}}$ as shown in Theorem 1, Theorem 2, Corollary 1 and Corollary 2, respectively, contain an integral term which is difficult to

evaluate in closed form, but it can be evaluated through numerical approaches using software such as MATLAB or Mathematica.

5 | MRC DECODING SCHEME

As the achievable data rate is limited by the inferior channel, in the MRC scheme, UE_1 and UE_2 will not decode the received signal in the first phase. UE_1 and UE_2 will instead conserve the signal and jointly decode the signal through the MRC scheme after receiving the decoded symbol x_1 and x_2 from R in the second phase. Therefore, the corresponding SINR during the second stage for x_1 and x_2 through the MRC scheme at UE_1 and UE_2 can be, respectively, given as:

$$\gamma_{\text{MRC}}^{x_1} = \frac{a_1 P X_2}{a_2 P X_2 + 1} + \frac{b_1 k\eta P X_1 X_4}{b_2 k\eta P X_1 X_4 + 1} \tag{25}$$

$$\gamma_{\text{MRC}}^{x_2} = a_2 P X_3 + b_2 k\eta P X_1 X_5 \tag{26}$$

5.1 | EC and ESC Analysis for the MRC Decoding Scheme

By using the Equations (7), (9), (15), and (26), the achievable data rate of UE_1 associated with the symbol x_1 based on TS and NOMA for the MRC scheme can be given as:

$$C_{MRC}^{x_1} = \frac{(1-\alpha)}{2}\log_2\left(1 + \min\left(\gamma_R^{x_1}, \gamma_{UE_2}^{x_1}, \gamma_{UE_2}^{x_1,II}, \gamma_{MRC}^{x_1}\right)\right) \tag{27}$$

Theorem 3. *The EC of* UE_1 *using TS and NOMA for the MRC decoding scheme can be expressed as:*

$$C_{\text{MRC-Ana}}^{x_1} = \frac{(1-\alpha)}{2\ln 2}\int_{\gamma=0}^{\frac{a_1}{a_2}} \frac{1}{1+\gamma}\left(e^{-\frac{\lambda_{h_3}\gamma}{P(a_1-\gamma a_2)}}\int_{x_1=\frac{\gamma}{P(a_1-\gamma a_2)}}^{\infty} e^{-\frac{\lambda_{h_5}\gamma}{k\eta P(b_1-b_2\gamma)x_1}} \times\left(\int_{z=c_3}^{\hat{z}} \frac{\lambda_{h_2}}{c_4} e^{-\frac{c_1}{c_4}} e^{\frac{\lambda_{h_2}c_3}{c_4}} e^{-\frac{(c_2c_4-c_1c_3)}{c_4 z}-\frac{\lambda_{h_2}z}{c_4}} dz + e^{-\frac{\lambda_{h_2}\gamma}{(a_1-a_2\gamma)P}}\right)\lambda_{h_1} e^{-\lambda_{h_1}x_1} dx_1\right) d\gamma \tag{28}$$

where $c_1 = \lambda_{h_4} P(a_2\gamma - a_1), c_2 = \lambda_{h_4}\gamma, c_3 = k\eta P x_1(b_1 - \gamma b_2), c_4 = k\eta P^2 x_1(b_1 a_2 - b_2(a_2\gamma - a_1)), \hat{z} = c_3 + c_4\frac{\gamma}{(a_1-a_2\gamma)P}$

Proof. The proof is given in Appendix C1. ∎

Now, by using Equations (10) and (25), the achievable data rate of UE_2 associated with the symbol x_2 based on TS and NOMA for the MRC scheme can be given as:

$$C_{\text{MRC}}^{x_2} = \frac{(1-\alpha)}{2}\log_2\left(1 + \min\left(\gamma_{\text{R}}^{x_2}, \gamma_{MRC}^{x_2}\right)\right) \tag{29}$$

Theorem 4. *The EC of* UE_2 *using TS and NOMA for the MRC decoding scheme can be expressed as:*

$$C_{\text{MRS-Ana}}^{x_2} = \frac{(1-\alpha)}{2\ln 2}\int_{\gamma=0}^{\infty} \frac{1}{1+\gamma}\left(\int_{x_1=\frac{\gamma}{a_2 P}}^{\infty} \lambda_{h_1}\lambda_{h_3}\frac{b_2 k\eta x_1}{b_2 k\eta\lambda_{h_3}x_1 - a_2\lambda_{h_5}} e^{-\frac{\lambda_{h_5}\gamma}{b_2 k\eta P x_1}-\lambda_{h_1}x_1} dx_1 - \int_{x_1=\frac{\gamma}{a_2 P}}^{\infty} \lambda_{h_3}\frac{b_2 k\eta x_1}{b_2 k\eta\lambda_{h_3}x_1 - a_2\lambda_{h_5}} e^{-\frac{\lambda_{h_5}\gamma}{b_2 k\eta P x_1}} e^{-\frac{(b_2 k\eta\lambda_{h_3}x_1 - a_2\lambda_{h_5})\gamma}{b_2 k\eta x_1 a_2 P}}\lambda_{h_1} e^{-\lambda_{h_1}x_1} dx_1 + e^{-\frac{(\lambda_{h_1}+\lambda_{h_3})\gamma}{a_2 P}}\right) d\gamma \tag{30}$$

Proof. The proof is given in Appendix D1. ∎

Now, by combining the Equations (28) and Equation (30), we get the analytical expression for the ESC of the considered system based on TS and NOMA with direct links for the MRC scheme.

It should again be noted that the final analytical expression of $C^{x_1}_{MRC-Ana}$, and $C^{x_2}_{MRC-Ana}$ as shown in Theorem 3, and Theorem 4, respectively, contain an integral term which is difficult to evaluate in closed form, but it can be evaluated through numerical approaches using software such as MATLAB or Mathematica.

6 | EC AND ESC OF OMA - FOR BENCHMARKING OF RESULTS

To evaluate the performance and demonstrate the capacity enhancement of our NOMA-SWIPT IoT relay system with a direct link, an OMA scheme using time-division multiple access (TDMA) referred to as OMA-TDMA, is considered. In the OMA-TDMA scheme, the time slots, each of the duration T, can be arranged into four time slots. In the first time slot, the BS broadcasts the signal x_1 to R and UE_1. Since R is an EH based relay, it first harvests the energy from the BS's signal for a period of αT and then uses the time $(1-\alpha)T$ for ID. In the second time slot, R now broadcasts the decoded symbol X_1 to UE_1. Similarly, the process is repeated for the symbol x_2 for the UE_2 through the direct link and via an EH based relay R in the next two time slots. For a fair comparison with our NOMA-SWIPT system model with direct links, similar to our discussion on the SDS and MRC scheme in the above section, the user nodes UE_1 and UE_2 in the OMA-TDMA scheme can also apply the SDS or MRC scheme. Also, it should be noted that in our model, the power of the BS and the EH based R node is divided by allocating the power allocation coefficients a_1, a_2, b_1 and b_2 and thus allowing BS and R to transmit x_1 and x_2 symbols with full power. OMA-TDMA scheme would not represent a fair and reasonable comparison with our NOMA-SWIPT model. Instead, we resort to allocating the same power allocation coefficients, b_1 and b_2 at the R in both the NOMA-SWIPT system model and the OMA-TDMA scheme.

In the OMA-TDMA scheme, the transmit power of the EH based DF relay node R is given by:

$$P_{R-OT} = \frac{\eta\alpha P|h_1|^2}{1-\alpha} \tag{31}$$

The EC of UE_1 for OMA-TDMA that is using the SDS scheme and the MRC scheme is given respectively by:

$$C^{x_1}_{\text{OMA-SDS}} = \frac{(1-\alpha)}{4}\log_2(1+\min(P|h_2|^2, P|h_1|^2, b_1P_{R-OT}|h_4|^2)) \tag{32}$$

$$C^{x_1}_{\text{OMA-MRC}} = \frac{(1-\alpha)}{4}\log_2(1+\min(P|h_1|^2, P|h_2|^2 + b_1P_{R-OT}|h_4|^2)) \tag{33}$$

Similarly, the EC of UE_2 for OMA-TDMA that is using the SDS scheme and the MRC scheme is given respectively by:

$$C^{x_2}_{\text{OMA-SDS}} = \frac{(1-\alpha)}{4}\log_2(1+\min(P|h_3|^2, P|h_1|^2, b_2P_{R-OT}|h_5|^2)) \tag{34}$$

$$C^{x_2}_{\text{OMA-MRC}} = \frac{(1-\alpha)}{4}\log_2(1+\min(P|h_1|^2, P|h_3|^2 + b_2P_{R-OT}|h_5|^2)) \tag{35}$$

Now, by combining Equations (32) and (34), we get the ESC of the OMA-TDMA model that is using the SDS scheme. Similarly, by combining Equations (33) and (35), we get the ESC of the OMA-TDMA model that is using the MRC scheme.

7 | NUMERICAL RESULTS AND DISCUSSIONS

In this section, we use Monte-Carlo simulations to test the correctness of our derived mathematical expressions for the EC and ESC of the system and make performance comparisons with the system model WDL and with the conventional OMA scheme. Unless otherwise stated, the simulation parameters used in the experiments are specified in Table 1. We used MATLAB for the Monte-Carlo experiments by averaging over 10^5 random realization of Rayleigh fading channels, i.e. h_1, h_2, h_3, h_4 and h_5. In all the results presented in this section, the legends in the figures 'SDS Ana' and 'SDS Sim' represent the analytical and simulation results for the NOMA-SWIPT model with direct links that is using the single signal detection scheme. Similarly, 'MRC Ana' and 'MRC Sim' represent the analytical and simulation results for the NOMA-SWIPT model with direct links that is using the MRC detection scheme. 'WDL

TABLE 1 Simulation parameters

Parameter	Symbol	Values
Distance between BS and R	d_1	2.0 m
Distance between BS and UE_1	d_2	3.0 m
Distance between BS and UE_2	d_3	1.5 m
Distance between R and UE_1	d_4	2.0 m
Distance between R and UE_2	d_5	1.0 m
Path loss exponent	v	3
BS transmit SNR	δ	0-45 dB
Energy harvesting efficiency	η	0.9
Power allocation factor for NOMA	a_1	0.8
Power allocation factor for NOMA	a_2	0.2
Power allocation factor for NOMA	b_1	0.8
Power allocation factor for NOMA	b_2	0.2

Abbreviation: SNR, Signal-to-noise ratio.

FIGURE 2 Ergodic Capacity of UE_1

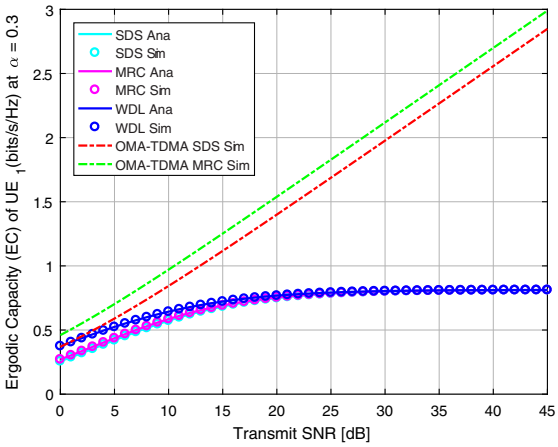

Ana' and 'WDL Sim' represent the analytical and simulation results of the NOMA-SWIPT system that is not using direct links, that is, without direct links stands for 'WDLs'. 'OMA-TDMA SDS Sim' and 'OMA-TDMA MRC Sim' represent the Monte-Carlo simulation results for the single signal detection and MRC scheme for the OMA-TDMA system model.

In Figures 2 and 3, we plot the ECs of UE_1 and UE_2 with the TS factor $\alpha = 0.3$ against the transmit SNR. As UE_1 is a distant user with poor channel conditions compared to UE_2, we observe that the EC of UE_1 is worse than that of UE_2. The ECs of UE_1 of the OMA-TDMA schemes that are using the SDS or MRC schemes are higher than our NOMA-SWIPT model with direct links. However, the EC for the NOMA-SWIPT model with direct links is superior to the OMA-TDMA scheme, as shown in Figure 3. As expected, the MRC scheme outperforms the SDS scheme. Also, one could argue this is not the case in Figure 2. Moreover, OMA-TDMA gives a more equal and fair sharing of capacity between UE_1 and UE_2.

In Figure 4, we plot the ESC at $\alpha = 0.3$ and $\alpha = 0.7$ against the transmit Signal-to-noise ratio (SNR) for all the schemes for a thorough comparison. We observe that the ESC is an increasing function with respect to increase in the transmit SNR for all of the schemes. At low transmit SNR, i.e. less than 10 dB, the OMA-TDMA MRC scheme has higher ESC than our NOMA-SWIPT model with direct links. However, as we increase the transmit SNR, the ESC of our NOMA-SWIPT model gives the overall higher ESC for the system. The reason for OMA-TDMA MRC scheme to have better ESC at low transmit

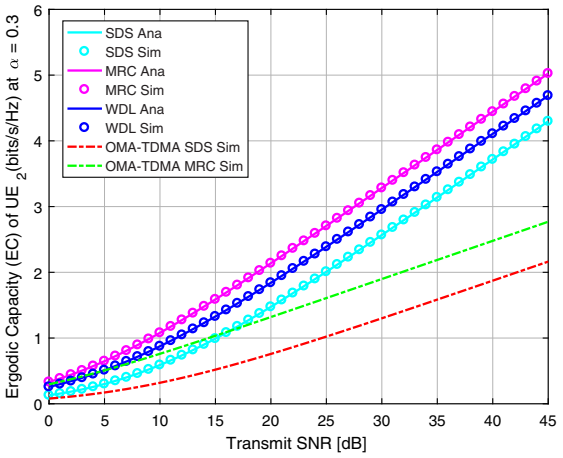

FIGURE 3 Ergodic capacity of UE_2

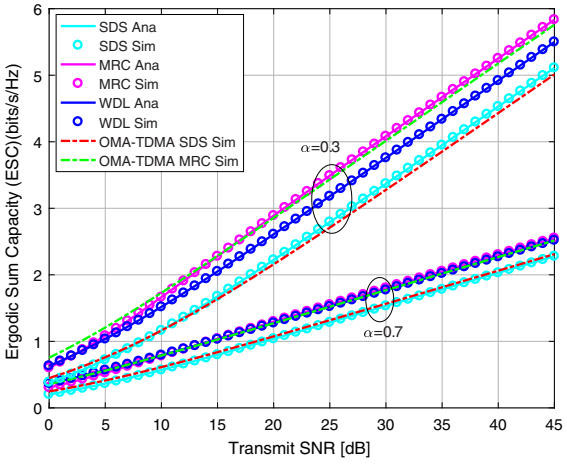

FIGURE 4 Ergodic sum capacity of considered system model for the NOMA-SWIPT with the direct link

SNR is that the BS transmits the signal for UE_1 and UE_2 with its full power of BS in two time slots whereas, in our considered NOMA-SWIPT model, the power of the BS is divided into two parts for the UE_1 and UE_2 using a single time slot. Also, it is interesting to note that the NOMA-SWIPT model WDLs has higher EC for UE_2 than our considered NOMA-SWIPT model with direct links that is using the SDS scheme. The reason for this is that the EC is dominated by the weakest link. Moreover, as we increase the α factor from 0.3 to 0.7, we see that the ESCs for all the models decrease. This indicates that a small α factor is sufficient for the system to harvest enough energy and the remaining time can be used for the data transmission.

In order to investigate the impact of α factor on the ESC performance, we plot the ESC against various α at the transmit SNR 25 dB and 10 dB in Figure 5. We observe that the ESC for all of the considered system models except the OMA-TDMA MRC scheme increases with an increase in α factor, until it reaches up to a maximum, and then it decreases again. This confirms that the ESC is a concave function that has a unique maxima at which the ESC of the system is maximized. The optimal α factor can be easily found, e.g., using the Golden section search method as in.[23] Also, as expected, a higher transmit SNR increases the ESC, as observed in Figure 5.

Since, the power allocation factor plays an important role in the NOMA-SWIPT system, in Figure 6, we plot the ESC against the power allocation coefficient factor b_1. When plotting the results in Figure 6, all other factors, such as $b_2 = 0.2$, $a_1 = 0.8$, and $a_2 = 0.2$ remained fixed and $\alpha = 0.3$. The reason for choosing to plot the ESC against the power allocation

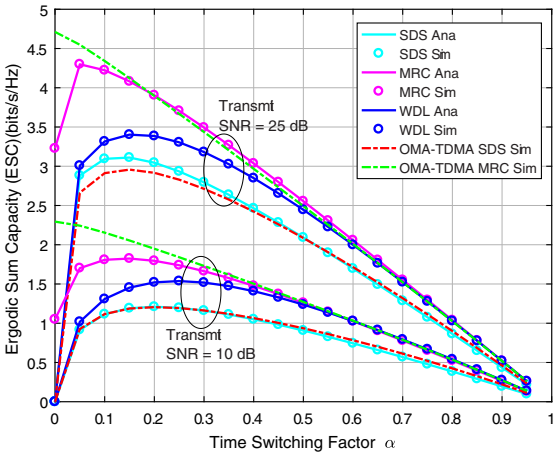

FIGURE 5 Ergodic sum capacity vs time switching factor

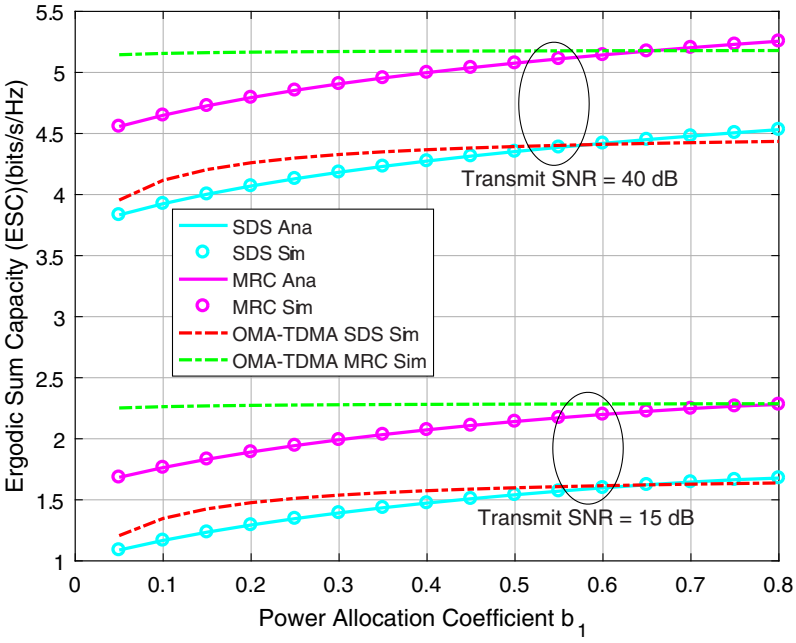

FIGURE 6 Ergodic sum capacity vs power allocation coefficient b_1

coefficient factor b_1 is that b_1 is the power allocated to the weak channel user UE_1, and b_1 factor determines the highest power allocation factor from the harvested energy at R that it is used for the data transmission to UE_1. We observe that the OMA-TDMA scheme outperforms our NOMA-SWIPT model with direct links when the power allocation coefficient factor b_1 is less than 0.6. When the value of b_1 increases beyond 0.6, the ESC of our NOMA-SWIPT model increases for both the SDS and MRC schemes. This confirms that the value of the power allocation coefficient factor needs to be selected carefully to achieve the best ESC performance.

Next, we intend to verify the ESC performance of our system model with the same power allocation coefficients of a_1 and a_2 for the OMA-TDMA system, to see the effect of ESC on the system. It should be noted that for the OMA-TDMA system, we assumed that the BS transmits the signals to UE_1 and UE_2 with the full power. However, for our NOMA-SWIPT model, the BS power is divided for the data transmission of the UE_1 and UE_2 by the power allocation coefficients a_1

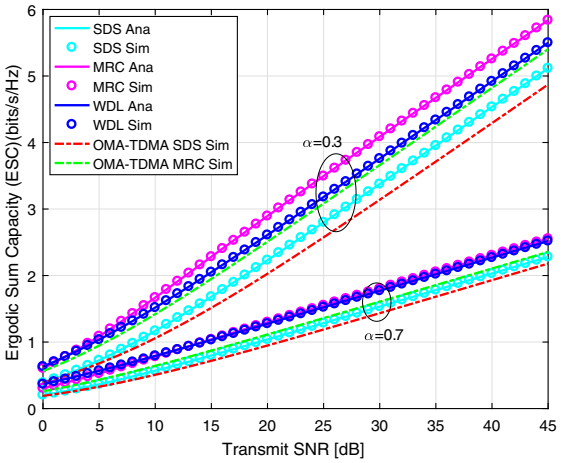

FIGURE 7 Ergodic sum capacity with the same power allocation coefficients a_1 and a_2

and a_2. Therefore, in Figure 7, we see that, if we allocate the same power allocation coefficients of a_1 and a_2 for the OMA-TDMA system for a fair comparison with our NOMA-SWIPT model with direct links, the ESC performance of our model outperforms the OMA-TDMA system model for both the MRC and SDS schemes. Also, it is observed that the ESC of the NOMA-SWIPT system model that is not using direct links outperformed the ESC performance of the OMA-TDMA system for both the SDS and MRC scheme. This indicates the performance gain in the ESC of the NOMA-SWIPT system over the OMA-TDMA SWIPT system.

8 | CONCLUSION

It is understood that consolidating direct links can significantly improve the efficiency of cooperative relaying systems when there are direct links between the BS and the users. Therefore, in this article, we investigated how direct links improve the capacity of the NOMA-SWIPT IoT relay systems with Rayleigh fading channels. Specifically, by employing the MRC scheme, we showed how direct links enhance the capacity of our NOMA-SWIPT system model with a TS EH architecture. For a detailed study and a fair comparison of the NOMA-SWIPT system model with direct links, we also studied the model without considering direct links and also other OMA-TDMA SWIPT models. The analytical expressions for the NOMA-SWIPT model with and WDLs for both MRC and SDS schemes were mathematically derived and analyzed and finally corroborated with the Monte-Carlo simulation results. Our results demonstrated that the MRC scheme can significantly enhance the ESC performance of the system compared to the SDS scheme. Moreover, we also showed that, with a proper selection of EH parameters, such as TS factor and power allocation factor for the NOMA, the ESC performance of the system can be further improved compared to the NOMA-SWIPT system that is not using direct links and compared to conventional OMA schemes.

ORCID

Ashish Rauniyar https://orcid.org/0000-0002-2142-9522

REFERENCES

1. Reinsel D, Gantz J, Rydning J. Data age 2025: the digitization of the world from edge to core. *Seagate*. 2018; Doc# US44413318:1-28. https://www.seagate.com/files/www-content/our-story/trends/files/idc-seagate-dataage-whitepaper.pdf.
2. Bockelmann C, Pratas NK, Wunder G, et al. Towards massive connectivity support for scalable mMTC communications in 5G networks. *IEEE Access*. 2018;6:28969-28992.
3. Al-Falahy N, Alani OY. Technologies for 5G networks: challenges and opportunities. *IT Professional*. 2017;19(1):12-20.
4. Singh S, Saxena N, Roy A, Kim H. Energy efficiency in wireless networks–a composite review. *IETE Tech Rev*. 2015;32(2):84-93.
5. Ali KS, Haenggi M, ElSawy H, Chaaban A, Alouini MS. Downlink non-orthogonal multiple access (NOMA) in poisson networks. *IEEE Trans Commun*. 2018;67(2):1613-1628.

6. Basharat M, Ejaz W, Naeem M, Khattak AM, Anpalagan A. A survey and taxonomy on nonorthogonal multiple-access schemes for 5G networks. *Trans Emerg Telecommun Technol*. 2018;29(1):e3202.
7. Wan D, Wen M, Ji F, Yu H, Chen F. Non-orthogonal multiple access for cooperative communications: challenges, opportunities, and trends. *IEEE Wirel Commun*. 2018;25(2):109-117.
8. Islam SR, Avazov N, Dobre OA, Kwak KS. Power-domain non-orthogonal multiple access (NOMA) in 5G systems: potentials and challenges. *IEEE Commun Surv Tutor*. 2016;19(2):721-742.
9. Zhang Y, Yang Z, Feng Y, Yan S. Performance analysis of cooperative relaying systems with power-domain non-orthogonal multiple access. *IEEE Access*. 2018;6:39839-39848.
10. Chen X, Jia R, Ng DWK. On the design of massive non-orthogonal multiple access with imperfect successive interference cancellation. *IEEE Trans Commun*. 2018;67(3):2539-2551.
11. Zhai D, Zhang R, Du J, Ding Z, Yu FR. Simultaneous wireless information and power transfer at 5G new frequencies: channel measurement and network design. *IEEE J Select Areas Commun*. 2018;37(1):171-186.
12. Liu X, Zhang X, Jia M, Fan L, Lu W, Zhai X. 5G-based green broadband communication system design with simultaneous wireless information and power transfer. *Phys Commun*. 2018;28:130-137.
13. Chae SH, Jeong C, Lim SH. Simultaneous wireless information and power transfer for internet of things sensor networks. *IEEE Internet Things J*. 2018;5(4):2829-2843.
14. Kader MF, Uddin MB, Islam A, Shin SY. Cooperative non-orthogonal multiple access with SWIPT over Nakagami-m fading channels. *Trans Emerg Telecommun Technol*. 2019;30(5):e3571.
15. Zaidi SK, Hasan SF, Gui X. SWIPT-aided uplink in hybrid non-orthogonal multiple access. Paper presented at: Proceedings of the IEEE Wireless Communications and Networking Conference (WCNC); 2018:1-6; IEEE.
16. Huang S, Yao Y, Feng Z. Simultaneous wireless information and power transfer for relay assisted energy harvesting network. *Wirel Netw*. 2018;24(2):453-462.
17. Aboelwafa MM, Abd-Elmagid MA, Biason A, Seddik KG, ElBatt T, Zorzi M. Towards optimal resource allocation in wireless powered communication networks with non-orthogonal multiple access. *Ad Hoc Netw*. 2019;85:1-10.
18. Huang J, Xing CC, Wang C. Simultaneous wireless information and power transfer: technologies, applications, and research challenges. *IEEE Commun Mag*. 2017;55(11):26-32.
19. Gu Y, Aissa S. RF-based energy harvesting in decode-and-forward relaying systems: ergodic and outage capacities. *IEEE Trans Wirel Commun*. 2015;14(11):6425-6434.
20. Nasir AA, Zhou X, Durrani S, Kennedy RA. Relaying protocols for wireless energy harvesting and information processing. *IEEE Trans Wirel Commun*. 2013;12(7):3622-3636.
21. Ding Z, Dai H, Poor HV. Relay selection for cooperative NOMA. *IEEE Wirel Commun Lett*. 2016;5(4):416-419.
22. Do NT, Da Costa DB, Duong TQ, An B. A BNBF user selection scheme for NOMA-based cooperative relaying systems with SWIPT. *IEEE Commun Lett*. 2016;21(3):664-667.
23. Rauniyar A, Engelstad P, Østerbø O. RF energy harvesting and information transmission based on NOMA for wireless powered IoT relay systems. *Sensors*. 2018;18(10):3254.
24. Rauniyar A, Engelstad PE, Østerbø ON. Performance analysis of RF energy harvesting and information transmission based on NOMA with interfering signal for IoT relay systems. *IEEE Sensors J*. 2019;19(17):7668-7682. https://doi.org/10.1109/JSEN.2019.2914796.
25. Kim JB, Lee IH. Non-orthogonal multiple access in coordinated direct and relay transmission. *IEEE Commun Lett*. 2015;19(11):2037-2040.
26. Kim JB, Lee IH, Lee J. Capacity scaling for D2D aided cooperative relaying systems using NOMA. *IEEE Wirel Commun Lett*. 2017;7(1):42-45.
27. Zhao N, Hu F, Li Z, Gao Y. Simultaneous wireless information and power transfer strategies in relaying network with direct link to maximize throughput. *IEEE Trans Veh Technol*. 2018;67(9):8514-8524.
28. Liu H, Ding Z, Kim KJ, Kwak KS, Poor HV. Decode-and-forward relaying for cooperative NOMA systems with direct links. *IEEE Trans Wirel Commun*. 2018;17(12):8077-8093.
29. Ha DB, Nguyen SQ. Outage performance of energy harvesting DF relaying NOMA networks. *Mobile Netw Appl*. 2018;23(6):1572-1585.
30. Zhong C, Suraweera HA, Zheng G, Krikidis I, Zhang Z. Improving the throughput of wireless powered dual-hop systems with full duplex relaying. Paper presented at: Proceedings of the IEEE International Conference on Communications (ICC); 2015:4253-4258; IEEE.
31. Gradshteyn IS, Ryzhik IM. *Table of Integrals, Series, and Products*. Cambridge, MA: Academic Press; 1980.

How to cite this article: Rauniyar A, Engelstad P, Østerbø ON. Capacity enhancement of NOMA-SWIPT IoT relay system with direct links over rayleigh fading channels. *Trans Emerging Tel Tech*. 2020;e3913. https://doi.org/10.1002/ett.3913

APPENDIX A

Proof of Theorem 1. The cumulative distributive function (CDF) of $\min(\gamma_{\mathrm{R}}^{x_1}, \gamma_{\mathrm{UE}_1}^{x_1,II}, \gamma_{\mathrm{UE}_2}^{x_1,II}, \gamma_{\mathrm{UE}_1}^{x_1}, \gamma_{\mathrm{UE}_2}^{x_1})$ can be given as:

$$F_\gamma(\gamma) = 1 - \Pr\left(\frac{a_1 PX_2}{a_2 PX_2 + 1} \geq \gamma\right) \Pr\left(\frac{a_1 PX_3}{a_2 PX_3 + 1} \geq \gamma\right) \Pr\left(\frac{a_1 PX_1}{a_2 PX_1 + 1} \geq \gamma, \frac{b_1 k\eta PX_1 X_4}{b_2 k\eta PX_1 X_4 + 1} \geq \gamma, \frac{b_1 k\eta PX_1 X_5}{b_2 k\eta PX_1 X_5 + 1} \geq \gamma\right)$$

$$F_\gamma(\gamma) = 1 - \Pr\left(X_2 \geq \frac{\gamma}{P(a_1 - \gamma a_2)}\right) \Pr\left(X_3 \geq \frac{\gamma}{P(a_1 - \gamma a_2)}\right) \times \underbrace{\Pr\left(X_1 \geq \frac{\gamma}{P(a_1 - \gamma a_2)}, X_4 \geq \frac{\gamma}{k\eta P(b_1 - b_2\gamma)X_1}, X_5 \geq \frac{\gamma}{k\eta P(b_1 - b_2\gamma)X_1}\right)}_{I_1}$$

$$F_\gamma(\gamma) = 1 - e^{-\frac{\gamma\lambda_{h_2}}{P(a_1 - \gamma a_2)}} e^{-\frac{\gamma\lambda_{h_3}}{P(a_1 - \gamma a_2)}} I_1$$

Conditioning I_1 on X_1, we get

$$F_\gamma(\gamma) = 1 - e^{-\frac{(\lambda_{h_2} + \lambda_{h_3})\gamma}{P(a_1 - \gamma a_2)}} \int_{x_1=0}^{\infty} \Pr\left(x_1 \geq \frac{\gamma}{P(a_1 - \gamma a_2)}, X_4 \geq \frac{\gamma}{k\eta P(b_1 - b_2\gamma)x_1}, X_5 \geq \frac{\gamma}{k\eta P(b_1 - b_2\gamma)x_1}\right) f_{X_1}(x_1) dx_1$$

$$F_\gamma(\gamma) = 1 - e^{-\frac{(\lambda_{h_2} + \lambda_{h_3})\gamma}{P(a_1 - \gamma a_2)}} \int_{x_1=\frac{\gamma}{P(a_1 - \gamma a_2)}}^{\infty} \Pr\left(X_4 \geq \frac{\gamma}{k\eta P(b_1 - b_2\gamma)x_1}, X_5 \geq \frac{\gamma}{k\eta P(b_1 - b_2\gamma)x_1}\right) f_{X_1}(x_1) dx_1$$

$$F_\gamma(\gamma) = 1 - e^{-\frac{(\lambda_{h_2} + \lambda_{h_3})\gamma}{P(a_1 - \gamma a_2)}} \int_{x_1=\frac{\gamma}{P(a_1 - \gamma a_2)}}^{\infty} \Pr\left(X_4 \geq \frac{\gamma}{k\eta P(b_1 - b_2\gamma)x_1}\right) \Pr\left(X_5 \geq \frac{\gamma}{k\eta P(b_1 - b_2\gamma)x_1}\right) f_{X_1}(x_1) dx_1$$

$$F_\gamma(\gamma) = 1 - e^{-\frac{(\lambda_{h_2} + \lambda_{h_3})\gamma}{P(a_1 - \gamma a_2)}} \int_{x_1=\frac{\gamma}{P(a_1 - \gamma a_2)}}^{\infty} e^{-\frac{\lambda_{h_4}\gamma}{k\eta P(b_1 - b_2\gamma)x_1}} e^{-\frac{\lambda_{h_5}\gamma}{k\eta P(b_1 - b_2\gamma)x_1}} \lambda_{h_1} e^{-\lambda_{h_1} x_1} dx_1$$

$$F_\gamma(\gamma) = 1 - \lambda_{h_1} e^{-\frac{(\lambda_{h_2} + \lambda_{h_3})\gamma}{P(a_1 - \gamma a_2)}} \int_{x_1=\frac{\gamma}{P(a_1 - \gamma a_2)}}^{\infty} e^{-\frac{(\lambda_{h_4} + \lambda_{h_5})\gamma}{k\eta P(b_1 - b_2\gamma)x_1} - \lambda_{h_1} x_1} dx_1$$

$$F_\gamma(\gamma) = 1 - \lambda_{h_1} e^{-\frac{(\lambda_{h_2} + \lambda_{h_3})\gamma}{P(a_1 - \gamma a_2)}} \left(\underbrace{\int_{x_1=0}^{\infty} e^{-\frac{(\lambda_{h_4} + \lambda_{h_5})\gamma}{k\eta P(b_1 - b_2\gamma)x_1} - \lambda_{h_1} x_1} dx_1}_{I_2} - \underbrace{\int_{x_1=0}^{\frac{\gamma}{P(a_1 - \gamma a_2)}} e^{-\frac{(\lambda_{h_4} + \lambda_{h_5})\gamma}{k\eta P(b_1 - b_2\gamma)x_1} - \lambda_{h_1} x_1} dx_1}_{I_3} \right)$$

The integral I_2 is in the form $\int_{x=0}^{\infty} e^{-\frac{\beta}{4x} - \gamma x}\, dx$ which can be solved using the formula in eq. 3.324.1 of Reference 31, as: $\frac{\beta}{\gamma} K_1(\sqrt{\beta\gamma})$, where $K_1(.)$ is a first order modified Bessel function of the second kind.

Similarly, the integral I_3 is in the form $\int_{x=0}^{a} e^{-\frac{c}{x} - bx}\, dx$, which can be solved in closed form[23] as: $\sum_{n=0}^{\infty} \frac{(-1)^n}{n!} b^n a^{n+1} E_{n+2}\left(\frac{c}{a}\right)$ where $E_{n+2}(.)$ is the exponential integral of order $n+2$.

Therefore,

$$F_\gamma(\gamma) = 1 - \lambda_{h_1} e^{-\frac{(\lambda_{h_2} + \lambda_{h_3})\gamma}{P(a_1 - \gamma a_2)}} \left(2\sqrt{\frac{(\lambda_{h_4} + \lambda_{h_5})\gamma}{k\eta P\lambda_{h_1}(b_1 - \gamma b_2)}} K_1\left(2\sqrt{\frac{(\lambda_{h_4} + \lambda_{h_5})\gamma\lambda_{h_1}}{k\eta P(b_1 - \gamma b_2)}}\right) - \sum_{n=0}^{\infty} \frac{(-1)^n}{n!} \lambda_{h_1}^n \left(\frac{\gamma}{P(a_1 - \gamma a_2)}\right)^{n+1} E_{n+2}\left(\frac{(\lambda_{h_4} + \lambda_{h_5})(a_1 - \gamma a_2)}{k\eta(b_1 - \gamma b_2)}\right) \right)$$

The EC in terms of CDF $F_\gamma(\gamma)$ can be written as:

$$C_{\text{SDS-Ana}}^{x_1} = \frac{(1 - \alpha)}{2 \ln 2} \int_{\gamma=0}^{\infty} \frac{1}{1 + \gamma} [1 - F_\gamma(\gamma)] d\gamma$$

Substituting $F_\gamma(\gamma)$ in the above equation, we get the final expression as in Equation (18).

This ends the proof of Theorem 1. ∎

APPENDIX B

Proof of Theorem 2. The CDF of $\min(\gamma_{\mathrm{R}}^{x_2}, \gamma_{\mathrm{UE}_2}^{x_2,II}, \gamma_{\mathrm{UE}_2}^{x_2})$ can be given as:

$$F_\gamma(\gamma) = 1 - \Pr\left(a_2PX_1 \geq \gamma, b_2k\eta PX_1X_5 \geq \gamma, a_2PX_3 \geq \gamma\right)$$
$$F_\gamma(\gamma) = 1 - \Pr\left(X_3 \geq \frac{\gamma}{a_2P}\right)\Pr\left(X_1 \geq \frac{\gamma}{a_2P}, X_5 \geq \frac{\gamma}{b_2k\eta PX_1}\right)$$

Now, conditioning $\Pr\left(X_1 \geq \frac{\gamma}{a_2P}, X_5 \geq \frac{\gamma}{b_2k\eta PX_1}\right)$ on X_1

$$F_\gamma(\gamma) = 1 - e^{-\frac{\lambda_{h_3}\gamma}{a_2P}}\int_{x_1=0}^{\infty}\Pr\left(x_1 \geq \frac{\gamma}{a_2P}, X_5 \geq \frac{\gamma}{b_2k\eta Px_1}\right)f_{X_1}(x_1)dx_1$$
$$F_\gamma(\gamma) = 1 - e^{-\frac{\lambda_{h_3}\gamma}{a_2P}}\int_{x_1=\frac{\gamma}{a_2P}}^{\infty}\Pr\left(X_5 \geq \frac{\gamma}{b_2k\eta Px_1}\right)f_{X_1}(x_1)dx_1$$
$$F_\gamma(\gamma) = 1 - \lambda_{h_1}e^{-\frac{\lambda_{h_3}\gamma}{a_2P}}\int_{x_1=\frac{\gamma}{a_2P}}^{\infty}e^{-\frac{\lambda_{h_5}\gamma}{b_2k\eta Px_1}-\lambda_{h_1}x_1}dx_1$$
$$F_\gamma(\gamma) = 1 - \lambda_{h_1}e^{-\frac{\lambda_{h_3}\gamma}{a_2P}}\left(\int_{x_1=0}^{\infty}e^{-\frac{\lambda_{h_5}\gamma}{b_2k\eta Px_1}-\lambda_{h_1}x_1}dx_1 - \int_{x_1=0}^{\frac{\gamma}{a_2P}}e^{-\frac{\lambda_{h_5}\gamma}{b_2k\eta Px_1}-\lambda_{h_1}x_1}dx_1\right)$$
$$F_\gamma(\gamma) = 1 - \lambda_{h_1}e^{-\frac{\lambda_{h_3}\gamma}{a_2P}}\left(2\sqrt{\frac{\lambda_{h_5}\gamma}{b_2k\eta P\lambda_{h_1}}}K_1\left(2\sqrt{\frac{\lambda_{h_1}\lambda_{h_5}\gamma}{b_2k\eta P}}\right) - \sum_{n=0}^{\infty}\frac{(-1)^n}{n!}\lambda_{h_1}^n\left(\frac{\gamma}{a_2P}\right)^{n+1}E_{n+2}\left(\frac{\lambda_{h_5}a_2}{b_2k\eta}\right)\right)$$

Now, the EC in terms of CDF $F_\gamma(\gamma)$ can be written as:

$$C_{\text{SDS-Ana}}^{x_2} = \frac{1}{2\ln 2}\int_{\gamma=0}^{\infty}\frac{1}{1+\gamma}[1 - F_\gamma(\gamma)]d\gamma$$

Substituting $F_\gamma(\gamma)$ in the above equation, we get the final expression as in Equation (20).

This ends the proof of Theorem 2. ∎

APPENDIX C

Proof of Theorem 3. The CDF of $\min(\gamma_{\mathrm{R}}^{x_1}, \gamma_{\mathrm{UE}_2}^{x_1}, \gamma_{\mathrm{UE}_2}^{x_1,II}, \gamma_{\mathrm{MRC}}^{x_1})$ can be given as:

$$F_\gamma(\gamma) = 1 - \Pr\left(\frac{a_1PX_3}{a_2PX_3+1} \geq \gamma\right)\Pr\left(\frac{a_1PX_1}{a_2PX_1+1} \geq \gamma, \frac{b_1k\eta PX_1X_5}{b_2k\eta PX_1X_5+1} \geq \gamma, \frac{a_1PX_2}{a_2PX_2+1} + \frac{b_1k\eta PX_1X_4}{b_2k\eta PX_1X_4+1} \geq \gamma\right)$$
$$F_\gamma(\gamma) = 1 - \Pr\left(X_3 \geq \frac{\gamma}{P(a_1-\gamma a_2)}\right)\underbrace{\Pr\left(X_1 \geq \frac{\gamma}{P(a_1-\gamma a_2)}, X_5 \geq \frac{\gamma}{k\eta P(b_1-b_2\gamma)X_1}, \frac{b_1k\eta PX_1X_4}{b_2k\eta PX_1X_4+1} \geq \gamma - \frac{a_1PX_2}{a_2PX_2+1}\right)}_{I_1}$$
$$F_\gamma(\gamma) = 1 - e^{-\frac{\gamma\lambda_{h_3}}{P(a_1-\gamma a_2)}}I_1$$

Conditioning I_1 on X_1, we get

$$F_\gamma(\gamma) = 1 - e^{-\frac{\lambda_{h_3}\gamma}{P(a_1-\gamma a_2)}}\int_{x_1=0}^{\infty}\Pr\left(x_1 \geq \frac{\gamma}{P(a_1-\gamma a_2)}, X_5 \geq \frac{\gamma}{k\eta P(b_1-b_2\gamma)x_1}, \frac{b_1k\eta Px_1X_4}{b_2k\eta Px_1X_4+1} \geq \gamma - \frac{a_1PX_2}{a_2PX_2+1}\right)f_{X_1}(x_1)dx_1$$
$$F_\gamma(\gamma) = 1 - e^{-\frac{\lambda_{h_3}\gamma}{P(a_1-\gamma a_2)}}\int_{x_1=\frac{\gamma}{P(a_1-\gamma a_2)}}^{\infty}\Pr\left(X_5 \geq \frac{\gamma}{k\eta P(b_1-b_2\gamma)x_1}, \frac{b_1k\eta Px_1X_4}{b_2k\eta Px_1X_4+1} \geq \gamma - \frac{a_1PX_2}{a_2PX_2+1}\right)f_{X_1}(x_1)dx_1$$

$$F_\gamma(\gamma) = 1 - e^{-\frac{\lambda_{h_3}\gamma}{P(a_1-\gamma a_2)}} \int_{x_1=\frac{\gamma}{P(a_1-\gamma a_2)}}^{\infty} e^{-\frac{\lambda_{h_5}\gamma}{k\eta P(b_1-b_2\gamma)x_1}} \Pr\left(\frac{b_1 k\eta P x_1 X_4}{b_2 k\eta P x_1 X_4 + 1} \geq \gamma - \frac{a_1 P X_2}{a_2 P X_2 + 1}\right) f_{X_1}(x_1) dx_1$$

$$F_\gamma(\gamma) = 1 - e^{-\frac{\lambda_{h_3}\gamma}{P(a_1-\gamma a_2)}} \int_{x_1=\frac{\gamma}{P(a_1-\gamma a_2)}}^{\infty} e^{-\frac{\lambda_{h_5}\gamma}{k\eta P(b_1-b_2\gamma)x_1}} \underbrace{\Pr\left(\frac{b_1 k\eta P x_1 X_4}{b_2 k\eta P x_1 X_4 + 1} \geq \gamma - \frac{a_1 P X_2}{a_2 P X_2 + 1}\right) f_{X_1}(x_1)}_{I_2} dx_1$$

Now, conditioning I_2 on X_2, we get

$$I_2 = \int_{X_2=0}^{\infty} \Pr\left(\frac{b_1 k\eta P x_1 X_4}{b_2 k\eta P x_1 X_4 + 1} \geq \gamma - \frac{a_1 P x_2}{a_2 P x_2 + 1}\right) f_{X_2}(x_2) dx_2$$

Now,

$$\gamma = \frac{a_1 P x_2}{a_2 P x_2 + 1} \rightarrow x_2 = \frac{\gamma}{(a_1 - a_2\gamma)P}$$

$$I_2 = \underbrace{\int_{x_2=0}^{\frac{\gamma}{(a_1-a_2\gamma)P}} \Pr\left(\frac{b_1 k\eta P x_1 X_4}{b_2 k\eta P x_1 X_4 + 1} \geq \gamma - \frac{a_1 P x_2}{a_2 P x_2 + 1}\right) f_{X_2}(x_2) dx_2}_{J_1} + \underbrace{\int_{x_2=\frac{\gamma}{(a_1-a_2\gamma)P}}^{\infty} f_{X_2}(x_2) dx_2}_{J_2}$$

$$J_1 = \int_{x_2=0}^{\frac{\gamma}{(a_1-a_2\gamma)P}} \Pr\left(\frac{b_1 k\eta P x_1 X_4}{b_2 k\eta P x_1 X_4 + 1} \geq \frac{\gamma a_2 P x_2 + \gamma - a_1 P x_2}{a_2 P x_2 + 1}\right) f_{X_2}(x_2) dx_2$$

$$J_1 = \int_{x_2=0}^{\frac{\gamma}{(a_1-a_2\gamma)P}} \Pr\left(X_4 \geq \frac{P x_2(a_2\gamma - a_1) + \gamma}{\eta k P x_1((b_1 - \gamma b_2) + P x_2(b_1 a_2 - b_2(a_2\gamma - a_1))}\right) \lambda_{h_2} e^{-\lambda_{h_2} x_2} dx_2$$

$$J_1 = \int_{x_2=0}^{\frac{\gamma}{(a_1-a_2\gamma)P}} \lambda_{h_2} e^{-\frac{\lambda_{h_4} P x_2(a_2\gamma - a_1) + \gamma\lambda_{h_4}}{\eta k P x_1((b_1-\gamma b_2)+P x_2(b_1 a_2 - b_2(a_2\gamma - a_1))} - \lambda_{h_2} x_2} dx_2$$

Now, let $c_1 = \lambda_{h_4} P(a_2\gamma - a_1), c_2 = \lambda_{h_4}\gamma, c_3 = \eta k P x_1(b_1 - \gamma b_2), c_4 = \eta k P^2 x_1(b_1 a_2 - b_2(a_2\gamma - a_1))$

$$J_1 = \int_{x_2=0}^{\frac{\gamma}{(a_1-a_2\gamma)P}} \lambda_{h_2} e^{-\frac{c_1 x_2 + c_2}{c_3 + c_4 x_2} - \lambda_{h_2} x_2} dx_2$$

Now, let $c_3 + c_4 x_2 = z \rightarrow dx_2 = \frac{1}{c_4} dz$

Also, when $x_2 = 0, z = c_3$ and, when $x_2 = \frac{\gamma}{(a_1-a_2\gamma)P}, z = c_3 + c_4\frac{\gamma}{(a_1-a_2\gamma)P} \rightarrow \hat{z}$

$$J_1 = \int_{z=c_3}^{\hat{z}} \frac{\lambda_{h_2}}{c_4} e^{-\frac{c_1\frac{(z-c_3)}{c_4}+c_2}{z} - \lambda_{h_2}\left(\frac{z-c_3}{c_4}\right)} dz$$

$$J_1 = \int_{z=c_3}^{\hat{z}} \frac{\lambda_{h_2}}{c_4} e^{-\frac{c_1}{c_4}} e^{\frac{\lambda_{h_2} c_3}{c_4}} e^{-\frac{(c_2 c_4 - c_1 c_3)}{c_4 z} - \frac{\lambda_{h_2} z}{c_4}} dz$$

Now,

$$J_2 = \int_{x_2=\frac{\gamma}{(a_1-a_2\gamma)P}}^{\infty} f_{X_2}(x_2) dx_2 = \int_{x_2=\frac{\gamma}{(a_1-a_2\gamma)P}}^{\infty} \lambda_{h_2} e^{-\lambda_{h_2} x_2} dx_2$$

$$J_2 = e^{-\frac{\lambda_{h_2}\gamma}{(a_1-a_2\gamma)P}}$$

$$I_2 = J_1 + J_2$$

$$I_2 = \int_{z=c_3}^{\hat{z}} \frac{\lambda_{h_2}}{c_4} e^{-\frac{c_1}{c_4}} e^{\frac{\lambda_{h_2} c_3}{c_4}} e^{-\frac{(c_2 c_4 - c_1 c_3)}{c_4 z} - \frac{\lambda_{h_2} z}{c_4}} dz + e^{-\frac{\lambda_{h_2}\gamma}{(a_1-a_2\gamma)P}}$$

Furthermore,

$$F_\gamma(\gamma) = 1 - e^{-\frac{\lambda_{h_3}\gamma}{P(a_1-\gamma a_2)}} \int_{x_1=\frac{\gamma}{P(a_1-\gamma a_2)}}^{\infty} e^{-\frac{\lambda_{h_5}\gamma}{\eta k P(b_1-b_2\gamma)x_1}} I_2 f_{X_1}(x_1)dx_1$$

$$F_\gamma(\gamma) = 1 - e^{-\frac{\lambda_{h_3}\gamma}{P(a_1-\gamma a_2)}} \int_{x_1=\frac{\gamma}{P(a_1-\gamma a_2)}}^{\infty} e^{-\frac{\lambda_{h_5}\gamma}{\eta k P(b_1-b_2\gamma)x_1}} \left(\int_{z=c_3}^{\hat{z}} \frac{\lambda_{h_2}}{c_4} e^{-\frac{c_1}{c_4}} e^{\frac{\lambda_{h_2}c_3}{c_4}} e^{-\frac{(c_2c_4-c_1c_3)}{c_4 z} - \frac{\lambda_{h_2}z}{c_4}} dz + e^{-\frac{\lambda_{h_2}\gamma}{(a_1-a_2\gamma)P}} \right) \lambda_{h_1} e^{-\lambda_{h_1}x_1} dx_1$$

Now, the EC in terms of CDF $F_\gamma(\gamma)$ can be written as:

$$C^{x_1}_{\text{MRS-Ana}} = \frac{(1-\alpha)}{2\ln 2} \int_{\gamma=0}^{\infty} \frac{1}{1+\gamma}[1 - F_\gamma(\gamma)]d\gamma$$

Substituting $F_\gamma(\gamma)$ in the above equation, we get the final expression as in Equation (27). ∎

This ends the proof of Theorem 3.

APPENDIX D

Proof of Theorem 4. The CDF of $\min(\gamma^{x_2}_{\text{R}}, \gamma^{x_2}_{\text{MRC}})$ can be given as:

$$F_\gamma(\gamma) = 1 - \Pr(a_2PX_1 \geq \gamma, a_2PX_3 + b_2k\eta PX_1X_5 \geq \gamma)$$

Conditioning on X_1, we get,

$$F_\gamma(\gamma) = 1 - \int_{x_1=0}^{\infty} \Pr\left(x_1 \geq \frac{\gamma}{a_2P}, a_2PX_3 + b_2k\eta Px_1X_5 \geq \gamma\right) f_{X_1}(x_1)dx_1$$

$$F_\gamma(\gamma) = 1 - \int_{x_1=\frac{\gamma}{a_2P}}^{\infty} \Pr(b_2k\eta Px_1X_5 \geq \gamma - a_2PX_3) f_{X_1}(x_1)dx_1$$

Again, conditioning on X_3, we get,

$$F_\gamma(\gamma) = 1 - \int_{x_1=\frac{\gamma}{a_2P}}^{\infty} \int_{x_3=0}^{\infty} \Pr(b_2k\eta Px_1X_5 \geq \gamma - a_2Px_3) f_{X_3}(x_3)dx_3 f_{X_1}(x_1)dx_1$$

Now, $\gamma = a_2Px_3 \rightarrow x_3 = \frac{\gamma}{a_2P}$

$$F_\gamma(\gamma) = 1 - \int_{x_1=\frac{\gamma}{a_2P}}^{\infty} \left(\int_{x_3=0}^{\frac{\gamma}{a_2P}} \Pr(b_2k\eta Px_1X_5 \geq \gamma - a_2Px_3) f_{X_3}(x_3)dx_3 + \int_{x_3=\frac{\gamma}{a_2P}}^{\infty} f_{X_3}(x_3)dx_3 \right) f_{X_1}(x_1)dx_1$$

$$F_\gamma(\gamma) = 1 - \int_{x_1=\frac{\gamma}{a_2P}}^{\infty} \left(\int_{x_3=0}^{\frac{\gamma}{a_2P}} \Pr\left(X_5 \geq \frac{\gamma - a_2Px_3}{b_2k\eta Px_1}\right) \lambda_{h_3} e^{-\lambda_{h_3}x_3} dx_3 + e^{-\frac{\lambda_{h_3}\gamma}{a_2P}} \right) f_{X_1}(x_1)dx_1$$

$$F_\gamma(\gamma) = 1 - \int_{x_1=\frac{\gamma}{a_2P}}^{\infty} \left(\int_{x_3=0}^{\frac{\gamma}{a_2P}} \lambda_{h_3} e^{-\frac{\lambda_{h_5}\gamma - \lambda_{h_5}a_2Px_3}{b_2k\eta Px_1} - \lambda_{h_3}x_3} dx_3 + e^{-\frac{\lambda_{h_3}\gamma}{a_2P}} \right) f_{X_1}(x_1)dx_1$$

$$F_\gamma(\gamma) = 1 - \int_{x_1=\frac{\gamma}{a_2P}}^{\infty} \left(\int_{x_3=0}^{\frac{\gamma}{a_2P}} \lambda_{h_3} e^{-\frac{\lambda_{h_5}\gamma}{b_2k\eta Px_1}} e^{-\frac{(b_2k\eta\lambda_{h_3}x_1 - a_2\lambda_{h_5})x_3}{b_2k\eta x_1}} dx_3 + e^{-\frac{\lambda_{h_3}\gamma}{a_2P}} \right) f_{X_1}(x_1)dx_1$$

$$F_\gamma(\gamma) = 1 - \int_{x_1=\frac{\gamma}{a_2P}}^{\infty} \left(\lambda_{h_3} \frac{b_2k\eta x_1}{b_2k\eta\lambda_{h_3}x_1 - a_2\lambda_{h_5}} e^{-\frac{\lambda_{h_5}\gamma}{b_2k\eta Px_1}} \left(1 - e^{-\frac{(b_2k\eta\lambda_{h_3}x_1 - a_2\lambda_{h_5})\gamma}{b_2k\eta x_1 a_2P}} \right) + e^{-\frac{\lambda_{h_3}\gamma}{a_2P}} \right) f_{X_1}(x_1)dx_1$$

$$F_\gamma(\gamma) = 1 - \int_{x_1=\frac{\gamma}{a_2P}}^{\infty} \lambda_{h_3} \frac{b_2k\eta x_1}{b_2k\eta\lambda_{h_3}x_1 - a_2\lambda_{h_5}} e^{-\frac{\lambda_{h_5}\gamma}{b_2k\eta Px_1}} \lambda_{h_1} e^{-\lambda_{h_1}x_1} dx_1$$

$$+\int_{x_1=\frac{\gamma}{a_2P}}^{\infty}\lambda_{h_3}\frac{b_2k\eta x_1}{b_2k\eta\lambda_{h_3}x_1-a_2\lambda_{h_5}}e^{-\frac{\lambda_{h_5}\gamma}{b_2k\eta Px_1}}e^{-\frac{(b_2k\eta\lambda_{h_3}x_1-a_2\lambda_{h_5})\gamma}{b_2k\eta x_1a_2P}}\lambda_{h_1}e^{-\lambda_{h_1}x_1}dx_1-\int_{x_1=\frac{\gamma}{a_2P}}^{\infty}e^{-\frac{\lambda_{h_3}\gamma}{a_2P}}\lambda_{h_1}e^{-\lambda_{h_1}x_1}dx_1$$

$$F_\gamma(\gamma)=1-\int_{x_1=\frac{\gamma}{a_2P}}^{\infty}\lambda_{h_1}\lambda_{h_3}\frac{b_2k\eta x_1}{b_2k\eta\lambda_{h_3}x_1-a_2\lambda_{h_5}}e^{-\frac{\lambda_{h_5}\gamma}{b_2k\eta Px_1}-\lambda_{h_1}x_1}dx_1$$

$$+\int_{x_1=\frac{\gamma}{a_2P}}^{\infty}\lambda_{h_3}\frac{b_2k\eta x_1}{b_2k\eta\lambda_{h_3}x_1-a_2\lambda_{h_5}}e^{-\frac{\lambda_{h_5}\gamma}{b_2k\eta Px_1}}e^{-\frac{(b_2k\eta\lambda_{h_3}x_1-a_2\lambda_{h_5})\gamma}{b_2k\eta x_1a_2P}}\lambda_{h_1}e^{-\lambda_{h_1}x_1}dx_1-e^{-\frac{(\lambda_{h_1}+\lambda_{h_3})\gamma}{a_2P}}$$

Now, the EC in terms of CDF $F_\gamma(\gamma)$ can be written as:

$$C^{x_2}_{\text{MRS-Ana}}=\frac{(1-\alpha)}{2\ln 2}\int_{\gamma=0}^{\infty}\frac{1}{1+\gamma}[1-F_\gamma(\gamma)]d\gamma$$

Substituting $F_\gamma(\gamma)$ in the above equation, we get the final expression as in Equation (30).

This ends the proof of Theorem 4. ∎

Paper XIII

Ergodic Capacity Performance of D2D IoT Relay NOMA-SWIPT Systems with Direct Links

Ashish Rauniyar, Paal E. Engelstad, Olav N. Østerbø

In: *IEEE 43rd International Conference on Telecommunications and Signal Processing (TSP), Milan, Italy, 7-9 July* (2020), pp. 1–7, DOI: 10.1109/TSP49548.2020.9163552.